Author:
Hussain, Yameen M

Title:
Fault Diagnostics of Electromechanical Actuators in Aerospace Safety Critical Applications

Fault Diagnostics of Electromechanical Actuators in Aerospace Safety Critical Applications

Yameen Monsur Hussain

A thesis submitted to the University of Bristol in accordance with the requirements of the degree of Engineering Doctorate in Systems in the Faculty of Engineering

Faculty of Engineering, March 2019

Word Count: 30,049

Abstract

Electromechanical Actuators (EMAs) are increasingly being considered for safety critical applications across the aerospace sector because of the potential benefits this technology can offer compared to traditional types of actuator. One of the main challenges for EMA implementation within safety critical applications is mitigating the single point of failure: ballscrew jamming. Better understanding of the onset of EMA ballscrew jamming, and consequences of jamming, would make EMAs a more viable option for aerospace safety critical applications.

Through Hierarchical Process Modelling (HPM) and review of previous literature, various diverse strategies were considered to mitigate EMA ballscrew jamming. The most favoured approach was fault diagnostics i.e. predicting the state of health of a component or onset of failure by monitoring system operation. Monitoring the state of health of a component in turn allows new maintenance strategies, for example Condition Based Maintenance (CBM). As part of a systems approach towards evaluating fault diagnostics, a Systems Dynamics (SD) study was conducted to capture the cost benefits of applying a CBM maintenance strategy to a fleet of aircraft in comparison to a conventional time-based maintenance strategy. Historical in-service data for EMAs was used in this study and it was notable that the reliability of EMAs had significantly improved over the timescale of the data, which meant the direct economic benefit of CBM was reduced. Therefore, the primary benefit of fault diagnostics was improving safety.

Sensing for fault detection was limited to using motor current alone, thus exploiting an existing sensor of the actuator system. A hybrid approach to fault diagnostics was proposed which utilises a combination of high-fidelity modelling of the system and experimental data to supplement the real application being monitored. Through simulations it was demonstrated that feature extraction of ballscrew dynamic frictional behaviour could be achieved through I_q current analysis. The results were also mapped to health states in a classification algorithm. The analysis was then extended to an industrial based case study for an Airbus A320 Nose Landing Gear extension-retraction system where it was demonstrated that EMA ballscrew stiction could be identified through motor current in the presence of aero loads.

The final outcome of this thesis was the development of a CBM technique for the A320 NLG extension-retraction system. The approach taken was to perform offline CBM checks on accumulated flight data (motor current signals) on a weekly basis. The diagnostics were based on extracting dynamic friction features of the EMA ballscrew through I_q currents and comparison of these with an analytical model in a hybrid approach.

Dedication

My late father Muhamed Shahadat Hussain always supported me throughout my EngD, as he has done all my life. His strength and courage gave me the determination and patience to complete this thesis.

Thank you for everything Abbu. You'll be sorely missed, and you'll always live on in my heart.

Acknowledgements

There are many who have been supportive and helpful during my EngD. I am very thankful -

To my supervisors,

Dr Steve Burrow for sharing his expert knowledge and experience in the field of electrical machines and drives. Steve was always there to provide technical support and guidance to ensure my project ran efficiently.

Professor Patrick Keogh for his valuable insight and wealth of knowledge on frictional dynamics. Patrick has been a great mentor and always provided very useful guidance.

Leigh Henson for guiding my research from an industrial standpoint. Leigh has always championed the importance of my research by ensuring my research outputs were made visible to Stirling Dynamics.

I am also grateful to Trajan Seymour for supporting my application onto the programme and his initial supervision.

To my academic peers,

There were a few within the university who have given me technical support. I give special appreciation to Dr Jason Yon and Dr Lindsay Clare for their time and effort during my test stand development.

My office colleagues have been a great source of motivation and banter! I give special thanks to my good friend Dr Jonathan Stevenson for his advice and encouragement.

The Systems Centre have done a wonderful job in ensuring the programme ran smoothly. I give special thanks to Sophie Causon-Wood and Dr Sean Shiels for always being there to meet the needs of the students.

To my family,

My mother supported me every step of the way and has been a great source of strength and determination. I thank my wife Sarah for all her support during my EngD journey and our son Reehan for bringing us joy.

Author’s Declaration

I declare that the work in this thesis was carried out in accordance with the requirements of the University’s Regulations and Code of Practice for Research Degree Programmes and that it has not been submitted for any other academic award. Except where indicated by specific reference in the text, the work is the candidate’s own work. Work done in collaboration with, or with the assistance of, others is indicated as such. Any views expressed in the thesis are those of the author.

Signed:

Date:

List of Publications and Awards

Journal Publications

1. ‘A High Fidelity Model-based Approach to Identify Dynamic Friction in Electromechanical Actuator Ballscrews using Motor Current’, Hussain, Y., Burrow, S., Henson, L., & Keogh, P. 2018, International Journal of Prognostics and Health Management, ISSN 2153-2648

2. ‘A Review of Techniques to Mitigate Jamming in Electromechanical Actuators for Safety Critical Applications’, Hussain, Y., Burrow, S., Henson, L., & Keogh, P. 2018, International Journal of Prognostics and Health Management, ISSN 2153-2648

3. ‘A Systems Dynamics Approach to Evaluate Component Availability under Condition Based Maintenance’, Hussain, Y., Burrow, S., Henson, L., & Keogh, P. International Journal of Prognostics and Health Management – In review

Peer Reviewed Conference Publications

1. Benefits Analysis of Prognostics & Health Monitoring to Aircraft Maintenance using System Dynamics’, Hussain, Y., Burrow, S., Henson, L., & Keogh, P. Third European Conference of the Prognostics and Health Management Society 2016, Bilbao

2. ‘Evaluating Strategies to Mitigate Jamming in Electromechanical Actuators for Safety Critical Applications’, Hussain, Y., Burrow, S., Henson, L., & Keogh, P. First Asia-Pacific Conference of the Prognostics and Health Management Society 2017, Jeju

3. ‘A Modelling Approach to Monitor Friction within Electromechanical Actuator Ballscrews using Motor Current’, Hussain, Y., Burrow, S., Henson, L., & Keogh, P. First Asia-Pacific Conference of the Prognostics and Health Management Society 2017, Jeju

Awards

Best Poster award for paper titled ‘Evaluating Strategies to Mitigate Jamming in Electromechanical Actuators for Safety Critical Applications’, First Asia-Pacific Conference of the Prognostics and Health Management Society 2017, Jeju

List of Abbreviations

AA	Airborne Attack
AC	Aircraft
AC	Alternating Current
AEA	All Electric Aircraft
AG	Advisory Generation
AIA	Airborne Inhabited Attack
ARP	Aerospace Recommended Practice
AUA	Airborne Uninhabited Attack
BITE	Built in Test Equipment
BLDC	Brushless Direct Current
BN	Ballnut
BS	Ballscrew
CBM	Condition Based Maintenance
CLD	Causal Loop Diagram
CNC	Computer Numerical Control
DA	Data Acquisition
DC	Direct Current
DM	Data Manipulation
DMC	Direct Maintenance Cost
EHA	Electrohydraulic Actuator
EMA	Electromechanical Actuator
EoL	End of Life
EPSRC	Engineering and Physical Sciences Research Council
FC	Flight Cycles
FFT	Fast Fourier Transform
FH	Flight Hours
FOC	Field Oriented Control
FMEA	Failure Mode and Effects Analysis
FMECA	Failure Mode, Effects & Criticality Analysis
HA	Health Assessment
HARAS	High Availability Redundant Actuation Systems
HPM	Hierarchical Process Model
IVHM	Integrated Vehicle Health Management
k-NN	k Nearest Neighbour

LG	Landing Gear
MD	Mean Downtime
MEA	More Electric Aircraft
MLG	Main Landing Gear
MTBF	Mean Time Before Failure
MTTR	Mean Time to Repair
NLG	Nose Landing Gear
NN	Nearest Neighbour
NPRD	Non Electronics Parts Reliability Database
OI	Operational Interrupts
PA	Prognosis Assessment
PHM	Prognostics and Health Monitoring
PMSM	Permanent Magnet Synchronous Motor
RPM	Revolutions per Minute
RPN	Risk Priority Number
RUL	Remaining Useful Life
SD	State Detection
SD	System Dynamics
SHM	Structural Health Monitoring
SoH	State of Health
SVM	Support Vector Machine
TCC	Thermal Contact Conductance
UAV	Unmanned Aerial Vehicle

List of Symbols

B	Motor Viscous Friction
D	Ball Diameter
D_s	Screw Pitch
d_s	Screw Diameter
F	Force
F_l	Load Force
F_{pf}	Pre-load Force
I_a	a Phase Current
I_b	b Phase Current
I_c	c Phase Current
I_d	d Axis Current
I_q	q Axis Current
I_α	α Axis Current
I_β	β Axis Current
J	Total System Inertia
J_{BS}	Ballscrew Inertia
J_l	Load Inertia
J_m	Motor Inertia
K_e	Motor Voltage Constant
K_t	Motor Torque Constant
k_c	Coulomb Friction Coefficient
k_s	Stribeck Friction Coefficient
k_v	Viscous Friction Coefficient
L	Lead
l	Length
L_d	d axis Inductance
L_q	q axis Inductance
m	Mass of Ballscrew
p	Number of Poles
R_s	Stator Resistance
T	Torque
T_c	Cogging Torque
T_e	Electromagnetic Torque
T_l	Load Torque

v_0	Velocity Range for Stribeck Effect
V	Linear Velocity
V_a	a Phase Voltage
V_B	Ball Linear Velocity
V_b	b Phase Voltage
V_{BN}	Relative Velocity between Ball and Nut
V_{BS}	Relative Velocity between Ball and Screw
V_c	c Phase Voltage
V_d	d Axis Voltage
V_q	q Axis Voltage
v_s	Sliding Velocity between Interacting Surfaces
V_α	α Axis Voltage
V_β	β Axis Voltage
α	Ballscrew Lead Angle
α_n	Contact Angle between Ball and Nut
α_s	Contact Angle between Ball and Screw
β	Lead Angle
θ	Rotor Angle
λ_{af}	Flux Induced by the Rotor Permanent Magnets
λ_d	d Axis Flux Linkage
λ_q	q Axis Flux Linkage
ρ	Density
τ_{fk}	Kinetic Friction
ω_b	Ball Angular Velocity
ω_{BN}	Relative Angular Velocity between Ball and Nut
ω_{BS}	Relative Angular Velocity between Ball and Screw
ω_m	Rotor Mechanical Angular Velocity
ω_r	Rotor Electrical Angular Velocity

Contents

List of Figures

List of Tables

Chapter 1: Introduction

This chapter provides background information regarding the research in to Health Monitoring of Aerospace Electromechanical Actuators (EMAs). The motivation behind this research stemming from the concept of More Electric Aircraft (MEA) is elaborated with the aim to make the implementation of EMAs more achievable for safety critical applications in Aerospace. Information regarding the key stakeholders involved in this Engineering Doctorate (EngD) is provided and is followed by a summary of the thesis layout.

1.1 Research Background and Motivation

1.1.1 Towards More Electric Aircraft (MEA)

Up until the 1970s, electrical power on commercial aircraft was predominantly used for electronic and utility functions with sparse application for other functions (Jones, 1999). With advances in permanent magnet materials and power electric devices, the use of electrically powered systems in place of traditional hydraulics and pneumatics appeared to become more advantageous thus prompting a drive towards All Electric Aircraft (AEA) near the end of the 1970s (Jones, 1999).

Studies conducted by NASA in the mid-1980s by Hoffman, Hansen, Beach, Plencner, Dengler, Jefferies & Frye, (1985) concluded that whilst the application of AEA technology is feasible and the benefits of achieving a reduction in operational costs due to the weight saving advantages and maintenance are possible, such wholesale changes would bring about more risk for the conservative and safety driven aerospace industry. This has prompted the aerospace industry to opt for an incremental adoption of electrical technology within secondary aircraft systems, thus the process is now known as More Electric Aircraft (MEA) (Jones, 1999).

1.1.2 The Shift from Hydromechanical to Electromechanical Systems

Much of the research for MEA has considered replacing traditional hydromechanical actuator systems with EMA systems. The often-cited drivers for this shift include reduced system weight, ease of maintenance and potential for greater precision in control (Hoffman et al., 1985). The introduction of EMAs to replace hydraulic systems could make for easier power distribution, using electrical cables in place of hydraulic pipes, as well as eliminating the maintenance infrastructure required for a hydraulic based system (Stridsberg, 2005). These positive drivers are equally valid for safety critical applications such as primary flight control systems and landing gear systems; however, the absence of reliable failsafe mechanisms and redundancy to mitigate the single point of failure (ballscrew jamming) has made it challenging to introduce EMAs to such systems (Balaban, Bansal, Stoelting, Saxena, Goebel & Curran, 2009a).

Actuation systems on a typical commercial aircraft are found on various subsystems. This includes the flight control surfaces as shown in Figure 1.

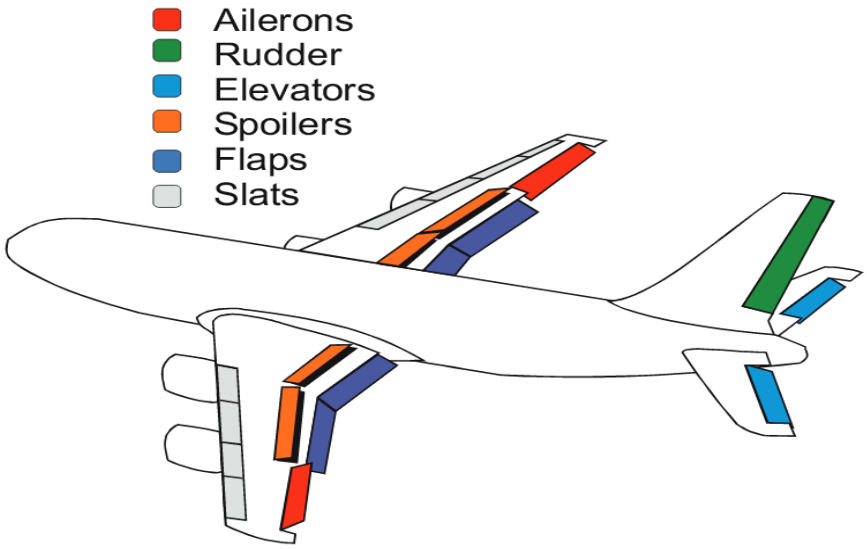

Figure 1. Flight Control Surfaces (Bennett J, 2010). *Reproduced by permission of Newcastle University under the Creative Commons Attribution Licence*.

The ailerons, rudder and elevators are classified as primary control surfaces and are safety critical applications. Another safety critical application that uses actuation systems is the landing gear system, in particular the extension/retraction mechanisms. Figure 2 shows an example of a typical main landing gear system.

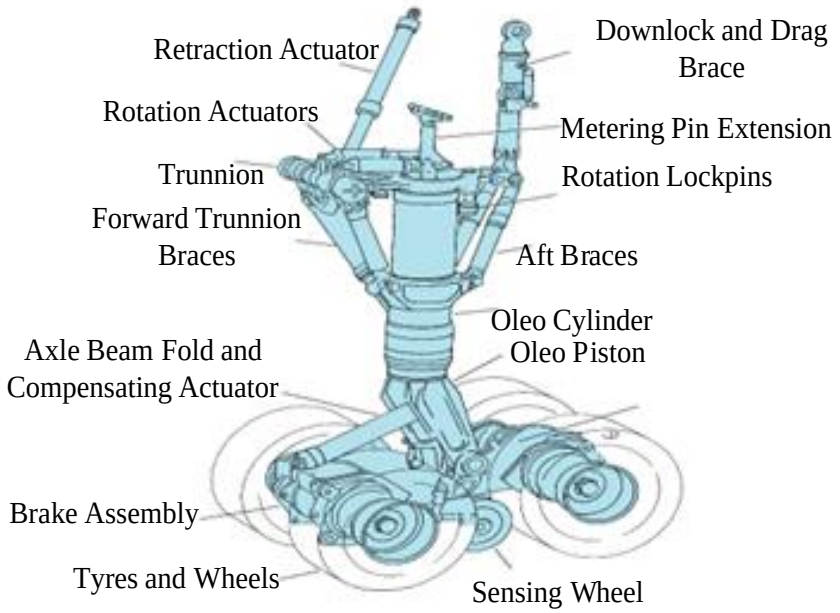

Figure 2. Main Landing Gear (Mouritz, 2012). *Reproduced by permission of Elsevier.*

Given the sparse implementation of EMAs in today's commercial aircraft actuation systems, Electro-hydraulic Actuators (EHAs) are considered to be the intermediate solution between hydromechanical and electromechanical actuation systems (Bennett, 2010). EHAs are essentially a hybrid electrical and

hydraulic device where the actuator is hydraulically operated with the hydraulic fluid self-contained and pressurised by an inbuilt motor to drive the actuation mechanism (Churn, Maxwell, Schofield, Howe and Powell, 1998). Figure 3 shows an example of an EHA.

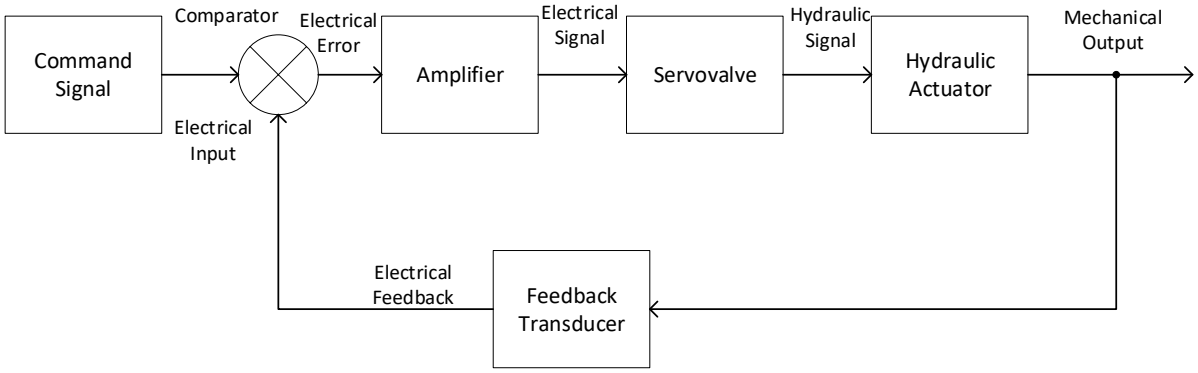

Figure 3. Electrohydraulic Actuator System Block Diagram.

EHAs are viewed as advantageous over conventional hydraulic systems with increased fluid pressure thus power density during actuation (Moir & Seabridge, 2008). Loss of operation would inhibit the hydraulic rod in exerting a force thus defaulting to damping action allowing for an adequate fail-safe mechanism by enabling other actuators to fulfil the actuation (Bennett, 2010). The added redundancy makes hydraulic actuation the preferred choice over EMAs in safety critical applications today.

1.1.3 Electromechanical Actuators (EMA)

EMAs generally consist of a motor, gearing and either a leadscrew, rollerscrew or ballscrew to provide incremental linear motion powered by the motor. Figure 4 shows a schematic of a typical EMA system.

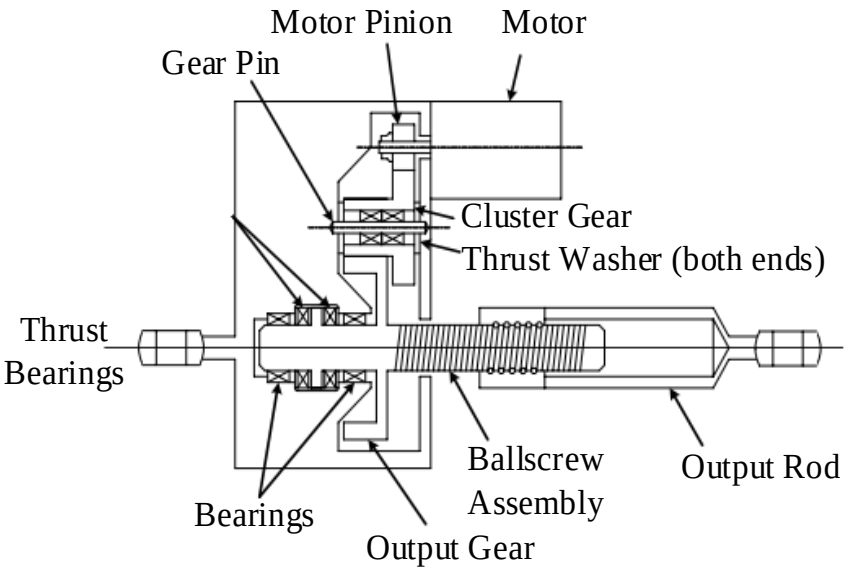

Figure 4. EMA System (Bodden, Clements, Schley & Jenney, 2007). *Reproduced by permission of the Institute of Electrical and Electronics Engineers (IEEE).*

1.1.3.1 EMA Trade Offs

There are different types of linear EMAs available today in production and usage in terms of the mechanical arrangement of the screw. A trade off study of the three common types of screw (Leadscrew, rollerscrew, ballscrew) is generally conducted to aid the design development of an EMA for a specific application based on technical and economic factors (Exlar, 2014). The basic principle behind screw based actuators is to provide linear motion from rotation of the actuator nut thus moving the screw shaft in a line.

The leadscrew assembly is usually constructed using a nut and screw coupling as male-female rubbing surfaces. They are known to experience high frictional energy losses compared to rollercrews and ballscrews, and therefore are usually not considered for use in high power applications.

Figure 5. Example Lead Screw (Abssac, 2020). *Reproduced by permission of Abssac.*

The rollerscrew is unique in mechanical design in that it comprises of several threaded helical rollers which are arranged in a planetary assembly around a typical threaded screw as shown in Figure 6.

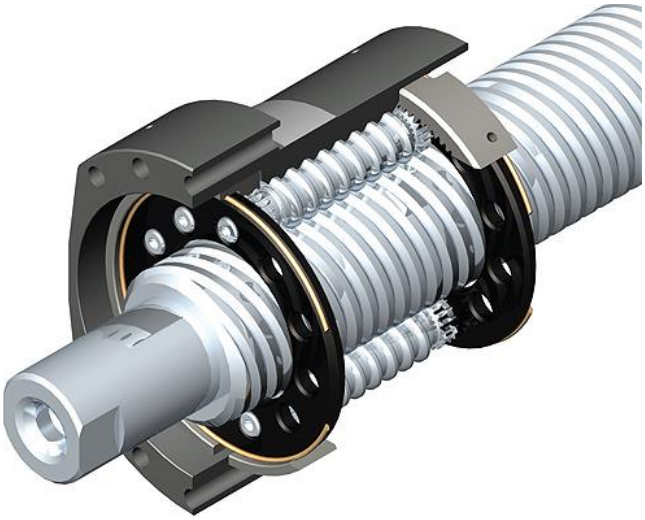

Figure 6. Example Rollerscrew (Shelton, 2010). *Reproduced by permission of Design World.*

This configuration is known to be the most efficient out of the three options and often the preferred choice for high precision, high speed, heavy load and high endurance applications. Rollerscrews, however, are complex in construction and therefore expensive to manufacture.

Like the rollerscrew, the ballscrew exhibits low friction and operates as a feed screw with the ball underdoing rolling motions between screw axis and nut. The screw threaded shaft contains a helical raceway for ball bearing travel which acts as the precision screw. Figure 7 shows an example ballscrew.

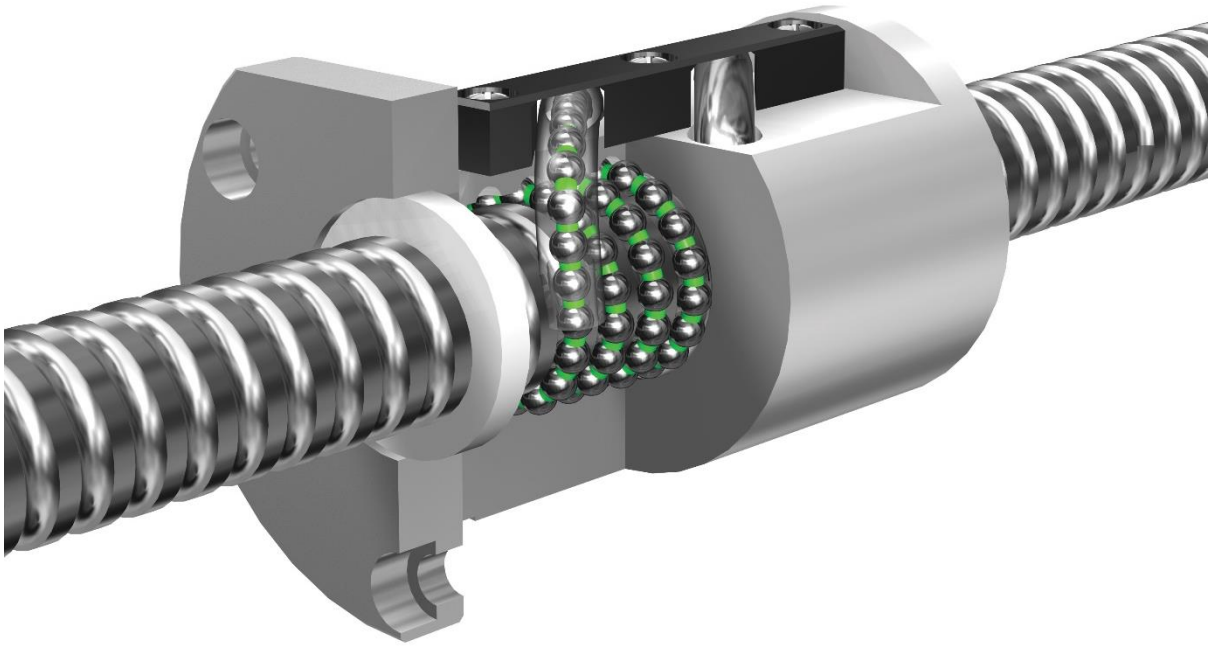

Figure 7. Example Ballscrew with Cutaway Section showing Ball Recirculation chamber (Design World, 2015). *Reproduced by permission of Design World.*

The ballscrew has been the generally favoured arrangement for industrial and aerospace applications due to its high efficiency, high load bearing capabilities, cheaper (compared to rollerscrew) design construction, thus the ballscrew is the main focus for this investigation of this thesis.

1.1.4 Previous Investigations on EMA Implementation in the Aerospace Sector

EMA ballscrew jamming (a single point of failure) was identified as a major factor in preventing EMAs from being considered more thoroughly as an actuator for safety critical applications (AIR5713, 2008). Another issue also arises on whether EMA redundancy can be designed to equal the flight safety reliability of dual/triple redundant hydromechanical systems (Leonard, 1984). For example, for an Airbus A320 aircraft landing gear extension-retraction system, gravity extension can be applied to mitigate a catastrophic event in the event of losing all hydraulic systems (Airbus, 1998).

Lucas Aerospace has also been involved in EMA research development from 1968 with early focus on missile control surfaces (Croke & Herrenschmidt, 1994). Lucas Aerospace went on to design and develop EMAs for aircraft actuation systems in 1988. The design considered an EMA with a brushless DC motor powered by a 270 VDC bus. The initial design was implemented only for test bench purposes,

however, advancements were made with preliminary designs factoring in installation to an aircraft envelope (with the assistance of a commuter jet manufacturer) (Cooper, 2014).

Boeing introduced EMAs to aircraft actuation systems in their Boeing 777 aircraft in the early 1990s. The EMAs were implemented as an electrical backup arrangement for the flaps and slats (Rea, 1993). EMAs also feature on the Airbus A380 slats and tail horizontal stabiliser (Adams, 2001). On more recent aircraft, EMAs have also been implemented on the Boeing 787 on 4 (out of 14) spoilers (Mare, 2016). The spoilers are considered secondary (non-safety critical) aircraft systems. EMAs have also been implemented for wheel braking on Boeing 787s. Whilst wheel braking is considered to be a safety critical item, the loss of braking on one wheel would not inhibit braking altogether with adequate redundancy in place.

1.2 EngD in Systems Programme and Stakeholders

This doctorate level research was pursued in collaboration with the industrial sponsor Stirling Dynamics. The University of Bristol is the awarding body of the EngD and are joint academic partners of the Systems Centre (funded by Engineering and Physical Sciences Research Council (EPSRC) along with the University of Bath. Stirling Dynamics is a small-medium sized company that specialises in the design, development and supply of highly complex and safety critical systems to a diverse range of customers within the aerospace, marine and energy sectors (Stirling Dynamics, 2018). Stirling Dynamics has also been involved in supporting the aerospace sector in developing innovative technologies to increase aircraft efficiency and safety with broad experience in aircraft systems design, integration and test services (Stirling Dynamics, 2018).

The research topic is aligned with Stirling Dynamics' objective to enhance capabilities in developing health monitoring functionality to make EMAs more technically viable for aerospace safety critical applications. This is also part of a long-term strategy at Stirling Dynamics to develop a prognostics functionality to diagnose and detect the onset of failure and therefore nullify any catastrophic events for one of its existing EMA products.

The EngD in systems research involves four stakeholders, these include the principal stakeholder which is the EngD researcher, 1st academic supervisor from University of Bristol, 2nd academic supervisor from University of Bath and industrial supervisor from Stirling Dynamics. Table 1 provides a summary of the key stakeholders and their objectives with respect to this research.

Table 1: Stakeholder Objectives

Stakeholder	Objectives
EngD Researcher	Conduct systems engineering based academic research to solve a technical problem in industry.
Academic Supervisors	Ensure that the researcher conducts novel research and follows an academic approach to solve technical problems.
Industrial Supervisor	Ensure that the research is conducted with a well-defined methodology and is closely aligned with industry objectives.

1.3 Thesis Chapter Summary

Chapter 1: Introduction

In this chapter, a research background for MEA is provided with explanation of research motivation, which is to make EMAs more technically viable for implementation on aerospace safety critical applications. The EngD programme with associated stakeholder objectives from academic and industrial standpoints are also highlighted.

Chapter 2: EMA Ballscrew Jamming: Previous Work, Data Collection, Research Problem and Objectives

This chapter provides a review of the current state-of-the-art with respect to mitigating EMA ballscrew jamming, as well as highlighting existing challenges from current approaches. The different types of failures encountered in EMA systems in aerospace are also documented, with a view to identifying the precursors and corresponding parameters needed for Fault Diagnostics development. This chapter also captures the experiences of industry professionals who use EMA ballscrews across various industries as well as capturing their views on health monitoring. Historical failure rate data of EMAs are also reviewed. Subsequently, a summary of the problem statement is given followed by the thesis objectives.

The work in this chapter has been published in the International Journal of Prognostics and Health Management titled 'A Review of Techniques to Mitigate Jamming in Electromechanical Actuators for Safety Critical Applications' in 2018 (Hussain Y. M., Burrow, Keogh, & Henson, 2018b).

Chapter 3: High Fidelity EMA System Modelling

This chapter presents a high fidelity model of a linear direct drive EMA system to aid better understanding of system behaviour as well as to analyse EMA ballscrew degradation through motor current. Through simulation studies, feature extraction of EMA ballscrew dynamic friction is demonstrated using motor current, which feeds into an algorithm design.

The work in this chapter has been published in the International Journal of Prognostics and Health Management titled 'A High Fidelity Model-based Approach to Identify Dynamic Friction in Electromechanical Actuator Ballscrews using Motor Current' in 2018 (Hussain Y. M., Burrow, Keogh, & Henson, 2018a).

Chapter 4: EMA Test Stand Analysis

The chapter presents the findings from a series of tests from an EMA test stand. These tests served as validation against the systems modelling and simulations presented in Chapter 4. The results from a series of seeded failure tests are also presented with analysis.

Chapter 5: Aircraft Landing Gear Extension-Retraction System Study

This chapter forms a case study based on an Airbus A320 Nose Landing Gear (NLG) extension-retraction system. Based on the high fidelity systems modelling approach from Chapter 4, this case study presented a remodelled actuation system with real A320 NLG extension-retraction end load data included. The simulations demonstrated feature extraction of dynamic friction behaviour in the system through motor current signals whilst factoring in NLG extension-behaviour and aerodynamic loads.

Chapter 6: Summary and Discussion - Towards a Feature Driven Algorithm to Detect EMA Ballscrew Jamming

This chapter brings together the outcomes of the earlier chapters with key findings highlighted as inputs towards a proposed algorithm design. The discussion is centred around a proposed hybrid algorithm for the A320 NLG extension-retraction EMA system by combining all the knowledge learnt from all the analyses conducted so far.

Chapter 7: Conclusions

This chapter provides a summary of the thesis and key findings. It also considers the impact of the research to Stirling Dynamics. Final comments are made on the technical feasibility of EMA implementation to safety critical applications in aerospace considering the findings from this research. The limitations of the research future research opportunities are also discussed.

Chapter 2: EMA Ballscrew Jamming: Previous Work, Data Collection, Research Problem and Objectives

This chapter provides a holistic review on the issue of EMA ballscrew jamming. This includes a review of literature on previously applied techniques to mitigate jamming as well as the existing challenges. Furthermore, data collection was conducted which included a failure analysis of an EMA system as well as capturing industrial experience from EMA users and repairers through semi-structured interviews to highlight technical challenges in mitigating ballscrew failures. Subsequently, a summary of the research problem and objectives are provided. [1]

2.1 Review of Current State-of-the-Art in EMA Ballscrew Jamming Mitigation

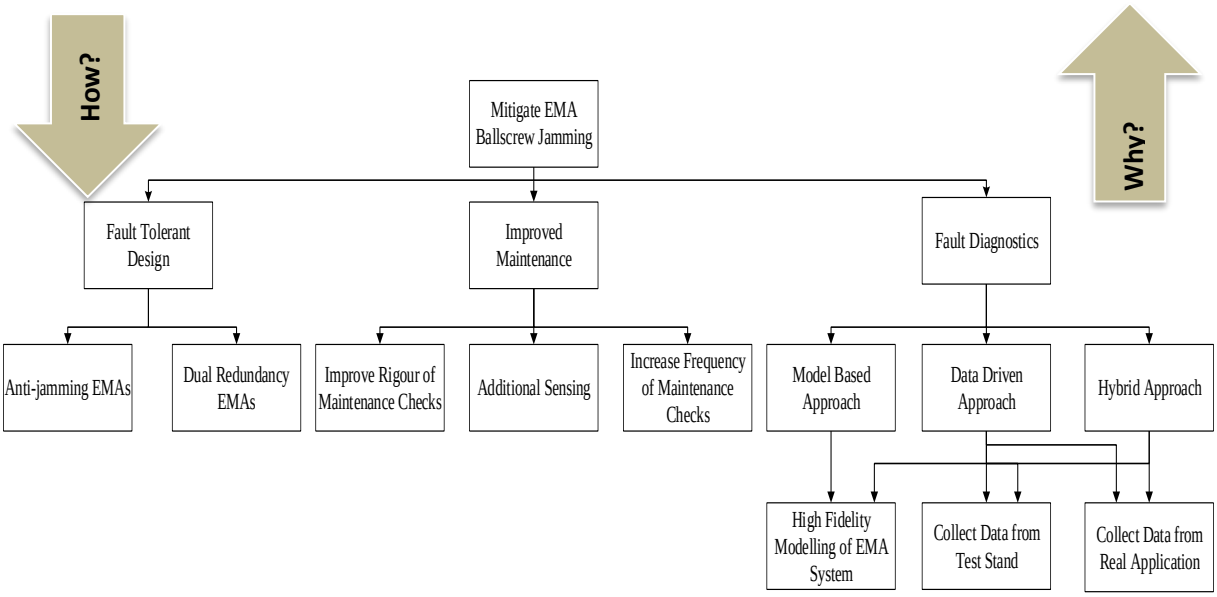

Figure 8. Hierarchical Process Model.

A Hierarchical Process Model (HPM) was constructed to act as a framework from which to consider existing approaches to mitigate EMA ballscrew jamming.

[1] Some of the work in this chapter has been published in the International Journal of Prognostics and Health Management titled *'A Review of Techniques to Mitigate Jamming in Electromechanical Actuators for Safety Critical Applications'* in 2018 (Hussain Y. M., Burrow, Keogh, & Henson, 2018b).

HPM can be a useful way to manage complexity to a single problem. HPM intends to show hierarchy with each level representing a more detailed decomposition of processes indicating transformational entities. HPM is driven by the need to support effective decision making whilst acknowledging issues related to risk and uncertainty. Pidd (2004) identified the need behind HPM by describing nature as being hierarchically organised with emergent properties at various levels of complexities.

The structure of a typical HPM stems from an initial purpose statement, which then branches downwards by exploring how it could be achieved through various system levels, as more detail is added (Checkland & Poulter, 2007). Figure 8 shows the HPM with purpose statement 'Mitigate EMA ballscrew jamming'. At the same time, it is possible to establish purpose and reasoning of a solution when viewing the HPM 'bottom up' (Checkland & Poulter, 2007).

The HPM in Figure 8 describes three top-level approaches to mitigate jamming: fault tolerant design, improved maintenance, and fault diagnostics. Fault tolerant design and fault diagnostics are further considered in Sections 2.1.1 and 2.1.2 of this chapter, respectively. The 'improved maintenance' node is not considered further in this study as the methods of analysis have limited similarity with the other two, requiring evaluation of assumed usage profiles and the impact on existing maintenance policy, for example, covered by the Maintenance Review Board (Robelin, 2010). Additional maintenance actions also incur ongoing costs due to increased labour and aircraft downtime (Jennions, 2012).

2.1.1 Fault Tolerant Design

Fault tolerant design describes a range of techniques, applied at either a system or component level, that provide 'fail operational' or 'fail safe' behaviour, typically through introducing redundancy.

The are several examples in the literature achieving fault tolerant behaviour on electric drive systems (the first section of an EMA) for aerospace applications. For example, at the electrical machine level, this could be achieved with dual/triple motor redundancy or by the use of poly-phase machines. Bennett, Mecrow, Atkinson and Atkinson (2011) suggest that with each lane including an independent converter, a fault tolerant electrical drive can withstand failures associated with power supply and control interface and therefore increasing the number of lanes would skew the EMA reliability figure towards the level for mechanical components. Figure 9 shows an EMA fault tree with dual lane fault tolerant electric drive derived by Bennett et al. (2011).

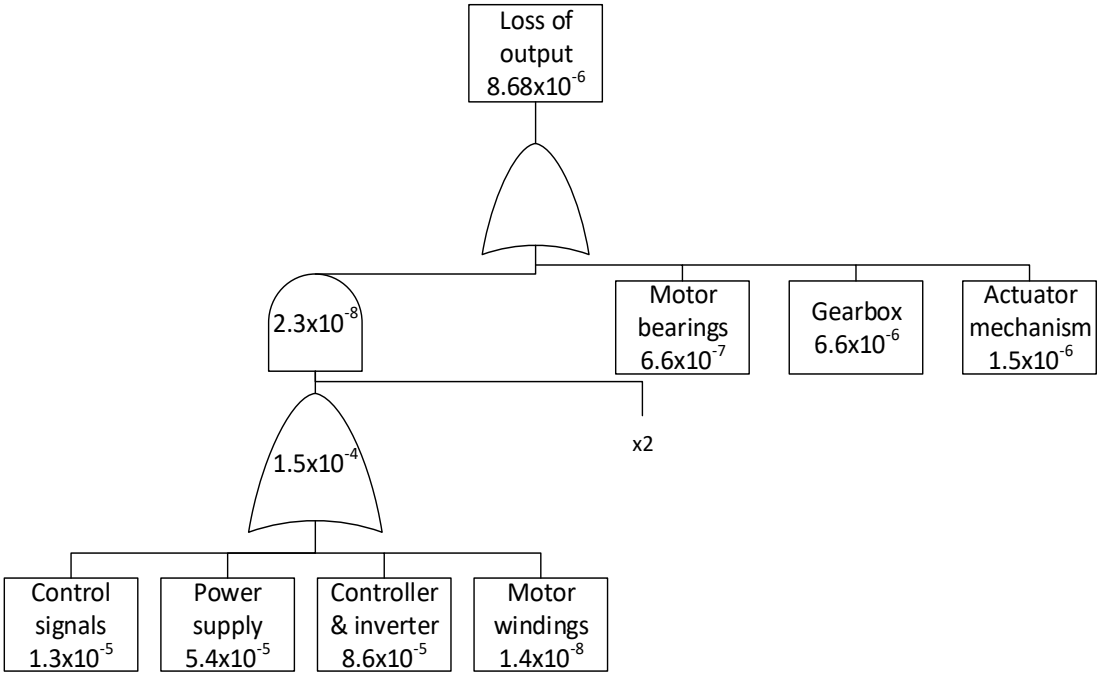

Figure 9. EMA Fault Tree with Dual Lane Fault Tolerant Electric Drive (Bennett et al. 2011). *Reproduced by permission of the Institution of Engineering & Technology.*

Providing fail operational behaviour for the mechanical components of the EMA is less well developed and summarised in the following sections.

2.1.1.1 Anti-Jamming EMAs

There have been a few EMA designs which have factored in mechanical modifications in an attempt to prevent jamming.

(i) Cronin (1985) proposed an EMA system with hydraulic coupling as a means to protect against mechanical jamming. The proposed arrangement included an EMA connected to a control surface through an EHA (without a pump). The backup EHA exerted the same amount of force as the primary EMA, however, such an arrangement adds significant weight and complexity to the overall system thus deeming such a solution unsuitable for implementation to safety critical aircraft actuation systems.

(ii) More recently, Nguyen, Behar and Mckay (2014) proposed an EMA design for jam tolerance, which incorporates a damper assembly that becomes coupled to the output rod (connected to the moveable surface) during the event of a mechanical jam. This in turn decouples the ballnut from the output rod. The damper system ultimately enables a passive, controlled rate return of the EMA output to a fail-safe position along with a latch that holds the position (within a fail-safe mode). The overall process relies on a complex mechanical arrangement which may in turn require additional scheduled maintenance actions and possibly condition monitoring.

2.1.1.2 Dual Redundancy EMAs

There have also been EMA design considerations with built-in redundancy in the event of ballscrew jamming.

(i) Collins and Sunstrand (2004) proposed a dual actuator system acting on a single flight control surface over a summing lever. The summing lever position corresponds with the sum of the positions of the actuators attached to it. Jamming of one of the actuators would require the other actuator to compensate for the malfunctioning one in order to bring the flight control surface to a neutral position. The proposed design would include two EMAs and a link arm, which not only adds weight but increases design complexity.

(ii) There is current research by Triumph Actuation Systems U.K Limited, in collaboration with Kugel Motion Limited and Nema Limited, looking into High Availability Redundant Actuation Systems (HARAS) since November 2015 (Triumph Actuation Systems - U.K, Ltd., 2015). The research programme is specific to developing fault tolerant electrical actuation solutions for primary flight control systems on Unmanned Aerial Vehicle (UAV). This initiative indicates that there is still an industry need to implement EMAs for flight safety-critical systems.

Aside from achieving a jam-tolerant EMA system, aircraft manufacturers face other technical challenges for EMA implementation to flight safety critical systems. Todeschi (2011) highlights constraints in installation of EMAs (for flight control systems) whereby space may be limited to accommodate a complex EMA system architecture. Todeschi (2011) also emphasised that weight would be another constraint during the design phase as well as design complexity which could impact maintenance scheduling and introduce further health monitoring. Given the criteria described by Todeschi (2011), the designs presented for anti-jamming EMAs could bring about operator concerns on reliability, weight and implementation.

Following the review of anti-jamming and dual redundancy EMAs, it can be concluded that fault tolerant EMAs are at an early stage with work to develop a redundant system for aircraft safety critical systems still ongoing.

2.1.2 Fault Diagnostics

Fault diagnostics is an element in the broader topic of Prognostics and Health Monitoring (PHM), involving the process of identifying an instance of a component or system behaviour that is different from the expected behaviour and locating the origin and cause of that behaviour. PHM takes this further by attempting to provide insight into a component's health, and determine its Remaining Useful Life

(RUL); PHM can thus increase availability by reducing unscheduled removals and reducing downtime, ultimately reducing Direct Maintenance Costs (DMC) (Jennions, 2012).

There have been several research projects exploring fault diagnostics to detect the onset of ballscrew jamming both within academia and industry. The following sections evaluate the progress made in fault diagnostics (for mitigating EMA jamming) considering the main approaches to developing the features correlated to damage i.e. modelling approaches, data-driven (experimental) approaches and hybrids of both.

2.1.2.1 Model-based Approaches

Modelling of a system to understand the physics of failure by monitoring system parameters is viewed as a cheaper alternative and is less time consuming and labour intensive compared to building a corresponding test stand. Figure 10 provides an overview of the processes involved in a model-based approach in the context of diagnosing system health.

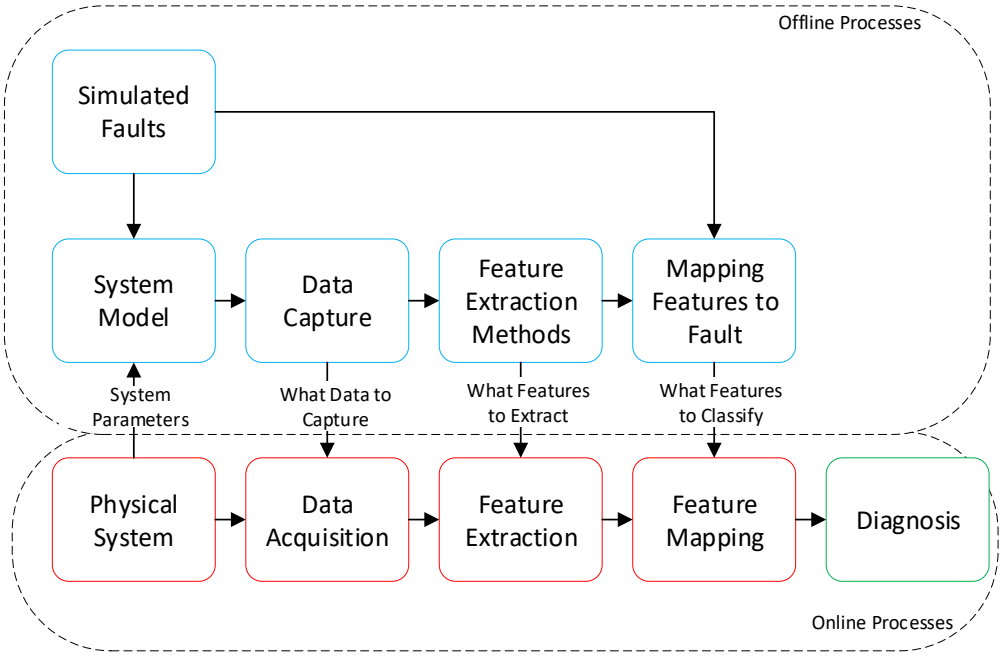

Figure 10. Model-based Approach.

A model-based approach through high fidelity modelling of an EMA system for fault detection and failure prediction is considered to be a useful preliminary step in understanding system behaviour under normal and abnormal conditions (Byington and Stoelting, 2004). Modelling an EMA system in detail can enable the prognostics design engineer to trace back failure modes to relatable physical system parameters thus providing the engineer with helpful diagnostic information. Two examples are as follows:

(i) Byington and Stoelting (2004) presented a model-based approach to PHM for EMAs on flight control actuators. The methodology was centred around diagnosing failures associated to the motor, gear slippage and bearings. Failures were selected based upon the highest number of

occurrences from in-service events. A mathematical dynamic model of the EMA system was developed using Matlab/Simulink, which was linked to the physical processes that drive the health monitoring of the EMA. This included emphasis on modelling friction coefficients at key elements of the EMA drivetrain such as the motor, gearbox and ballscrew. This was varied to understand the impact on response time, motor current and load.

(ii) Maggiore, Vedova, Pace and Desando (2014) developed a Matlab/Simulink model of an EMA system to be utilised for fault analysis associated with mechanical failures due to progressive wear; this included friction, backlash, coil short circuit and rotor static eccentricity. The research was focused on characterising and building system-representative models for these failure modes. The modelled EMA system was typical of an arrangement for a primary flight control system comprising a control and power drive electronics, a Brushless Direct Current (BLDC) motor, gearing and a ball/rollerscrew. Motor current, angular speed and position were the parameters being monitored. Subsequent failure maps were derived for fault detection/evaluation based on simulations of the different types of failures.

A high fidelity and exhaustive model of the system features can enable identification of parameters that are associated with the build-up of a specific failure mode. This can therefore allow utilisation of parametric estimation for diagnostics application and state of health estimation, however, this is dependent on the level of modelling effort and granularity.

Whilst modelling is a useful means to get an initial perspective of a system, it is never a 'true' representation of the actual behaviour. For instance, Byington and Stoelting's (2004) approach utilised variation of friction coefficients as a means to perform sensitivity analysis to evaluate mechanical losses in the drivetrain. The reality, however, is that friction is prevalent in many areas of the drivetrain, therefore, it would be difficult to ascertain the location of the friction build-up. It would require one to quantify the amount of mechanical losses attributed due to friction by mitigating the effects of external loads, backlash and any other unwanted non-linear effects. It is therefore imperative that in the case for modelling the physics of failure behind ballscrew jamming, a more robust approach is taken in terms of modelling wear and friction by considering the main areas of friction within such systems.

Maggiore et al. (2014) gave importance to the build-up of friction as a pre-cursor to the onset of jamming. The corresponding failure maps of motor current provided useful information in terms of evaluating friction torque at a system level by assigning thresholds for the onset of a failure. It, however, was not clear whether friction monitoring at local levels for the main contact regions in the ballscrew (ball and nut, and ball and screw) could be characterisable, especially when trying to diagnose for jamming faults from these contact areas.

2.1.2.2 Data-Driven Approaches

Data-driven approaches to fault diagnostics can be split up into two methods:

(a) Retrieving data from a real application such as an in-service EMA;

(b) Retrieving data from a representative test stand.

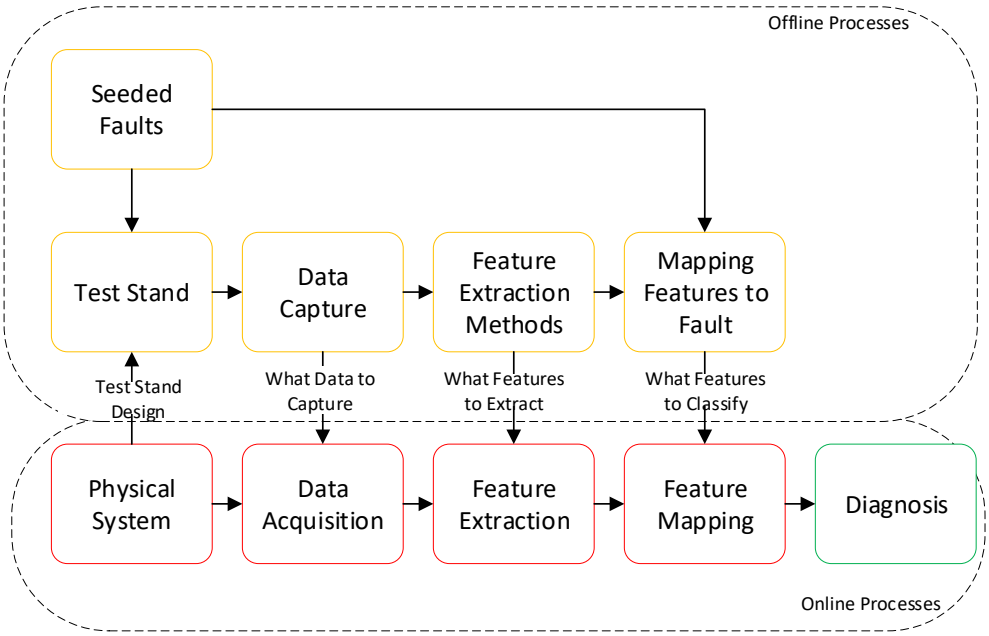

Figure 11. Data-Driven Approach.

Obtaining data from an in-service EMA may be as advantageous as the information generated will be a true representation of the application usage profile and system behaviour. By this, aerodynamic loads and other environmental effects are factored in. The issue, however, is the limited quantity of data obtained. Aircraft manufacturers and operators are reluctant to have additional sensing due to added weight implications and reliability (Donald, Garg, Hunter, Guo & Semega, 2004), thus requiring diagnostics engineers to isolate a problem like jamming within the EMA drivetrain based on existing sensor signals alone. Such an approach, however, is considered within a PHM framework through a combination of physical modelling and test stand data, which is discussed later in this chapter.

The building of a bespoke EMA test stand can enable run-to-failure tests as well as seeded failure tests to be performed. The advantage here is that more sensors can be added to improve the understanding of the system behaviour as well as characterise different types of failures modes. A significant amount of research has been conducted in this area with particular focus on seeded failure tests to EMA test stands.

(i) Bodden et al. (2007) seeded contaminant to an EMA test stand and cycled it until failure. The amount of debris was the key parameter for setting the rate at which jamming would occur. A measure of actuator efficiency was quantified by taking the ratio of power output and power

input of the system. It was found that as heat and vibration energy increased, the power input to the system increased and therefore increased the motor current demand. The test stand was also fitted with other sensors in order to identify other pre-cursors such as temperature and vibration in addition to motor current. Temperature readings were recorded (thermistors mounted on the rear of the motor housing) with increased temperatures observed which were attributed to the higher level of friction in the system due to the induced debris. Such readings, however, were not characterisable against the nature of the simulated fault therefore making it difficult to isolate the actual location of the increased friction in reality.

(ii) An EMA test stand was built with airworthy equipment in which in-flight data was post processed on the ground (Balaban, Saxena, Goebel, Byington, Watson, Bharadwaj & Smith, 2009b). This followed the philosophy of taking the data off aircraft and performing prognostics on the ground. Jamming faults were simulated on the test stand with results showing good agreement with developed thermal and mechanical models. The issue, however, was the abrupt nature in which the jamming occurs making it challenging to design a prognostics algorithm based on such data. Using the same test stand, Balaban, Saxena, Narasimhan, Roychoudhury, Goebel and Koopmans (2010) also introduced spalling to the ballscrew to understand the effects on the system response of the EMA. Indentations were created in the test ballscrew at high stress contact points at dimensions of 0.3 mm depth and widths ranging from 0.3-0.5 mm to evaluate how the size of the initial spall affects the nature of its growth. An accelerometer was fitted to the nut of the ballscrew to monitor the frequency of the system. The results showed that there was increased vibration in the ballscrew due to the induced spalling.

Unless certain fault modes can be characterised through EMA test stand analysis, it may be challenging to isolate and identify a particular fault mode such as ballscrew jamming.

Additionally, the failure analysis conducted through experimental analysis has largely involved simulating faults. By this, faults were artificially implemented through seeding debris and introducing structural damage to the ballscrew. Run-to-failure tests are an effective means to obtain data corresponding to naturally occurring faults. However, this can be time consuming and expensive, particularly when trying to obtain data for ballscrew jamming, as other failure modes may manifest in performing run-to-failure tests.

2.1.2.3 Hybrid Approach to Fault Diagnostics

The methods discussed so far have considered a modelling approach or a data-driven approach in isolation. Narasimhan, Roychoudhury, Balaban and Saxena (2010) explained that a modelling approach works well for deriving analytical models for specific faults only. The data-driven approach requires a lot of data under varying experimental conditions for training a classifier. Furthermore, the classifier

would need to consider all types of faults and other conditions, therefore increasing the size and complexity of the classifier.

A hybrid approach to fault diagnostics would entail employing a detailed model of an EMA system against an equivalent physical EMA system to capture any discrepancies from normal behaviour. This would then enable identification of faults prompting further investigation.

Narasimhan et al. (2010) presented a hybrid diagnostic approach that involved the fusion of model-based and data-driven based methods. The data-driven method was based on the previously built flyable EMA test stand by Balaban et al. (2009a). A top-level diagram of the hybrid approach followed is shown in Figure 12.

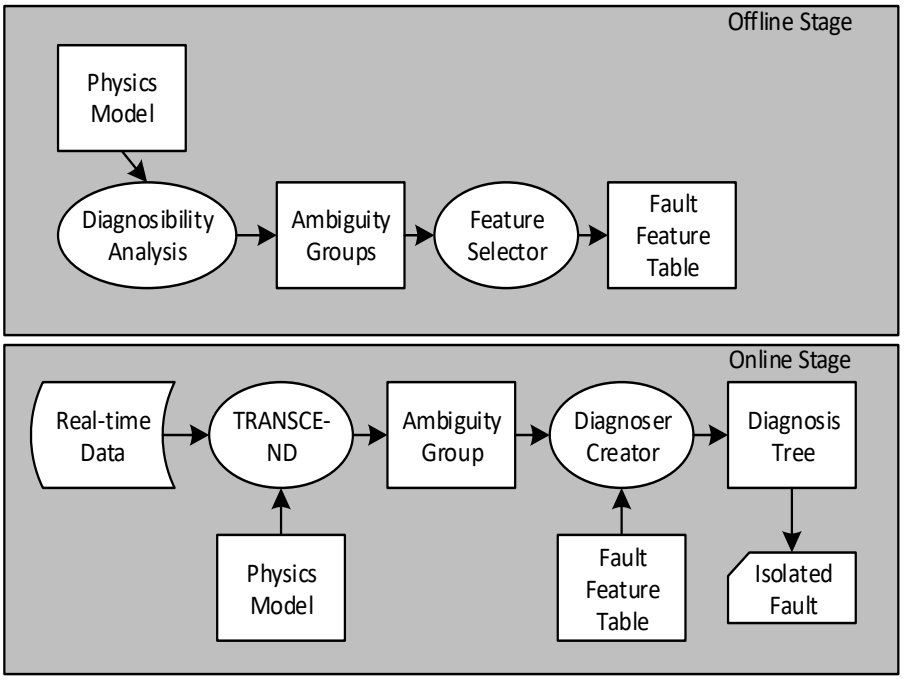

Figure 12. Hybrid Diagnostics (Narasimhan et al. 2010). *Reproduced by permission of the Prognostics and Health Management Society.*

The hybrid diagnostics approach presented by Narasimhan et al. (2010) not only combined model-based and data-driven methods, but considered offline and online stages in the diagnostic process. The offline stage involved use of an EMA system physical model to generate repeatable fault signatures, which were then categorised into fault feature tables. The online stage utilised real-time data (from the flyable EMA test stand) from which anomalies were detected and isolated using the physical model before classifying ambiguity groups.

Saxena (2010) provided a holistic view of the PHM processes whereby the online modules involve a sequence of data acquisition and manipulation, state detection, health assessment, prognosis assessment and decision making. Emphasis is given to what can be learned from the offline modules.

The offline modules are dependent on a fusion of data from experimental analysis and system modelling. A data fusion approach can be seen as advantageous as the combination of modelling and data-driven analysis can help to isolate and identify certain types of faults by comparing predicted and observed system behaviour.

There are limitations in obtaining in-service EMA data due to manufacturers' concerns around reliability and the addition of more sensors, due to space and weight constraints (Donald et al, 2004). Therefore, in the context of mitigating EMA ballscrew jamming, a combination of a high fidelity EMA model and extraction of relevant test stand data is proposed as the optimal approach in performing fault diagnostics for this case.

Following a review of existing approaches to EMA fault diagnostics, a bespoke approach for ballscrew jamming mitigation has been proposed as illustrated in Figure 13. Critically, the parallel test stand and simulated system models provide complimentary functions: the test stand providing true behaviours for a limited number of conditions that can be used to tune the system model, which in turn can provide simulations of broad ranging operational conditions.

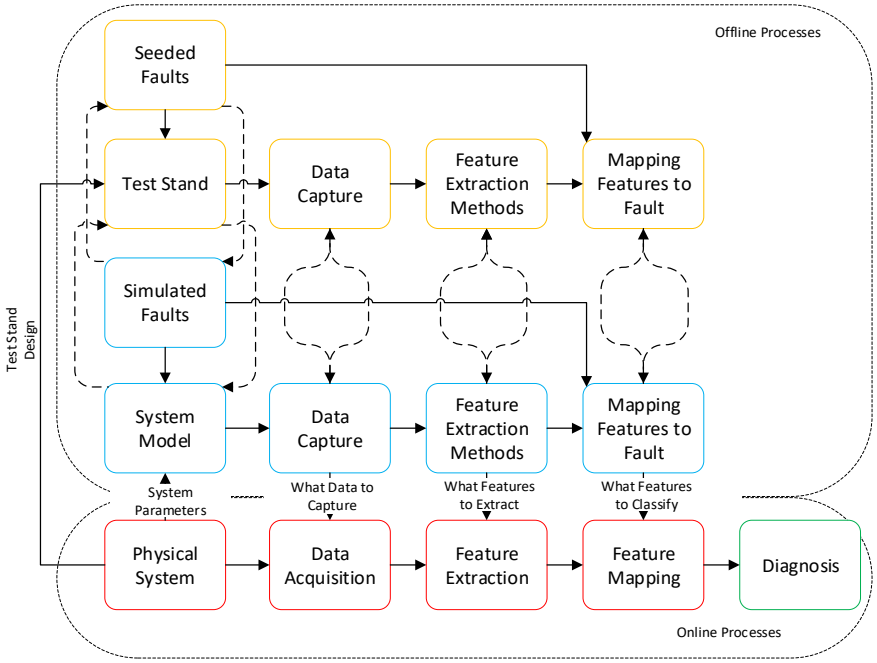

Figure 13. Hybrid Approach to EMA Fault Diagnostics.

2.2 Existing Challenges in Mitigating EMA Ballscrew Jamming through Fault Diagnostics

The combination of a model-based and data-driven approach can improve the overall prediction accuracy, therefore, a hybrid approach to fault diagnostics of the EMA jamming case was considered to be the optimal approach. The success of the hybrid approach would, however, still relies on the robustness of the modelling and data generated from an EMA test stand and/or real application. This section highlights challenges which need to be addressed in trying to create a more robust fault diagnostics algorithm.

2.2.1 Challenges for Data-Driven Approaches

Most reported examples have used seeded fault tests to EMA ballscrews by introducing debris as well as physical damage to the screw. Technical challenges were identified in trying to characterise fault modes from seeded faults as well as reproducing more realistic fault cases. These challenges are further described in the following sub-sections.

2.2.1.1 Ballscrew Thermal Expansion

Previous research has investigated the effects of seeding debris and damage to the ballscrew to simulate wear. Consideration should also be given to simulate the effects of ballscrew ball deformation due to thermal expansion. The balls within the ballnut of a ballscrew system can undergo thermal expansion due to heat caused by friction (Jeong & Park, 1992). This can lead to a degradation in performance and positioning accuracy. Jeong & Park (1992) demonstrated this with temperature variations due to different ballnut preloads and Thermal Contact Conductance (TCC) using finite difference methods.

Such conditions could be considered in test stand analysis by seeding deformed or appropriately larger balls in the ballscrew to simulate and evaluate the effects of ball deformation due to thermal expansion.

2.2.1.2 Seeded Failure Tests

Whilst useful information can be obtained from simulating seeded faults to a healthy actuator (Balaban et al, 2009b) limitations still exist in understanding the true nature from which a particular failure mode may initially manifest. Therefore, more run-to-failure tests could be conducted to learn from naturally occurring faults and to validate seeded fault test results. This should include the re-use of older actuators that would have started to exhibit wear and degradation naturally from in-service application. This could enable the distinguishing and characterisation of properties for systems with lower mechanical efficiencies as well as to validate seeded fault test results.

2.2.2 Challenges for Model-Based Approaches

In the reviews of previous research, a clear theme emerged that a high-fidelity approach is required for model-based approaches to identify the onset of ballscrew jamming. The following sub-sections highlight areas where limitations currently exist in modelling EMA systems for fault diagnostics based investigations.

2.2.2.1 Gearbox Modelling

For direct drive EMA systems, the absence of gearing simplifies the analysis in diagnosing ballscrew related failures (Gerada & Bradley, 2008). For gear driven EMA systems, previous approaches have modelled the gearbox using efficiency terms to model losses. Losses in the gearbox would need to be modelled in more detail to account for non-linearities. Losses in gear systems are attributed primarily to gear tooth friction and lubrication churning losses (Schlegel, Hösl , & Diel, 2009). Detailed modelling of these losses would improve the accuracy in decomposing losses across the drivetrain.

2.2.2.2 Motor Modelling

EMA systems have been modelled mainly using simple motor models, with only a few exceptions when more complex models have been used. Simple models typically consider torque and motor current as being directly proportional without considering motor dynamic behaviour. The research conducted by Maggiore et al. (2014) provides an advancement to this by modelling a BLDC system with power drive electronics that evaluated the torque generated by the motor as a function of the voltages generated by a 3-phase electrical power regulator. For future model-based approaches, it is proposed that the modelling could consider Field Oriented Control (FOC) techniques, which can capture magnetic behaviour. FOC can be applied where 3-phase AC quantities (I_a, I_b, I_c) can be reduced to DC quantities (I_d, I_q) using Park's transform (Park, 1929).

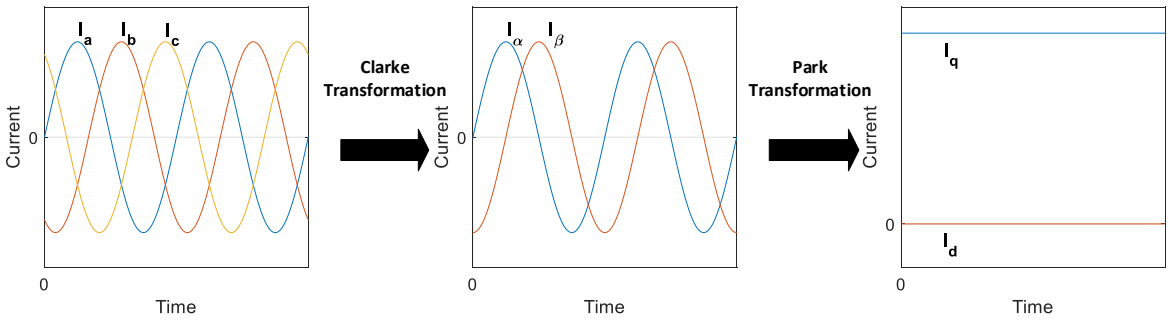

Figure 14. 3-phase to 2-phase Stationary and 2-phase Stationary to 2-phase Rotating Reference Frame.

This can enable simplified analysis by reducing AC quantities to DC quantities whilst still capturing motor dynamics (such as inductance saliency) for condition monitoring and fault detection within the EMA drivetrain. Whilst FOC modelling can be used for EMA condition monitoring through analysing time series I_q currents, there may be limitations in correctly diagnosing the origin of a fault if analysing the I_q current signal alone. This approach also relies on the accurate estimation of rotor angle position.

2.2.2.3 Ballscrew Kinematics

Buildup of friction is considered a pre-cursor to EMA ballscrew jamming (Balaban, et al., 2009b). Model-based approaches have often parameterised friction through industry standard coefficients. It is therefore proposed that modelling the main areas of friction within the ballscrew (ball and nut, and ball and screw (Vahid-Araghi & Golnaraghi, 2011)) to a high fidelity could improve the characterisation of such features for fault detection. This could be achieved by modelling the ballscrew kinematics in more detail by considering the ball and nut, and the ball and screw interactions as shown in Figure 15.

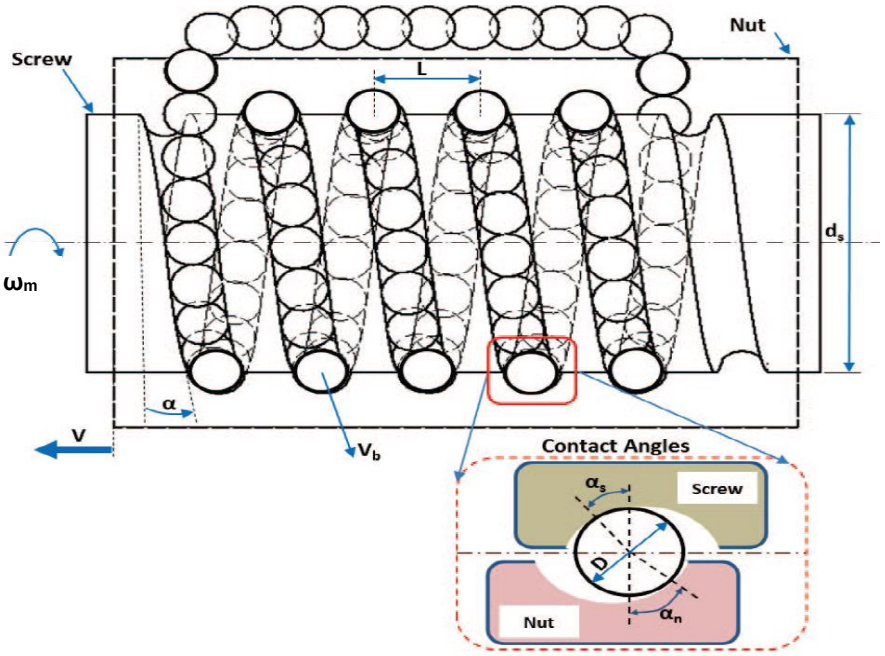

Figure 15. Ballscrew Kinematics (Ismail, Balaban, & Spangenberg, 2016). *Reproduced by permission of the Institute of Electrical and Electronics Engineers (IEEE).*

This can enable a more accurate representation of the contact mechanics between the ball and nut, and ball and screw and also consider the effects of slip.

2.3 EMA Failure Analysis

Conducting a detailed failure analysis of a linear EMA could enhance the understanding of how it fails. In general, specialised failure analysis engineers would determine the root cause of a failure to prevent it from happening and thus improve the performance and reliability. As part of the systems approach

being taken for this research, failure analysis can be conducted for this EMA, which involves the full decomposition of the component followed by the listing of as many failure modes as possible of each sub-item followed by the effects at a local, equipment and system level. This is presented along with the anticipating features which could become apparent at the onset of a failure thus enabling options for possible prognostics techniques. The analysis in this section intends to pave the way to identify the most frequently occurring and the most critical failure mode and to also analyse the existing sensing arrangements to determine the precursors for each failure. This will aid the understanding of health as these are the key attributes in extracting the most appropriate data features and parameters in the development of a fault diagnostics algorithm.

2.3.1 EMA Parts Decomposition and Corresponding Failures and Effects

Tables 2 – 3 shows all the different types of failures modes for associated EMA parts for a linear ballscrew system based on previously published work by Balaban et al. (2009a). Additional columns have been included to show the effects of these failures at a local and system level, the type of failure in terms of degrading or abrupt, precursors and possible health monitoring solutions based on available sensors.

Table 2 shows the failure modes for the mechanical assembly with focus on the ballscrew assembly – ballscrew, ballnut, ball return(s) and balls. The corresponding ballscrew assembly parts were collected from analysis previously conducted by Balaban et al. (2009a). Table 3 shows the failure modes for a motor system. The corresponding motor assembly parts were collected from analysis previously conducted by Balaban et al. (2009a). As mentioned in Section 2.1.1, EMAs on an aircraft system would have multiple back-up motors in the event of one failing, therefore, there would be sufficient redundancy against a single point of failure.

Table 2. Mechanical Assembly Failure Modes.

Part (Balaban et al. 2009a)	Failure Mode (Balaban et al. 2009a)	Effects		Failure Type (Degrading/ Abrupt)	Precursors	Possible Health Monitoring Techniques
		Local Level (Balaban et al. 2009a)	System Level			
Ballscrew	Spalling	Increased noise and vibration	Slower extension-retraction times	Degrading	Misalignment, increased friction and vibration, and slower extension-retraction times.	Actuator efficiency analysis through motor current.
	Excessive wear/backlash	Increased noise and vibration, severe backlash	Slower extension-retraction times	Degrading	Misalignment, increased friction and vibration, and slower extension-retraction times.	Actuator efficiency analysis through motor current.
Ballnut	Spalling	Increased noise and vibration	Slower extension-retraction times	Degrading	Increased friction and vibration, and slower extension-retraction times.	Actuator efficiency analysis through motor current.
	Backlash	Increased noise and vibration, severe backlash	Slower extension-retraction times	Degrading	Misalignment, increased friction and vibration, and slower extension-retraction times.	Actuator efficiency analysis through motor current.
	Binding/sticking	Ballnut does not rotate on screw	Loss of extension-retraction	Abrupt	Misalignment, and increased friction and vibration	Abrupt failure, however, motor current analysis could identity precursors

Part (Balaban et al. 2009a)	Failure Mode (Balaban et al. 2009a)	Effects		Failure Type (Degrading/ Abrupt)	Precursors	Possible Health Monitoring Techniques
		Local Level (Balaban et al. 2009a)	System Level			
	Bent	Ballnut does not rotate on screw	Loss of extension-retraction	Abrupt	Misalignment, binding/sticking, and increased friction and vibration	Abrupt failure, however, motor current analysis could identity precursors
Ball Return(s)	Jamming	Ballnut does not rotate on screw	Loss of extension-retraction	Abrupt	Binding/sticking, and increased friction and vibration	Abrupt failure, however, motor current analysis could identity precursors
Bearings	Spalling	Increased noise and vibration, metal flakes separating	Slower extension-retraction times	Degrading	Misalignment, increased friction and vibration, and slower extension-retraction times.	Actuator efficiency analysis through motor current.
	Binding/Sticking	Jamming of bearing	Loss of extension-retraction	Abrupt	Misalignment, and increased friction and vibration	Abrupt failure, however, motor current analysis could identity precursors
	Corrosion	Increased noise and vibration, metal flakes separating, leading to jamming	Slower extension-retraction times	Degrading	Foreign object contamination, increased friction and vibration, and slower extension-retraction times.	Actuator efficiency analysis through motor current.

Part (Balaban et al. 2009a)	Failure Mode (Balaban et al. 2009a)	Effects		Failure Type (Degrading/ Abrupt)	Precursors	Possible Health Monitoring Techniques
		Local Level (Balaban et al. 2009a)	System Level			
	Backlash	Increased vibration and disintegration	Slower extension-retraction times	Degrading	Increased friction and vibration, and slower extension-retraction times.	Actuator efficiency analysis through motor current.
Dynamic Seals	Wear	Increased vibration	Slower extension-retraction times	Degrading	Increased friction and vibration, and slower extension-retraction times.	Actuator efficiency analysis through motor current.
	Structural failure	Increased vibration and disintegration	Slower extension-retraction times	Abrupt	Increased friction and vibration, and slower extension retraction times.	Abrupt failure, however, motor current analysis could identity precursors
Static Seals	Structural failure	Increased vibration and disintegration	Slower extension-retraction times	Abrupt	Increased friction and vibration, and slower extension retraction times.	Abrupt failure, however, motor current analysis could identity precursors
Balls	Spalling/deformation	Increased vibration, metal flakes separating, leading to jamming	Slower extension-retraction times	Degrading	Foreign object contamination, increased friction and vibration, and slower extension-retraction times.	Actuator efficiency analysis through motor current.

Part (Balaban et al. 2009a)	Failure Mode (Balaban et al. 2009a)	Effects		Failure Type (Degrading/ Abrupt)	Precursors	Possible Health Monitoring Techniques
		Local Level (Balaban et al. 2009a)	System Level			
	Excessive wear	Backlash	Slower extension-retraction times	Degrading	Misalignment and increased vibration, and slower extension-retraction times	Actuator efficiency analysis through motor current.
Mountings	Structural failure: Crack(s), play	Increased vibration and disintegration	Slower extension-retraction times	Abrupt	Misalignment, increased vibration.	Abrupt failure, however, motor current analysis could identity precursors
Lubricant	Contamination	Increased vibration and disintegration	Slower extension-retraction times	Degrading	Foreign object contamination, increased friction and vibration, and slower extension-retraction times	Actuator efficiency analysis through motor current
	Run-dry	Increased vibration, metal flakes separating, leading to jamming	Loss of extension-retraction	Abrupt	Foreign object contamination, increased friction and vibration	Abrupt failure, however, motor current analysis could identity precursors

Table 3. Motor Assembly Failure Modes.

Part (Balaban et al. 2009a)	**Failure Mode (Balaban et al. 2009a)**	**Effects**		**Failure Type (Degrading/ Abrupt)**	**Precursors**	**Possible Health Monitoring Techniques**
		Local Level (Balaban et al. 2009a)	**System Level**			
Connectors	Intermittent contact	Disconnection	Loss of motor, extension-retraction function by back-up motors	Abrupt	Increased vibration and intermittent operation	Abrupt failure, however, intermittent operation trend monitoring could identify precursors
Stator	Stator coils fail open	Coil failure	Loss of motor, extension-retraction function by back-up motors	Abrupt	Increased vibration and temperature	Abrupt failure, however, motor temperature monitoring could identify precursors
	Insulation deterioration/ wire chafing	Short circuit	Loss of motor, extension-retraction function by back-up motors	Degrading[2]	Increased temperature	Motor temperature monitoring
Resolver	Coils fails open	Coil failure	Loss of motor, extension-retraction function by back-up motors	Abrupt	Increased vibration and temperature	Abrupt failure, however, motor temperature monitoring could identify precursors

[2] While some faults develop over an extended period, the onset of noticeable effect will be abrupt.

Part (Balaban et al. 2009a)	Failure Mode (Balaban et al. 2009a)	Effects		Failure Type (Degrading/ Abrupt)	Precursors	Possible Health Monitoring Techniques
		Local Level (Balaban et al. 2009a)	System Level			
	Intermittent coil failures	Coil failure	Loss of motor, extension-retraction function by back-up motors	Abrupt	Increased vibration, temperature and intermittent operation	Abrupt failure, however, temperature and intermittent operation trend monitoring could identify precursors
	Insulation deterioration / wire chafing	Short circuit	Loss of motor, extension-retraction function by back-up motors	Degrading[3]	Increased temperature	Motor temperature monitoring
Rotor and Magnets	Rotor-magnets chemical bonds deterioration	Complete magnet separation leading to motor failure	Loss of motor, extension-retraction function by back-up motors	Degrading[3]	Misalignment, and increased vibration and temperature	Motor temperature monitoring
	Rotor eccentricity	Support bearing failure	Loss of motor, extension-retraction function by back-up motors	Abrupt	Misalignment, and increased vibration, temperature and friction	Abrupt failure, however, motor temperature monitoring could identify precursors

[3] While some faults develop over an extended period, the onset of noticeable effect will be abrupt.

2.3.2 EMA Failures with Corresponding Criticality Index

Table 4 shows all the EMA failure modes (as presented in Section 2.3.1) against corresponding probability of occurrence and severity scores as devised by Balaban et al. (2009a). These two values are multiplied to get the Criticality Index (FMEA-FMECA, 2006). Loss of motor function was deemed as non-safety critical due to back up redundancy, therefore, this section focuses solely on the mechanical assembly.

Table 4. Mechanical Assembly Failure Modes and Criticality Index.

Part	**Failure Mode**	**Relative Occurrence (1 – 10, low to high)**	**Relative Severity (1 – 10, low to high)**	**Criticality Index**
Ballscrew	Spalling	5	3	15
	Excessive wear/backlash	7	3	21
Ballnut	Spalling	5	3	15
	Backlash	7	3	21
	Binding/sticking	3	3	9
	Bent	1	5	5
Ball return(s)	Jamming	5	8	40
Bearings	Spalling	5	3	15
	Binding/Sticking	2	4	8
	Corrosion	2	5	10
	Backlash	7	3	21
Dynamic seals	Wear	4	6	24
	Structural failure	3	8	24
Static seals	Structural failure	2	8	16
Balls	Spalling/deformation	5	3	15
	Excessive wear	7	5	35
Mountings	Structural failure: Crack(s), play	1	7	7
Lubricant	Contamination	8	5	40
	Run-dry	3	10	30

As can be seen from Table 4, the failure modes with the highest Risk Priority Number (RPN) are Ball return(s) jamming (40), Lubricant Contamination (40) and Ball Wear (35).

2.3.3 EMA Failure Analysis Findings

The EMA failure and RPN analysis has shown that mitigating ballscrew jamming in the ball return(s) is of highest importance given that it is a failure mode that could lead to a complete loss of function. Health monitoring to identify the precursors of this failure is possible, however, as discussed in Section 2.1, due to the conservative nature of the aerospace industry, sensing is limited to diagnosing such failure through motor current only (Donald et al., 2004).

2.4 Industrial Experience of EMA Ballscrews

So far, a review of literature and engineering failure analysis of EMAs has revealed insightful information relating to EMA failures. It has re-emphasised the importance of identifying the onset EMA ballscrew jamming through fault diagnostics to make EMAs a more viable solution for safety critical applications in aerospace systems. This section intends to gather industrial experience of EMA ballscrews from repairers, designers and manufacturers through semi-structured interviews.

Semi-structured interviews are a method of qualitative soft systems research (Edwards & Holland, 2013). The objective of such interviews is to maintain a theme around a particular research topic and also allow flexibility for digression and a more open discussion.

For the semi-structured interviews, ballscrew repairers were targeted as interview candidates, as it was felt that repairers could provide first-hand practical insight in to the types of ballscrew failures encountered from industry and could offer information relating to potential root causes with respect to the human factor element. The ballscrew repairers were also requested to comment on their perception on the topic of fault diagnostics and prognostics and what the existing limitations and challenges were. Designers and manufacturers were also seen as valuable interview candidates to obtain views about design evolution against certain ballscrew failures as well as collecting views about performing fault diagnostics and prognostics for critical failures. In summary, the following topics were covered during the semi-structured interviews:

1. Types of ballscrew failures;
2. Most common type of ballscrew failures;
3. Most critical type of failure;
4. Ballscrew failure root causes;
5. Comments on existing sensing solutions;
6. Perceptions of fault diagnostics and prognostics to mitigate ballscrew jamming across different industries and applications.

Three semi-structured interviews were conducted with the following United Kingdom based ballscrew companies:

i. 'The Ballscrew Company' on 23rd October 2017;
ii. 'Kugel Motion Limited' on 27th October 2017;
iii. 'Ballscrew Services Limited' on 5th December 2017.

Their responses are summarised in the following subsections.

2.4.1 The Ballscrew Company

The Ballscrew Company is a company that specialises in the repair of ballscrew and linear guides for industrial applications (The Ballscrew Company, 2017). Dave Hughes was the technical representative from The Ballscrew Company who assisted in sharing their industrial experience with ballscrew failures. Due to constraints in time and travel, the interview was conducted through email correspondance.

On the types of ballscrew failures encountered:

The Ballscrew Company has received faulty ballscrews with broad ranging issues including ball track wear, backlash, ball wear, loss of preload, misalignment and jamming.

On the most common type(s) of ballscrew failures encountered:

Ball wear was noted to be the most common type of ballscrew failure. This has resulted in secondary failures such as increased backlash and loss of preload.

On the most critical type(s) of ballscrew failures encountered:

Ball rupture/breakage was the most critical failure which has led to ballscrew jamming and eventual system breakdown.

On ballscrew failure(s) root cause investigations:

The Ballscrew Company does evaluate the reasons for failure when ballscrews arrive for repair. The most common reason for failure was due to lack of maintenance. Examples include issues in using lubrication whereby the user uses to much lubricant or too less lubricant leading to run-dry conditions. There have also been operator errors in overriding machine parameters, which has resulted in thrust bearing collapse causing ballnut to run eccentric thus damaging the ballscrew to beyond repair.

On whether existing sensing solutions are fit for purpose:

Existing sensors were viewed as not being at fault. The problem is more associated to the lack of preventive maintenance due to the pressure and demands of production. More robust sensing could be

seen as beneficial (if used correctly), however, may not be seen a favourable strategy by the production managers.

On the use of fault diagnostics and prognostics to mitigate ballscrew jamming (in industrial applications i.e. CNC machines, 3D printers):

In such events, abrupt seizures like ballscrew jamming would result in shutting down the controller and not over compensating the system – this is viewed as the best form of health monitoring.

The Ballscrew Company does not receive many repair requests from the aerospace industry and, therefore, did not comment further on ballscrew jamming mitigation using health monitoring techniques.

2.4.2 Kugel Motion Limited

Kugel Motion Limited is a company that specialises in the design, manufacture, after sales service and repair of ballscrews and rollerscrews for industrial, aerospace and automotive applications (Kugel Motion Limited, 2018). As mentioned in Section 1.3.1.2, Kugel Motion Limited is also involved as part of a research collaboration to develop a dual redundancy EMA for use on primary flight control systems on UAVs. Alexander O'Neill is the Managing Director of the company and was able to share Kugel Motion Limited's experiences with ballscrews from various perspectives including design, manufacture and workshop repair.

On the types of ballscrew failures encountered:

Kugel Motion Limited has mainly encountered ballscrew failures from industrial applications. The types of failures include misalignment, brinelling and ballscrew wear. These were viewed as the most common type of ballscrew failure. Ballscrew jamming has also been encountered.

On the most critical type(s) of ballscrew failures encountered:

Alexander elaborated on the ballscrew failures already mentioned and described the secondary effects following these occurrences. Ballscrew misalignment had caused 'top and tailing' which had led to generation of excessive loads and therefore premature failing of the ballscrew through material fatiguing. Ballscrew brinelling had resulted in excessive vibration, which eventually leads to excessive loads to point beyond the bearings and ballnut can handle in terms of operating speed. Ballscrew wear occurred through life usage mainly in the ball track and balls resulting in fatigue. Reported jamming cases had caused subsequent system seizure and breakage.

On ballscrew failure(s) root cause investigations:

Root cause evaluations have revealed that misalignment problems have most often arisen because of improper installation by the customer. Ballscrew brinelling has generally manifested due to impact damage which, again, was attributed to improper installation by the customer as well as usage from excessive loads surpassing elastic load limits. As mentioned previously, ballscrew wear occurs mainly through life usage, however, there have been some reported cases of accelerated wear due to poor maintenance i.e. insufficient lubrication. Jamming cases were reported to have been caused by either improper installation and excessive lubrication which essentially acts as debris.

On whether existing sensing solutions are fit for purpose:

Alexander mentioned that poor preventive maintenance practices and improper installation of EMA systems have most often resulted in increased downtime of equipment. Therefore, existing sensing solutions are sufficient, especially load sensing on certain industrial equipment. Load sensing is viewed as useful, however, the resolution is not very good thus making it challenging to isolate faults along the EMA drivetrain. Therefore, more sophisticated and state-of-the-art sensing is desired to detect and track gradual degradations to prevent the onset of common ballscrew failures.

On the use of fault diagnostics and prognostics to mitigate ballscrew jamming (in industrial applications i.e. CNC machines, 3D printers):

The ballscrew jamming failure mode is rarely seen on industrial applications, however, implementation of a health monitoring functionality is viewed as a favourable strategy to monitor ballscrew wear. A robust health monitoring schedule would make it easier to plan maintenance and therefore reduce equipment downtime.

On the use of fault diagnostics and prognostics to mitigate ballscrew jamming (in safety critical aerospace applications i.e. landing gear, flight control systems):

Alexander explained the importance of having a robust health monitoring solution to mitigate ballscrew jamming in aerospace safety critical applications. Ballscrews (for aerospace use) tend to be designed with more backlash, axial play and less preload to account for ball thermal expansion especially for applications that exhibit high energy and a rigorous duty cycle (Kugel Motion Limited, 2018). Given this, any debris (dust, metal flakes) can build-up within the balls and become embedded within the ball track and continue to move along the screw due to force. This build-up of debris can lead to loss of efficiency and jamming, and so it is imperative to develop a reliable and robust health monitoring functionality to identify the onset of jamming.

2.4.3 Ballscrew Services Limited

Ballscrew Services Limited is a company that specialises in ballscrew repair as well as offering like for like ballscrew replacements for industrial and aerospace applications (Ballscrew Services Limited, 2015). Joe Grey is the owner of Ballscrew Services Limited and provided his technical and industrial experience with ballscrews.

On the types of ballscrew failures encountered:

Ballscrew Services Limited has received ballscrew repair requests mainly from machine tool (i.e. CNC machines) users. Reported faults include loss of preload leading to ball wear, backlash and brinelling.

On the most critical type(s) of ballscrew failures encountered:

The loss of preload has often resulted in ballscrew stiffness which has led to loss of axial play and eventually ball wear. Joe elaborated that many of these issues, especially at an early stage, get masked by the electronics whereby the user refers to the speed/position control compensation of the motor drive to get an indication of system health. The accumulation of backlash has also led to race ball track wear. Joe also provided some samples of failed in-service ballscrews from customers to exemplify some of the problems. Figure 16 shows an example of a 20mm diameter machined ballscrew removed from a CNC milling machine. As shown in Figure 17, there is visible evidence of ball track wear and surface brinelling along the screw thread where the system had undergone most usage from frequent ball nut travel. The ballnut had only travelled a certain distance along the screw through normal operation which was evident in the visibly pristine condition of the screw ends as shown in Figure 18.

Figure 16. 20mm Diameter Ballscrew from CNC Milling Machine.

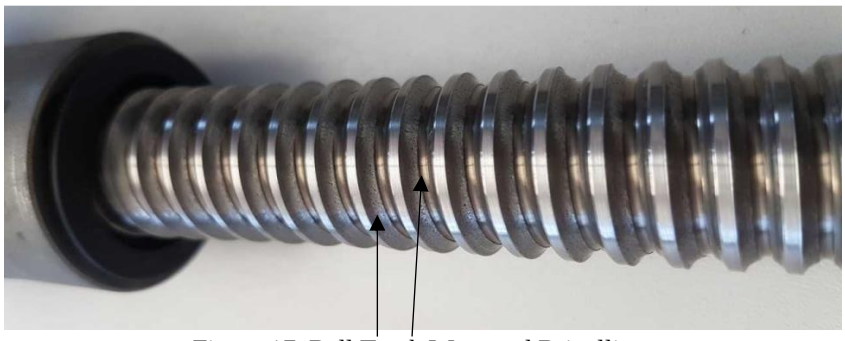

Figure 17. Ball Track Wear and Brinelling.

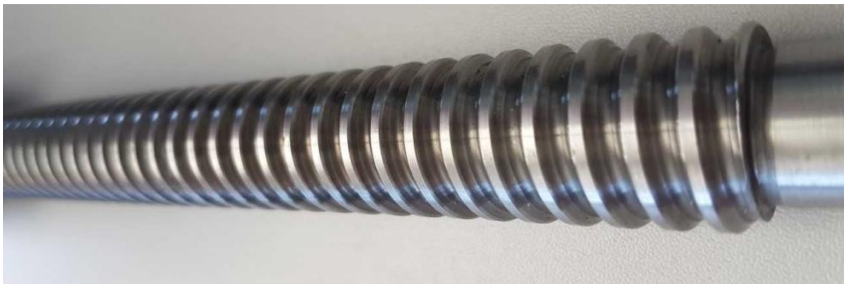

Figure 18. Ballscrew End with No Visible Track Wear.

Figure 19 shows an example of severe ballscrew corrosion. This ballscrew was removed from an industrial application where negligence in scheduled maintenance was apparent. Joe further elaborated the issue of electronics masking the problems within the mechanical drivetrain, therefore making it challenging to detect the onset of the fault using existing sensors and signals.

Figure 19.Ballscrew Corrosion.

On ballscrew failure(s) root cause investigations:

Joe described that many of these ballscrew failures have manifested themselves due to poor maintenance, and incorrect installation and usage. On poor maintenance, it was also mentioned that even if the recommended scheduled maintenance were being adhered to, the user has sometimes made errors when conducting particular maintenance tasks. An incorrect lubricant may have been used, thus going against manufacturer recommendation. For example, use of grease with suspended solid particles in high speed and low temperature applications can contribute to debris build-up and clogging in the ball return system. Excessive lubrication has also seen instances of increased ballscrew stiffness and seizure.

As mentioned previously, through customer feedback, many of the impending fault symptoms are masked by the electronics which, therefore, makes it challenging for the operator to diagnose problems within the mechanical side of the EMA drivetrain.

On whether existing sensing solutions are fit for purpose:

Joe mentioned that firstly, more could be done by the operator in better utilising the existing sensing solutions. Motor drive electronics masking a lot of the ballscrew degradation has made it challenging to isolate faults within the drive train and, therefore, more sensing is necessary to monitor vibration and

noise in the system to ascertain the ballscrew state of health and EMA efficiency. Heat generation should also be monitored in instances where excessive friction is taking place between the ballscrew mating parts.

On the use of fault diagnostics and prognostics to mitigate ballscrew jamming (in industrial applications i.e. CNC machines, 3D printers):

Effective and robust health monitoring is viewed as being a useful methodology to mitigate ballscrew jamming issues in industrial applications, however, it would depend on the culture of applying general line maintenance. As highlighted earlier, operators can be prone to missing scheduled maintenance actions due to time constraints to meet production deadlines, and so, such operators are content for having ballscrews available and ready to replace in the event of a failure. Generally, the operators are inclined towards following the manufacturer guarantee as a guideline towards approximating the ballscrew end of life.

On the use of fault diagnostics and prognostics to mitigate ballscrew jamming (in safety critical aerospace applications i.e. landing gear, flight control systems):

Ballscrew Services Limited also receives a high volume of ballscrews for repair from aerospace customers. Joe agrees that health monitoring is an essential step to mitigate ballscrew jamming to make EMAs more technically feasible for use in aerospace safety critical applications.

2.4.4 Concluding Remarks from Semi-structured Interviews

Three industry professionals participated in a semi-structured interview to gather their industrial experience on the use of ballscrews with respect to failures, root causes of failures, issues in sensing and maintainability, as well as health monitoring to mitigate jamming for industrial and aerospace applications.

In general, there has been a broad range of ballscrew failures with ballscrew wear being the most common. All the interviewees cited ballscrew jamming as the most critical type of failure which manifests itself as a secondary failure because of misalignment, debris build-up, incorrect lubricant application and ball rupture.

Root cause investigations and customer feedback have generally shown that poor maintainability and incorrect installation of EMA systems were a cause for a lot of the ballscrew failures. All three interviewees agreed that following the manufacturer instructions on scheduled maintenance, installation and operation would help alleviate many of these problems. This would also optimise the use of the existing sensing solutions.

Fault diagnostics methodology was viewed as a favourable approach to take in mitigating EMA ballscrew jamming for existing systems. However, before considering fault diagnostics, it was also emphasised that some operators need to ensure scheduled maintenance actions are being correctly followed. This would minimise the occurrence of faults that lead to reactive maintenance and downtime. It was also highlighted that more sensing i.e. vibration, temperature, noise etc. would be required to supplement a robust health monitoring solution due to issues in motor drive electronics masking a lot of issues in the mechanical drivetrain. This problem was substantiated for aerospace applications where a fault diagnostics algorithm would need to be designed for detecting the onset of ballscrew jamming through motor current only.

2.5 EMA Reliability in Aerospace Applications[4]

Despite their inherent advantages over other technologies, EMAs have seen little use to date in safety critical aircraft applications due to the potential for jamming, creating a single point of failure even when configured in parallel redundant formats (Balaban, et al. 2011). It has, however, been suggested widely that the next generation of fly-by-wire aircraft could benefit from EMA technology if PHM could be successfully incorporated (Balaban, et al. 2011).

A typical EMA is a linear ballscrew that provides linear motion when driven by a rotary electric motor. This consists of a single actuator assembly driven by a brushless DC motor via a single stage gearbox with the motor mating with a single pinion in the ballscrew assembly (Bodden et al., 2007). EMA ballscrew actuator failures are often a result of gradual degradation of the ballscrew surface through metal to metal contact of the re-circulating balls to the hardened metal surface of the ball screw shaft, eventually leading to jamming (Jin et al., 2013). Typical PHM schemes measure a parameter correlated with degradation (feature extraction) and then map this to a damage state through a diagnostic algorithm.

To get a better understanding of EMA reliability, historical in-service EMA failure data are evaluated from the 'Non Electronic Parts Reliability Database' (NPRD). The NPRD intends to provide a comprehensive database of field failure rate data on a variety of electrical, mechanical and electromechanical parts and assemblies to assist in reliability analyses and assessments (Quanterion, 2016). The NPRD has been publishing since the early 1970s with a cumulative compilation of data at each up-issue every 5-6 years.

[4] This work forms part of a case study conducted as part of the EngD to evaluate the benefits of applying PHM to aircraft maintenance through System Dynamics. The work was presented at the Third European Conference of the Prognostics and Health Management Society 2016 and published in a peer-reviewed conference paper titled 'Benefits Analysis of Prognostics & Health Monitoring to Aircraft Maintenance using System Dynamics' (Hussain Y., Burrow, Henson, & Keogh, 2016). This work is also under review for publication in the International Journal of Prognostics and Health Management titled 'A System Dynamics Approach to Evaluate Component Availability Under Condition Based Maintenance' – a draft of the Journal paper can be found in Appendix A.

The 2016 edition added an extra 138,000 parts and 370 billion part hours, representing a 400% increase in data compared to the previous edition in 2011 (Quanterion, 2016). Table 5 compares failure rate data for linear EMAs between data published in 1991 and in 2016.

Table 5. Linear EMA failure, NPRD data (Quanterion, 2016).

Years	**Part**	**Total Failed**	**Operating Hours 10^6**	**Failures per 10^6 Hours**
~1970-1991	Linear EMA	460	0.5256	875.2
~1970-2016	Linear EMA	1725	100.6478	17.14

It can be seen from the data collected in Table 5, the rate of failure was much higher between the early 1970s and 1991 than compared to between early 1970s and 2016. This may be attributed to improvements in actuator design for safety and reliability as well as improvements in maintenance. Usage profiles are not made apparent within the NPRD and so the nature of how the failures occurred is unclear. The failure rate data for 2016 can be further decomposed to show the rates for each application environment, these are shown in Table 6.

Table 6. Linear EMA failure by application, NPRD 2016 (Quanterion, 2016).

Application Environment	**Total Failed**	**Operating Hours (10^6)**	**Failures per 10^6 Hours**
Airborne Attack (AA)	806	3.3384	241.43
Airborne Uninhabited Attack (AUA)	229	2.1928	104.43
Airborne Inhabited Attack (AIA)	10	0.3655	27.36
Airborne Commercial (AC)	680	94.7512	7.18

Given the data in Table 6, a clear distinction can be made in failure rates between applications on military and commercial platforms. For military aircraft, there are a higher number of removals, which can be attributed to the fact that military aircraft are generally designed for enhanced performance and operate beyond the performance envelope of commercial aircraft.

It is challenging for aircraft operators and maintenance teams using CBM when the component degrades at a faster rate (Li et al., 2014). Early stage abrupt failures could arise from actuator misalignment leading to mechanical seizure of the ballscrew assembly (Balaban et al., 2015). Failures exhibiting a

gradual degradation initially before experiencing a jam can be attributed to abrupt seizures in the bearings of the screw from a build-up of debris or loss of lubrication (Balaban et al., 2015).

2.6 Problem Statement Summary and Thesis Objectives

Based on the background research, the main challenge has been to implement EMAs to aerospace safety critical applications in the drive towards MEA. This has been primarily due to the single point of failure in EMAs, which is ballscrew jamming.

Through HPM, fault tolerant designs and fault diagnostics were identified as the key methods to mitigate EMA ballscrew jamming. A review of the existing state-of-the-art revealed that due to weight constraints and design complexity, fault tolerant designs of EMAs were viewed as having low technical maturity to be considered for implementation on aircraft safety critical systems. A review of fault diagnostics solutions to mitigate ballscrew jamming showed that whilst many advancements were made through model-based and data-driven approaches, many challenges remain in obtaining a robust approach. In particular, this problem is made more challenging where sensing is limited to using motor current alone in the context of an aerospace safety critical application.

A hybrid approach (as shown in Figure 13) through combining model-based and data-driven methods against physical system data was considered to be the optimal approach in achieving a more robust and reliable means to predict and mitigate ballscrew jamming. Such an approach relies on producing characterisable fault modes from use of EMA test stands through data-driven approaches. A successful hybrid approach is also dependent on ensuring a high fidelity modelling approach is followed by modelling the motor dynamics and ballscrew kinematics in greater detail as stipulated in Section 2.2.2.

Following a review of literature on the existing challenges and desired approach to use fault diagnostics to mitigate EMA ballscrew jamming, the objectives of this thesis are as follows:

i. Evaluate the benefits of applying hybrid fault diagnostics to an aircraft EMA system to assess the impact on availability through Condition Based Maintenance (CBM) and associated cost effectiveness. This work forms part of a case study that is separate to this thesis but conducted as part of the EngD with Stirling Dynamics to evaluate the benefits of applying PHM to aircraft maintenance through System Dynamics. This work is currently under Journal paper publication, and a draft version can be found in Appendix A.
ii. Produce a high fidelity model of an EMA system to include:

a. Motor modelling using FOC techniques to analyse 3-phase AC quantities reduced to DC quantities using Park's transform to provide an in-depth learning of motor dynamics.
b. Ballscrew kinematics modelling to model the main areas of friction to improve the characterisation of impending jamming faults to aid fault detection.

iii. Through EMA test stand analysis, analyse and identify ballscrew jamming precursors through motor current alone.

iv. Utilising a combination of high fidelity EMA system modelling and test stand analysis, provide a feature driven algorithm to monitor and detect the onset of EMA ballscrew jamming.

Chapter 3: High Fidelity EMA System Modelling

This chapter presents an enhanced model-based approach to monitor friction within EMA ballscrews using motor current alone. Through simulations, feature extraction of EMA ballscrew dynamic friction is demonstrated through motor current as part of the hybrid fault diagnostics based algorithm design.[5]

3.1 Background

As documented in Chapter 1, there is a move towards a MEA within the aerospace industry, which has prompted aircraft manufacturers to consider replacing traditional hydromechanical solutions for EMAs in actuation systems. EMAs are being considered in safety critical applications such as primary flight control systems and landing gear systems (Balaban et al., 2011).

3.2 Previously Published Work and Objectives

Research in this area has considered many strategies and technologies using PHM. Whilst research has been conducted in terms of applying PHM to EMAs, an optimum solution to mitigating jamming is still sought. This section reviews previously published work using a data-driven approach and a model-based approach.

3.2.1 Data-Driven Approach

Research has been previously undertaken to isolate jamming failures by utilising test rig analysis for seeded failure tests and run-to-failure data. An example of this, is work undertaken by Balaban, Saxena, Goebel, Byington, Watson, Bharadwaj and Smith (2009b) where jamming faults were injected into a custom made EMA test stand. The results show good agreement with developed thermal and mechanical models. The issue, however, is the abrupt nature in which the failure occurs making it difficult to detect the onset of this failure. Bodden et al. (2007) also conducted seeded failure testing on an EMA test stand. The methodology evaluated actuator efficiency by monitoring overall power output

[5] The work in this chapter has been published in the International Journal of Prognostics and Health Management titled *'A High Fidelity Model-based Approach to Identify Dynamic Friction in Electromechanical Actuator Ballscrews using Motor Current'* in 2018 (Hussain Y. M., Burrow, Keogh, & Henson, 2018a).

against input. The analysis revealed that it was difficult to ascertain the origin of the fault at a local level.

Therefore, the main challenges in employing a data-driven analysis include the difficulty to simulate naturally occuring faults as well as isolating a particular fault within the drivetrain.

3.2.2 Model-based Approach

Modelling an EMA system in detail can enable the prognostics design engineer to trace back failure modes to relatable physical system parameters thus providing the engineer with informative diagnostic information. Maggiore, Vedova, Pace and Desando (2014) developed a Matlab/Simulink model of an EMA system for fault analysis associated with mechanical failures due to progressive wear. The modelled EMA system was typical of an arrangement for a primary flight control system comprising of control and power drive electronics, a Brushless Direct Current (BLDC) motor, gearing and a ball/rollerscrew. The study conducted by Maggiore et al. (2014) emphasised on modelling the build up of friction since this is a pre-cursor for ballscrew jamming. The results show that useful information could be obtained in terms of evaluating friction torque at a system level. However, it was not clear whether friction monitoring at a local level (for the main areas of friction within the ball/rollerscrew) could be characterisable, therefore making it challenging to diagnose for jamming faults.

Previous approaches have also generally used simple motor models. The investigation has therefore been limited to analysing electromagnetic torque and motor current without considering the dynamic effects of the motor. The research conducted by Maggiore et al. (2014) provided an advancement by modelling a BLDC system with power drive electronics that evaluated the torque generated by the motor as a function of the voltages generated by a 3-phase electrical power generator.

Therefore, identification of ballscrew degradation within EMAs using motor current alone can be enhanced through modelling the magnetic behaviour of the motor to gain a more in-depth understanding of the motor dynamics. Detailed modelling of ballscrew kinematics should also be enhanced using a more accurate representation of the contact mechanics.

3.3 Methodology for EMA Systems Modelling

The first part of the methodology consists of a series of procedures and equations for EMA modelling to develop an enhanced understanding of the baseline linear EMA system.

Secondly, the methodology describes how motor current can be used to aid fault detection and diagnostics of the ballscrew. This is followed by a description of the test cases and conditions to be simulated for healthy, degrading and failure states of the ballscrew.

3.3.1 EMA Modelling

The system being modelled is a baseline linear EMA system. The modelling was conducted using Matlab/Simulink where the key components consisted of the motor controller, the Permanent Magnet Synchronous Motor (PMSM) and the ballscrew. Figure 20 shows a high level view of the EMA system being modelled for speed and current control.

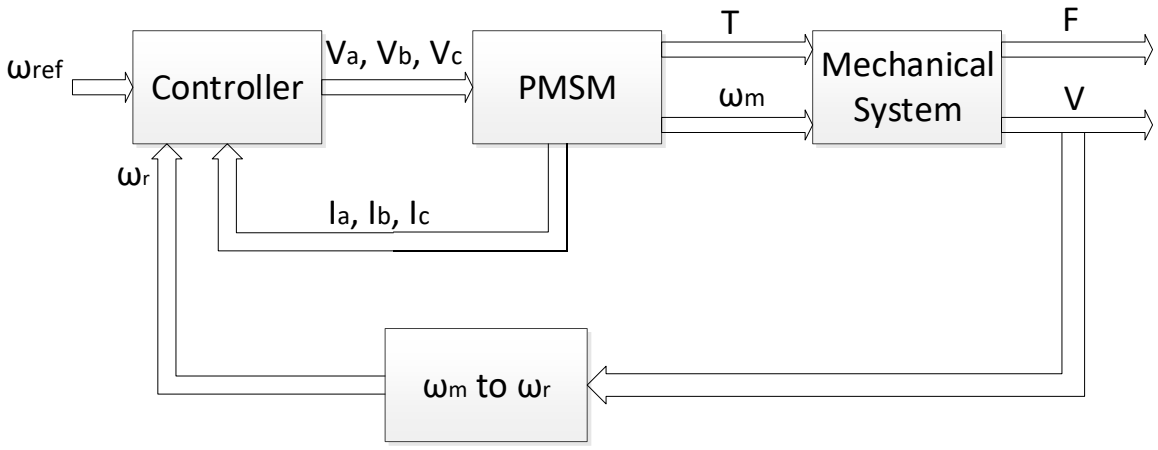

Figure 20. EMA Block Diagram.

PMSM's use permanent magnets rather than windings in the rotor. Electronic excitation control with integrated power inverter and rectifier, sensor, and inverter electronics are required for practical operation (Vas, 1996). The PMSM was modelled using 'dq-axis transformation' theory, which involves Park's transform. This reduces 3-phase AC quantities (I_a, I_b, I_c) to DC quantities (I_d, I_q) (Park, 1929). The transform to DC quantities reduces the complexity of the system and therefore more understanding of the drivetrain system can be achieved by modelling the PMSM in this way. Figure 21 shows the equivalent electrical circuit for the PMSM whereby, R_S is the resistance, L_d and L_q are the inductances in the d and q axis respectively, ω_r is the electrical angular velocity of the rotor, and λ_d and λ_q are the flux linkages in the d and q directions respectively.

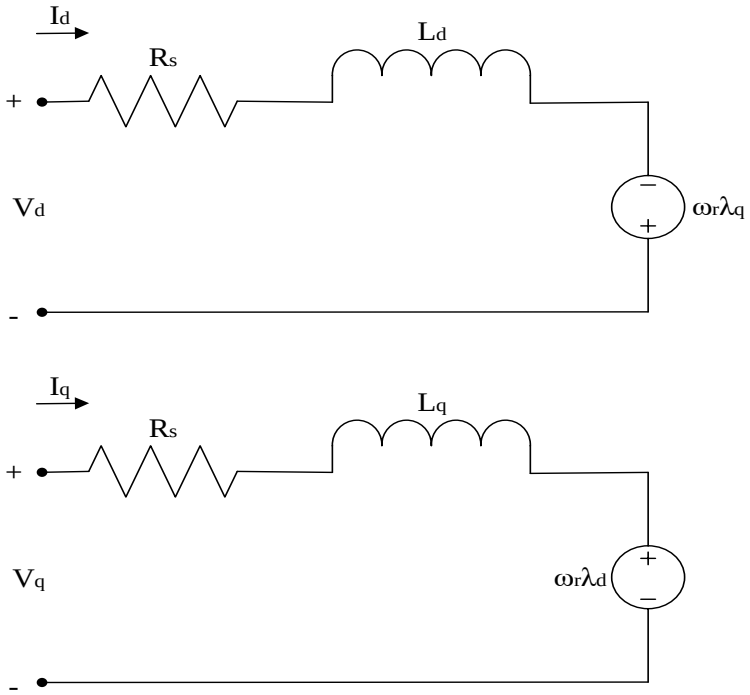

Figure 21. PMSM Equivalent Electric Circuit in Rotating Reference Frame (DQ).

The transformation converts vectors in the 3-phase reference frame to 2-phase and then a rotating 2-phase reference frame as shown in Figure 22.

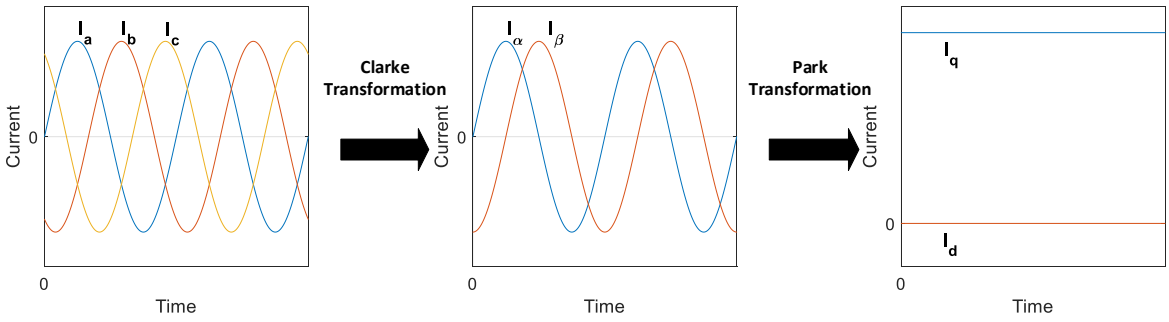

Figure 22. 3-phase to 2-phase Stationary and 2-phase Stationary to 2-phase Rotating Reference Frame.

This enables simplified analysis of these DC quantities before performing the inverse transform to the 3-phase results. This will provide in-depth motor understanding for condition monitoring and fault detection.

The PMSM was modelled in accordance to an industrial servomotor (Emerson) with parameters listed in Table 7.

Table 7. PMSM Parameters.

Parameter	Value
Resistance, R_s	1.1 ohm
Motor Voltage Constant, K_e	98 V/KRPM
Motor Torque Constant, K_t	1.6 Nm/A
Peak Torque, T	45.9 Nm
Peak Current, I	28.7 A
Poles, p	6
Inductance on q-axis, L_q	7.4 mH
Inductance on d-axis, L_d	7.4 mH
Motor Inertia, J_m	0.0138 kg.m^2

The electrical and mechanical elements of the PMSM were modelled within the PMSM block shown in Figure 20 using the equations as listed below.

Firstly, the 3-phase supply voltages were converted to 2-phase quantities using Park's transform:

$$\begin{bmatrix} V_d \\ V_q \\ V_0 \end{bmatrix} = \frac{2}{3}\begin{bmatrix} cos\theta & cos\left(\theta - \frac{2\pi}{3}\right) & cos\left(\theta + \frac{2\pi}{3}\right) \\ -sin\theta & -sin\left(\theta - \frac{2\pi}{3}\right) & -sin\left(\theta + \frac{2\pi}{3}\right) \\ \frac{1}{2} & \frac{1}{2} & \frac{1}{2} \end{bmatrix}\begin{bmatrix} V_a \\ V_b \\ V_c \end{bmatrix} \quad (1)$$

The PMSM electrical model consists of the stator resistance, inductances (d and q axes), number of poles as well as the flux induced by the rotor permanent magnets in the stator phases to get the I_q and I_d currents:

$$V_d = R_s I_d + \frac{d}{dt}\lambda_d - \omega_r \lambda_q \quad (2)$$

$$V_q = R_s I_q + \frac{d}{dt}\lambda_q + \omega_r \lambda_d \quad (3)$$

where

$$\lambda_d = L_d I_d + \lambda_{af} \quad (4)$$

where λ_{af} is the flux induced by the rotor permanent magnets and

$$\lambda_q = L_q I_q \quad (5)$$

The electromagnetic torque of the PMSM is derived from:

$$T_e = \frac{3p}{4}\left(\lambda_d I_q - \lambda_q I_d\right) = \frac{3p}{4}\left(\lambda_{af} I_q + \left(L_d - L_q\right) I_d I_q\right) \quad (6)$$

The mechanical subsystem of the PMSM model to calculate mechanical torque and rotor mechanical speed is given by

$$T_e = T_L + B\omega_m + J\frac{d\omega_m}{dt} \quad (7)$$

where B is the motor viscous friction.

Equation (7) can be rearranged for rotor mechanical speed:

$$\omega_m = \int \left(\frac{T_e - T_L - B\omega_m}{J}\right) dt \quad (8)$$

whereby the relationship between the electrical speed (ω_r) and the rotor mechanical speed (ω_m) is given by

$$\omega_m = \omega_r \left(\frac{2}{p}\right) \quad (9)$$

Given the modelled PMSM electrical and mechanical properties, the d and q axis currents are transformed back into 3-phase quantities and subsequently fed back in to the PMSM controller block (as shown in Figure 34). The inverse Park transform was used to return the 3-phase currents:

$$\begin{bmatrix} I_a \\ I_b \\ I_c \end{bmatrix} = \begin{bmatrix} cos\theta & -sin\theta & 1 \\ cos\left(\theta - \frac{2\pi}{3}\right) & -sin\left(\theta - \frac{2\pi}{3}\right) & 1 \\ cos\left(\theta + \frac{2\pi}{3}\right) & -sin\left(\theta + \frac{2\pi}{3}\right) & 1 \end{bmatrix} \begin{bmatrix} I_d \\ I_q \\ I_0 \end{bmatrix} \quad (10)$$

The PMSM controller was modelled for speed and torque control. This enables real time control of torque variation demand, mechanical speed and regulation of the phase currents, which ultimately reduces the occurrence of current spikes during transient operation. Figure 23 shows a block diagram of the PMSM speed and current control system. The PI gains for the speed and current controllers were manually tuned with the following values: For PI (1), $K_p = 5$ and $K_i = 1.5$, for PI (2), $K_p = 1.5$ and $K_i = 1$, and for PI (3), $K_p = 3$ and $K_i = 2$.

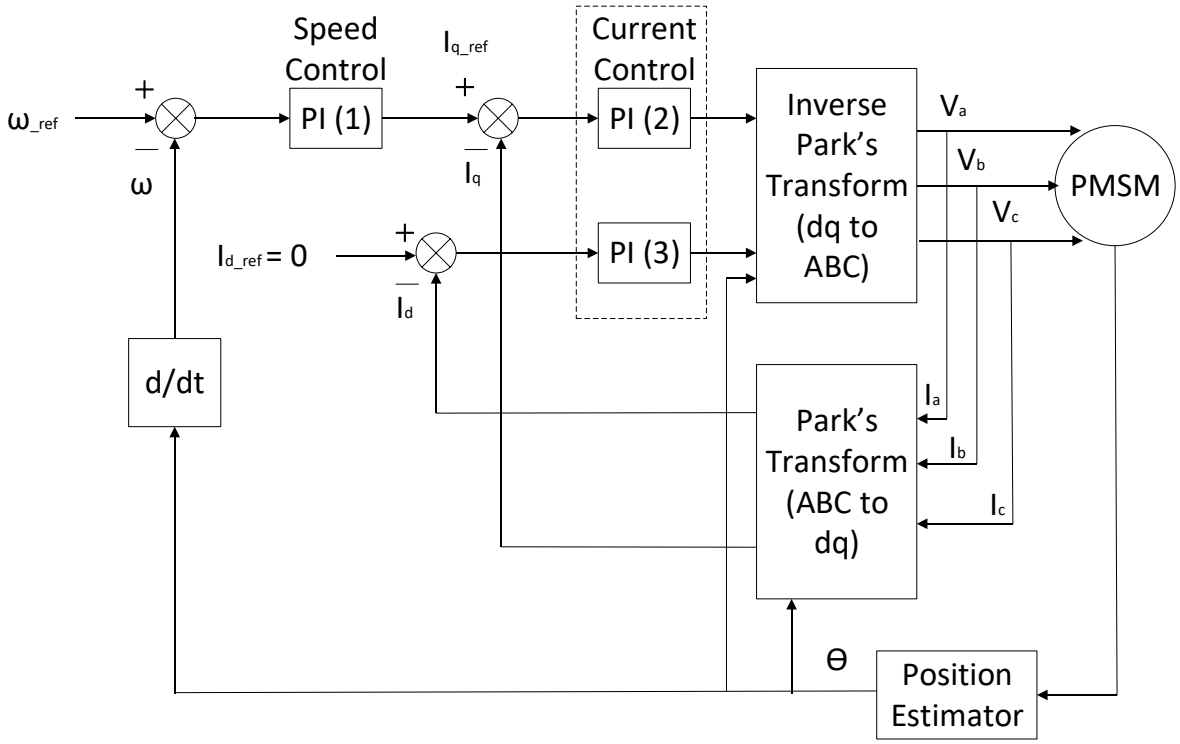

Figure 23. PMSM Speed and Current Controller.

The ballscrew was modelled by taking the generated mechanical torque and rotor speed values and converting them in to end loads and linear speeds. The ballscrew specification is presented in Table 8.

Table 8. Ballscrew Parameters.

Parameter	**Value**
Lead, *L*	5
Length, *l*	300 mm
Screw Diameter, d_s	16 mm
Ball Diameter, *D*	3.15 mm
Ballscrew Lead Angle, α	7°
Density, ρ	7750 kg/m^3
Ballscrew coefficient of friction, μ	0.01

The equations used for ballscrew modelling are listed below:

For this analysis, the total system inertia is given the summation of motor, ballscrew and load inertia:

$$J = J_m + J_{BS} + J_l \quad (11)$$

J_m is known from the motor manufacturer specification as given in Table 7. J_{BS} was modelled as a cylinder based on density, radius and length:

$$J_{BS} = \frac{\pi l \rho d_s^4}{32} \quad (12)$$

J_l is the load inertia reflected back to the motor:

$$J_l = \frac{mL^2}{2\pi} \times 10^{-6} \quad (13)$$

The load torque reflected to the motor is composed by the load force, F_l and pre-load force, F_{pf}:

$$T_l = \frac{F_l L}{2\pi\eta} + \mu \frac{F_{pf} L}{2\pi\eta} \quad (14)$$

The relative velocities between ball and screw, V_{BS} and ball and nut V_{BN}, needed to be factored in. Relative speeds of these regions are critical for this study as they largely dictate the magnitude of instability when the ballscrew experiences a fault (Jiang, Song, Xu, Tang, Zhang & Han, 2010). The corresponding relative angular velocities are given by

$$\omega_{BS} = \frac{V_{BS}}{0.5(D_s - D)} \quad (15)$$

$$\omega_{BN} = \frac{V_{BN}}{0.5 d_n} \quad (16)$$

Information regarding the rotor mechanical speed, (ω_m) is known therefore the angular velocities were calculated using a detailed kinematic analysis. Wei and Lin (2004) determined the relationship between the angular velocities, ω_{BS} and ω_{BN} as

$$\frac{\omega_{BS}}{\omega_{BN}} = \frac{(1+\delta cos\alpha_n)(cos\alpha_s + tan\beta sin\alpha_s)}{(1-\delta cos\alpha_s)(cos\alpha_n + tan\beta sin\alpha_n)} \quad (17)$$

β is the lead angle and δ is a relationship between ball diameter and screw pitch given by

$$\delta = \frac{D}{D_s} \quad (18)$$

The contact angles (between ball and nut, α_n, and ball and screw, α_s) are depicted in Figure 24.

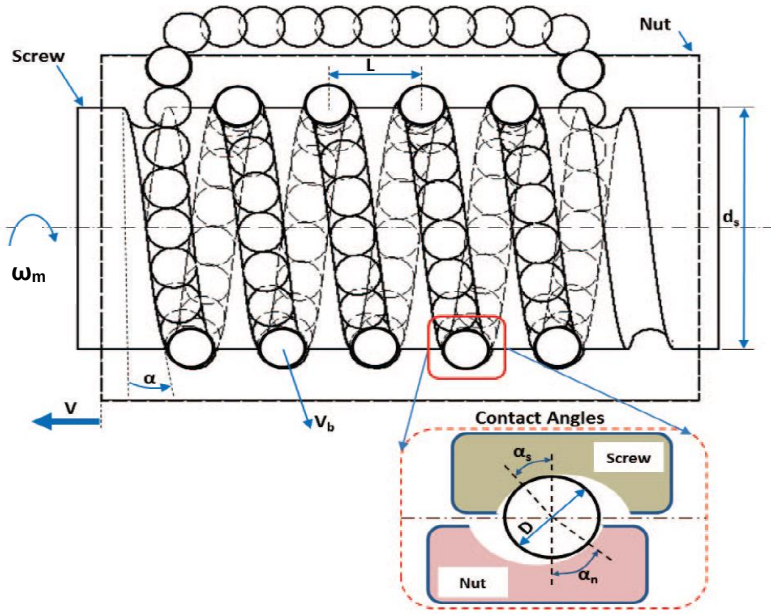

Figure 24. Ballscrew Kinematics (Ismail, Balaban & Spangenberg, 2016). *Reproduced by permission of the Institute of Electrical and Electronics Engineers (IEEE).*

Friction is mostly prevalent between the ball and screw thread (Vahid-Araghi & Golnaraghi, 2011). Friction also occurs between the ball and nut and therefore the analysis focuses on these areas of interaction within the ballscrew. A kinematic analysis of this region was required in order to understand these contact areas in more detail and to evaluate friction as a function of sliding velocity. A schematic depicting the ballscrew kinematics is shown in Figure 24.

A thorough mathematical model of ballscrew kinematics has been developed by Wei and Lin (2004), therefore this was utilised partially for this segment of the research.

In order to calculate the relative angular velocities (ω_{BS} and ω_{BN}), ball linear velocity, V_B needs to be ascertained. Assuming the relative slip speed between ball and nut is negligible, V_B can be calculated as follows (Song, Jian, Zhao-tan, Xian-yin & Bao-min, 2005):

$$V_B = \frac{\omega_m(d_s - D\sin\alpha)\cos\beta}{2} \quad (19)$$

where the lead angle, β is determined from

$$\tan\beta = \frac{L}{\pi D} \quad (20)$$

Given equation (19), the corresponding ball angular velocity, ω_b is given by:

$$\omega_b = \frac{V_B}{0.5D_s} \quad (21)$$

The relative angular velocity between ball and screw, ω_{BS} depends on ball angular velocity, ω_b and ballscrew angular velocity, ω_m (Wei & Lin, 2004), hence

$$\omega_{BS} = (\omega_m - \omega_b)cos\alpha \quad (22)$$

The relative angular velocity between ball and nut, ω_{BN} depends only on the ball angular velocity, ω_b (Wei & Lin, 2004) therefore:

$$\omega_{BN} = -\omega_b cos\alpha \quad (23)$$

Given that ω_{BS} and ω_{BN} can now be calculated as a function of ball angular velocity, ω_b, equations (22) and (23) can be substitued into equation (17) and rearranged to obtain

$$\omega_{BS} = \omega_{BN} \frac{(1+\delta cos\alpha_n)(cos\alpha_s + tan\beta sin\alpha_s)}{(1-\delta cos\alpha_s)(cos\alpha_n + tan\beta sin\alpha_n)} \quad (24)$$

$$\omega_{BN} = \omega_{BS} \frac{(1-\delta cos\alpha_s)(cos\alpha_n + tan\beta sin\alpha_n)}{(1+\delta cos\alpha_n)(cos\alpha_s + tan\beta sin\alpha_s)} \quad (25)$$

The next step is to formulate a velocity dependent coefficient of friction model given the relative velocities between the ball and nut, and ball and screw. The Stribeck friction model (Bowden & Tabor, 1950) was used to evaluate friction between the interacting surfaces in the ballscrew. This was used previously by Vahid-Araghi and Golnaraghi (2011) for a lead screw drive system. The velocity depdendent coefficient of friction is generally composed of:

(a) Coulomb friction – Constant friction force opposing motion.

(b) Viscous friction - Friction force proportional to the sliding velocity.

(c) Stribeck friction – Occurs at low sliding velocities and contains Coulomb and Viscous friction components as shown in Figure 25.

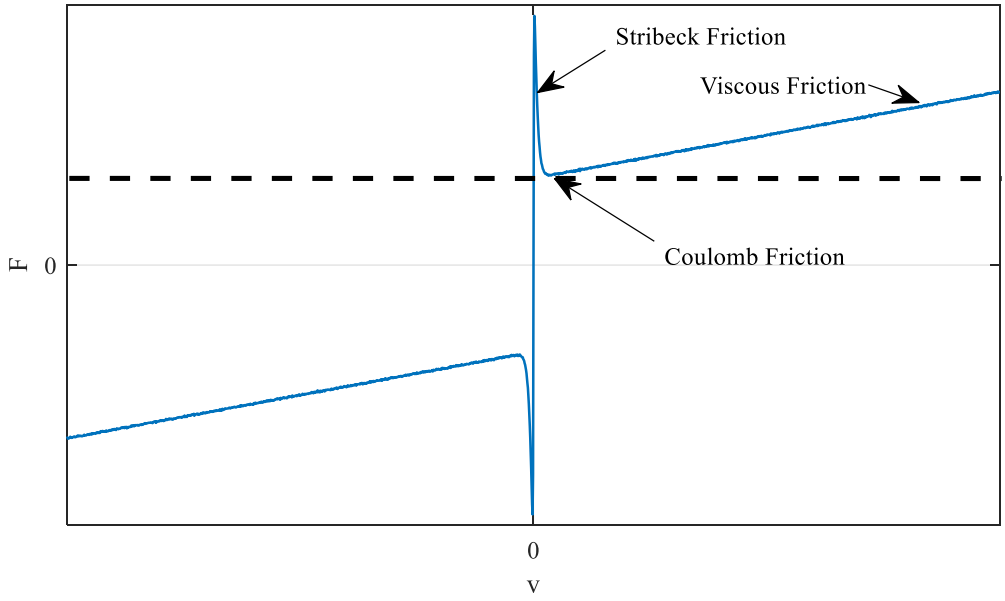

Figure 25. Velocity Dependent Friction Force.

Kinetic friction τ_{fk} is expressed by:

$$\tau_{fk}(\omega) = sign(\omega)\left(k_c + (k_s - k_c)e^{-\left|\frac{v_s}{v_0}\right|^{\delta v}}\right) + k_v\omega \quad (26)$$

Where k_c, k_v and k_s are the Coulomb, Viscous and Stribeck friction coefficients, respectively. v_s is the sliding velocity between interacting surfaces. This was treated as the relative speed between ball and nut, and ball and screw as described earlier in this section. v_0 controls the velocity range of the Stribeck effect.

The overall friction is then added into the end load model, which is then converted back into the reflected torque to the motor.

3.3.2 EMA Model Test Cases and Conditions

Using the model described in Section 3.3.1, a series of simulations were evaluated using different variables that include contact angles between ball and nut, and ball and screw, mechanical efficiencies and demand speeds. A typical landing gear extension/retraction cycle for a Boeing 757 lasts ~20 seconds (Boeing, 1994) therefore a cycle time of 20 seconds was used for this analysis.

It should be noted that no load profiles were modelled for this case study as one of the primary objectives was to identify the onset of ballscrew jamming through investigating ballscrew dynamic friction (between interacting ball and nut, and ball and screw) and ballscrew geometry through motor current. Using this model-based approach, test cases for simulation were created with respect to 3 states of health: Healthy, Degrading and Faulty.

Healthy State

Contact angles between ball and nut, and ball and screw typically range between 38-40° (Ninomiya & Miyaguchi, 1998). Therefore, these values were used to represent a healthy condition for the ballscrew and nut.

Mechanical efficiency is the measure of effectiveness of the EMA's input power over the output, which produces the end force and motion. Industry standard values were used for ballscrew mechanical efficiency, which is generally in the region of ~80-90% for healthy states (McNier, 2016).

Degrading State

Degrading states are conditions where the EMA is operable, but exhibits deteriorations in performance due to wear and build up of friction. Ballscrew and nut contact angles can vary upto 8% through deterioration, misalignment cases or incorrect selection (Xu, Yao, Sun & Shen, 2014). Therefore such instances were simulated by inducing variation in the contact angles of up to 8%.

Ballscrew mechanical efficiencies are also significantly lower therefore values between 35-65% were used in this state. Mechanical efficiencies of 70-80% were also tested for such cases of variation in contact angles.

Faulty State

The analysis is focused on one type of EMA failure mode, ballscrew jamming. The onset of jamming is of interest and so lower mechanical efficiency values (15-35%) were modelled to evaluate the effect on motor current.

The relative velocities (between ball and nut, and ball and screw) were set to zero to represent the jamming condition.

Table 9 summarises the test cases and conditions that were simulated.

Table 9. Test Cases and Conditions Summary.

State	Ball – Nut and Ball – Screw Angle of Contact (degrees)	Mechanical Efficiency (%)
Healthy	38-40	70-80
Degrading	35-43	70-80
		35-69
Faulted	Relative velocity set close to 0 (onset of jamming)	15-35

The contact angles were modelled using Equations (24) and (25) and were varied according to the values listed in Table 9 (in radians). The mechanical efficiencies were modelled using industry standard Viscous friction coefficients. Figure 26 shows a graph by Collins (2017) indicating typical ballscrew viscous coefficients corresponding to overall efficiency.

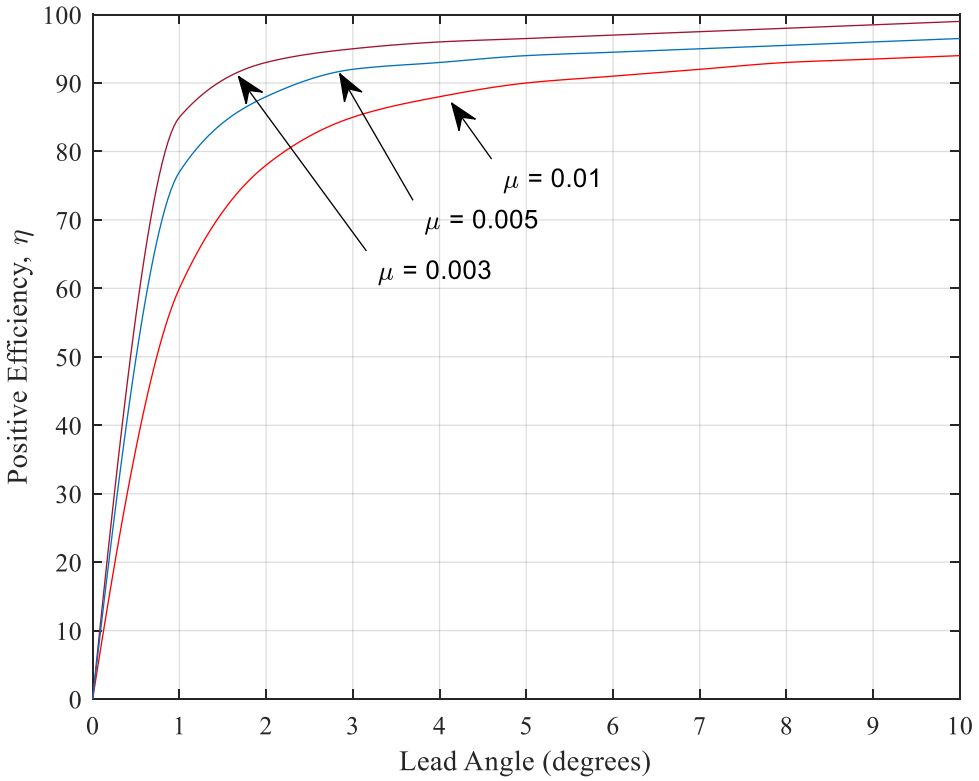

Figure 26. Ballscrew Efficiency (Collins, 2017). *Data points from Collins (2017) were used to produce this figure.*

The ballscrew lead angle was calculated using Equation (20), from which subsequent values of Viscous friction coefficients were deduced accordingly to represent each health state. The values of Viscous friction coefficient were modelled in Equation (26).

Simulations for each of the test cases for the different states were run for different motor command speeds: 500, 1500 and 3000 RPM.

In addition, external disturbances can occur in an EMA application, e.g. gust and aeroloads for a landing gear actuation system, which can induce uncertainty in ascertaining the true state of health. Therefore, an additional load of 20% was modelled to replicate these external disturbances.

Following the simulations, peak I_q motor currents were generated for post analysis and training for classification. A total of 667 I_q current datasets were generated which included different contact angle combinations and mechanical efficiencies (as shown in Table 9) as well as variations due to external disturbances for each of the test cases.

3.3.3 Data Classification Methodology

Classification of all the data was necessary in order to train and learn from the parameter readings for new data.

The classification of the simulated data was viewed as a process of 'supervised learning' from which the objective was to take the known set of input data and known responses to the data, and build a prediction model for responses to new data.

Various algorithms were considered for applying data classification techniques. These classification algorithms (for supervised learning) included decision trees, Support Vector Machine (SVM), Discriminant analysis, k-NN and Naïve Bayes. The selection of the classification algorithm was based on prediction accuracy, fitting and prediction speed and ease of interpretation.

Karter (2016) reviewed the use of these algorithms. Decision trees for classification was considered binary and therefore have low predictive accuracy. SVMs have high predictive accuracy and the data would need to have exactly two classes. If many support vectors are used, prediction speed and memory become compromised. k-NNs have good predictive accuracy in low dimensions even with large datasets. Discriminant analysis can have varying predictive accuracies depending on the modeling assumptions.

Therefore, given high predictive accuracy for large datasets with low dimensions, the datasets were trained and classified using the k-NN algorithm. This stores all trained cases and classifies new cases based on a measure of similarity (Murphy, 2012). By this, the k-NN algorithm measures the distance between a new scenario against the already set scenarios from the generated data sets which would enable an approximation for classification for a new query. Distance was evaluated using the Euclidean norm (Murphy, 2012):

$$d_{st}^2 = (x_s - y_t)(x_s - y_t)' \quad (27)$$

The datasets generated from Section 3.3.2 were organised and trained for all the different tests conditions and cases for classification using peak motor current values only. This was tested to evaluate the robustness and accuracy for new queries. New queries were selected for classification prediction using k-NN classifier. This was achieved using the built-in k-NN function in Matlab, the code for which can be found in the Appendix.

3.4 Simulation Results

This section shows the simulation results of the test cases described in Section 3.3.

3.4.1 Identifying Ballscrew Stribeck Behaviour Through Motor Current

Simulations were run for three trapezoidal speed profiles – 500, 1500 and 3000 RPM as shown in Figure 27.

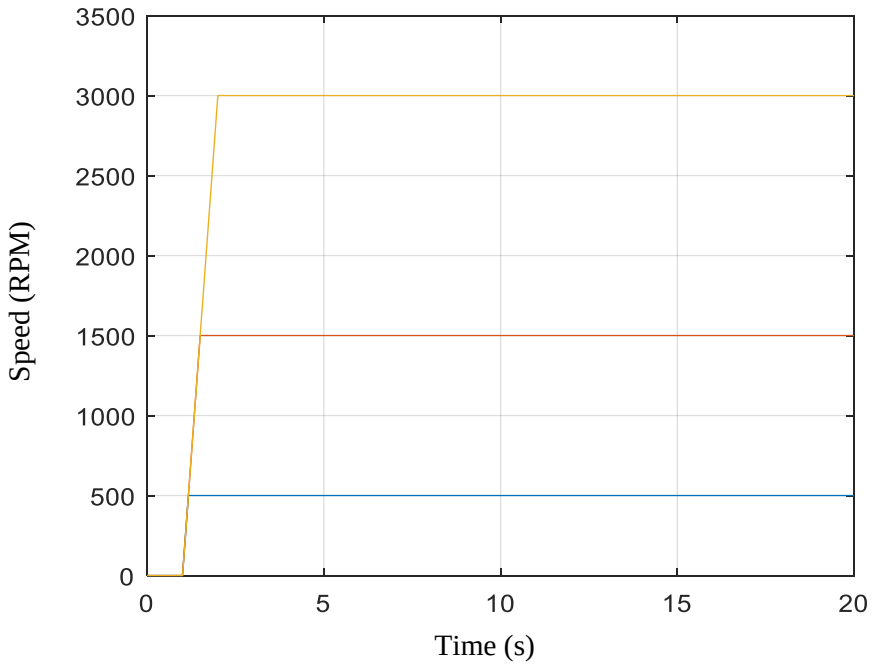

Figure 27. EMA Test Speed Profiles.

The corresponding 3-phase currents for 500 RPM is shown in Figure 28.

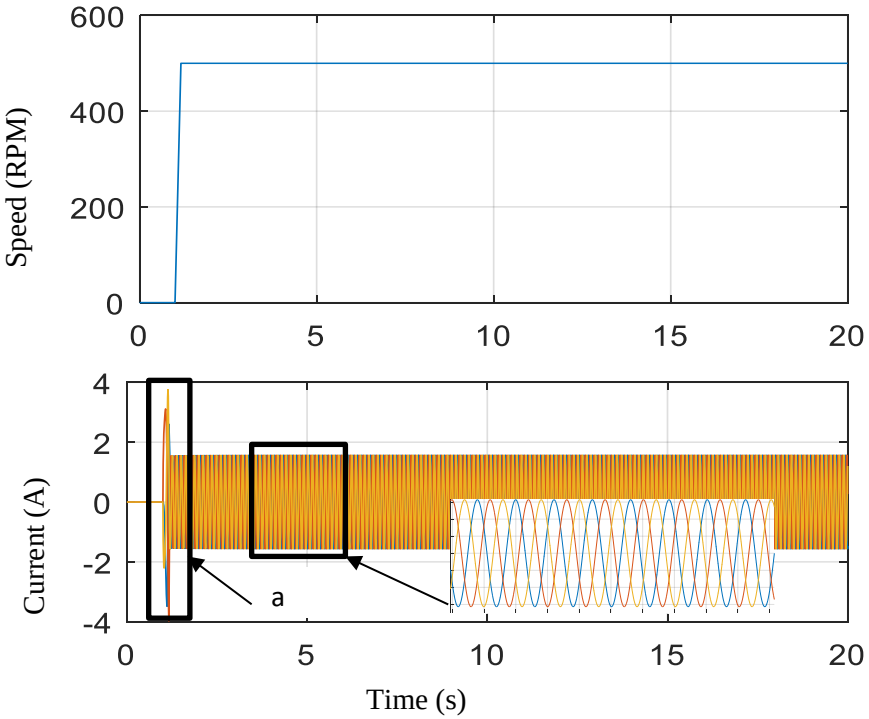

Figure 28. 3-Phase Currents at 500 RPM.

As can be seen from the region labelled ‘a’ in Figure 28, the motor starts to turn after 1 second, which corresponds to the initial ramp up as indicated in the speed profiles and is followed by a peak starting current. After reaching steady state, the sinusoidal 3-phase alternating currents exhibit constant amplitudes as well as fixed width waveforms.

The peak starting current occurs when an electrical motor is switched on in which the magnitude of the current drawn is dependent on the initial load on the motor (Park, 1929). Gao and Kang (2014) also demonstrated this effect through the modeling of a PMSM using vector control.

Park’s transform was performed to generate the equivalent I_q currents. These are shown for all speeds in Figure 29.

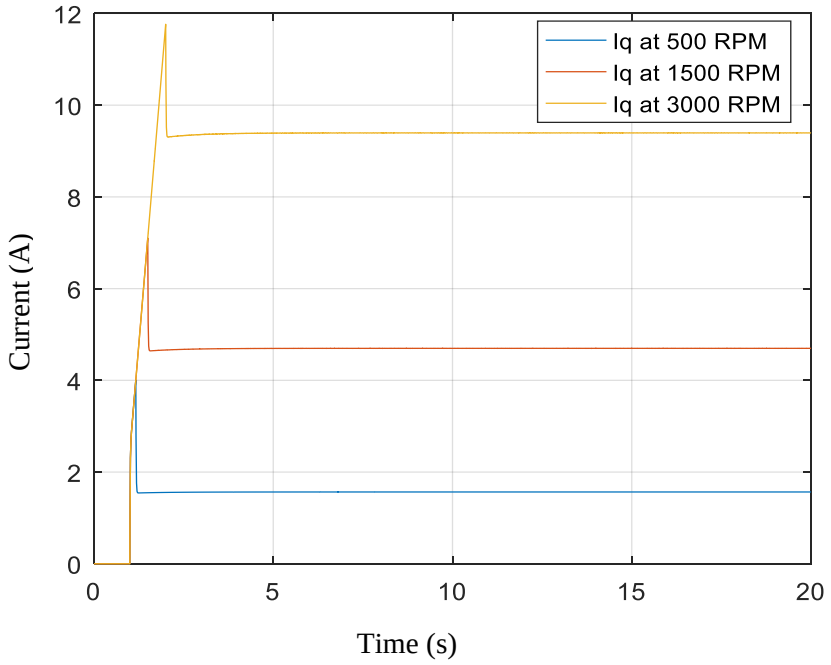

Figure 29. I_q Currents for All Speeds.

The transient period (at the first peak of the starting current) increases with command speed due to acceleration before settling to steady state currents. The next set of simulations were conducted to evaluate the effects of the ballscrew kinematics. Figure 30 shows the time domain 3-phase and I_q current signals without any load torque at 500 RPM.

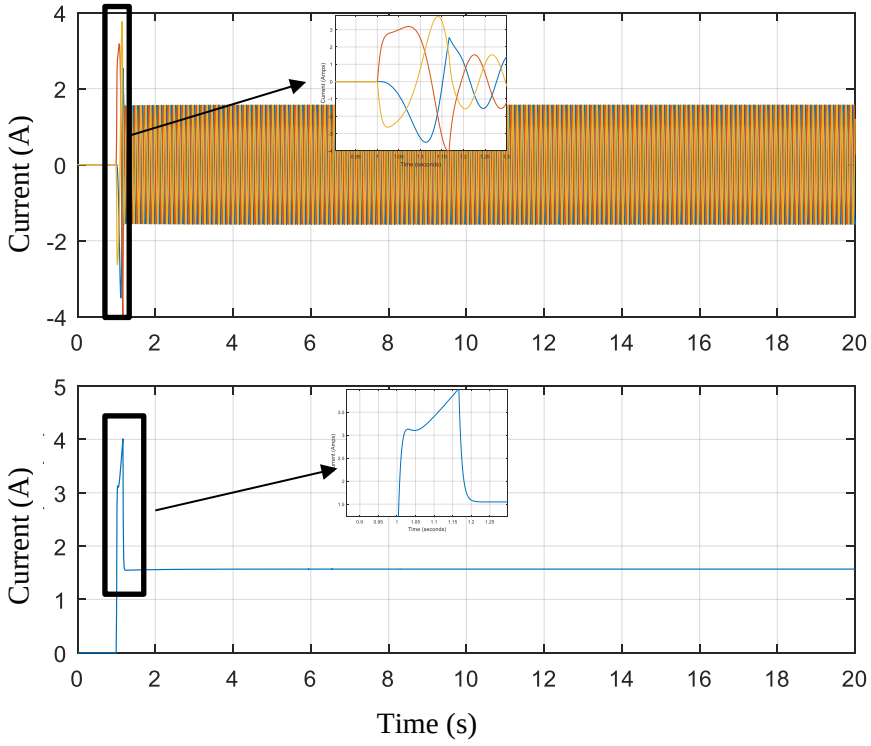

Figure 30. 3-phase and I_q Currents at 500 RPM with Ballscrew.

The zoomed views in Figure 39, in addition to the peak starting current show an additional current spike at the beginning of the starting current region. This is attributable to the Stribeck friction component of the ballscrew friction model. This occurs at low velocities at a transition between static and kinetic friction. This is further exemplified in Figure 31 when the Stribeck friction coefficient is increased.

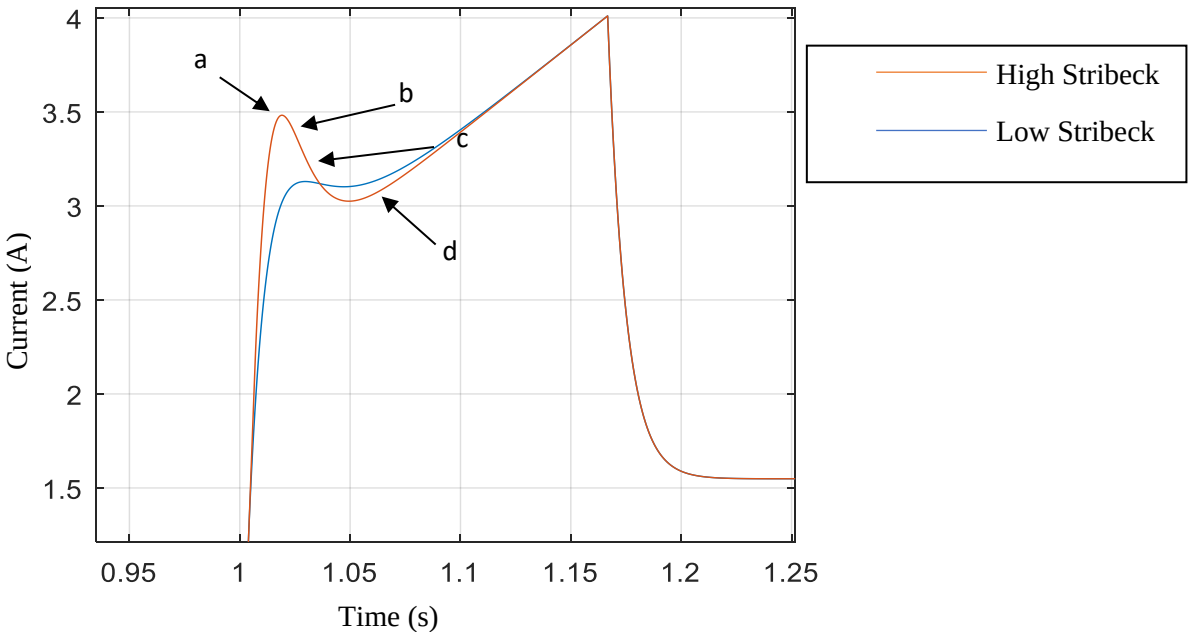

Figure 31. I_q Current with Increased Stribeck Effect in Ballscrew (Region 'a' is the static region from which the interaction behaves like a spring with micro-displacement proportional to the force (Armstrong-Helouvry , Dupont, & De Wit, 1994). Region 'b' exhibits boundary lubrication whereby the velocity increases, however, it not enough to build a fluid film between the surfaces. Region 'c' involves partial fluid lubrication and region 'd' includes full fluid lubrication whereby the relatively velocity is high enough for separation of the surfaces (Armstrong-Helouvry et al, 1994)).

Figure 32 shows a range of peak current values (from steady state behavior) against speed for the motor only as well as for the motor + ballscrew configurations (with Stribeck friction conditions as described above).

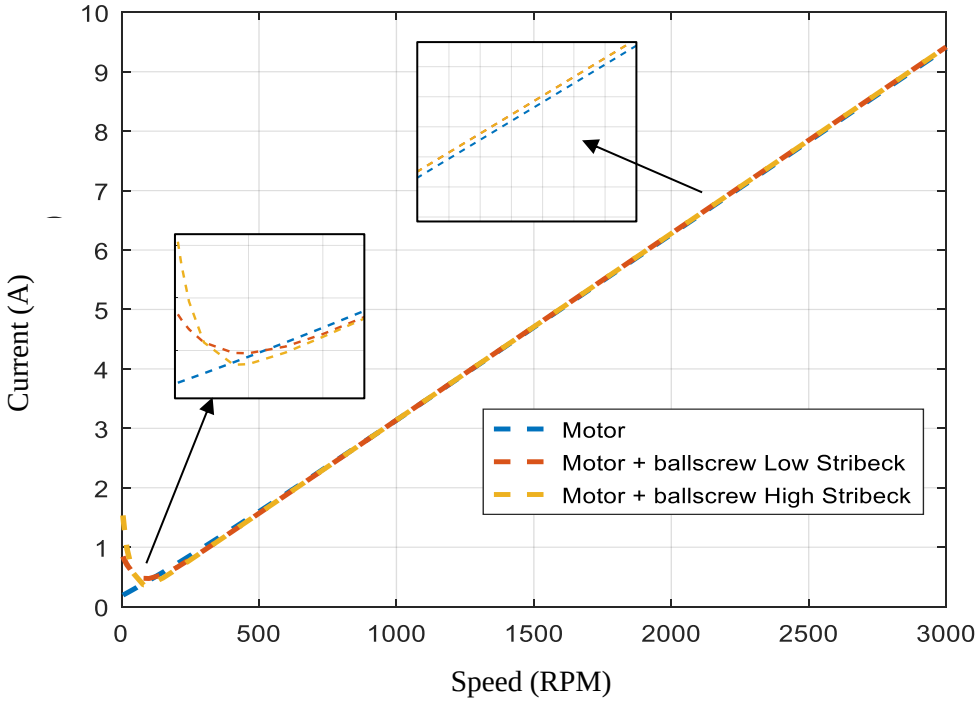

Figure 32. I_q Current Speed Range with Stribeck Effect.

For the 'motor only' configuration, the currents increase linearly due to the velocity dependent internal friction of the motor (it should be noted that the motor viscous friction was set at a high value (~0.1 kgm^2/s) to demonstrate this speed dependent feature across the speed range). This is also true for configurations with ballscrew included, however, there is a gradually increasing disparity in current with speed due to the presence of ballscrew Viscous friction component. Furthermore, higher current is noticeable at lower speeds due to the Stribeck effect for the motor + ballscrew configurations.

The effects of Viscous friction through motor current signals were simulated. Figure 26 in Section 3.3.2 provided a guideline to use for representative Viscous friction values as an indicative figure of ballscrew efficiency from industry standards. Progressively higher values of Viscous friction were used to represent a degrading and faulty ballscrew system. Resulting peak I_q currents across a speed range are shown in Figure 33.

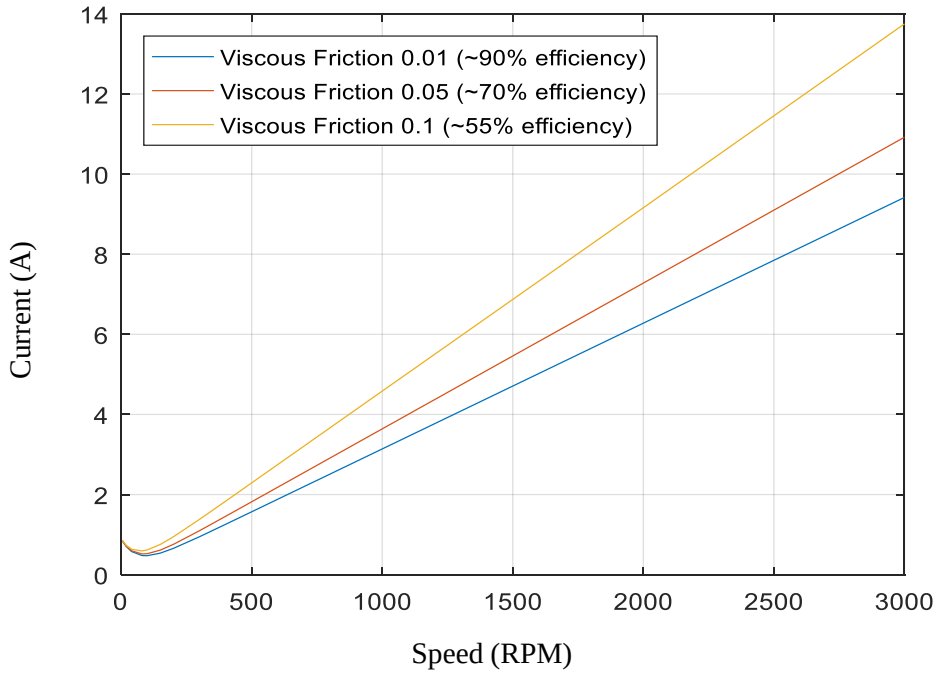

Figure 33. I_q Current Variation with Viscous Friction.

As can be observed, the I_q currents increase with Viscous friction, which is speed dependent. Hence, disparities between each condition become larger with speed.

The next step evaluated the effect of seeding a fault (change in ball and nut, and, ball and screw contact angle) on 3- phase and I_q current signals. A simulation was run at 500 RPM with a seeded fault in the form of a contact angle variation was modelled at 10 seconds.

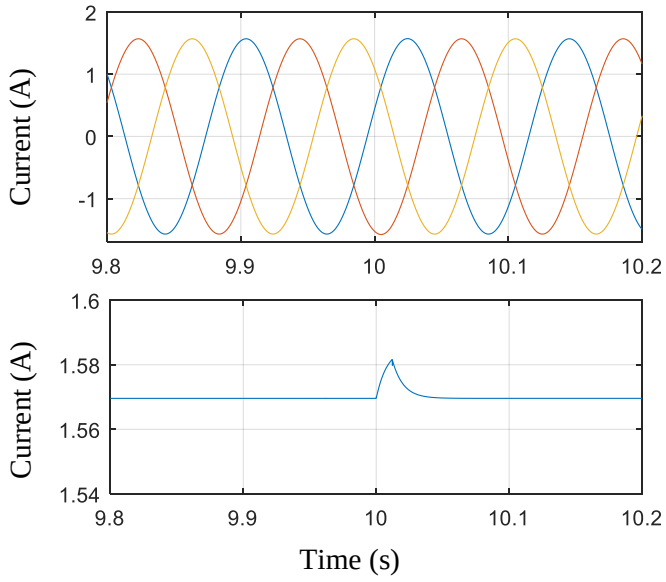

Figure 34. 3-phase Current (top) and I_q Current (bottom) Signals Following Seeded Fault.

From Figure 34, a resulting spike is noticeable through evaluation of the I_q current. Such method can be used to determine variation in ballscrew geometry for fault detection.

Simulations were then run for different contact angles and mechanical efficiencies added to evaluate the effect of I_q currents. The analysis considers the maximum I_q current from steady state period for each test case. Results are shown for Healthy, Degrading and Faulty conditions.

Healthy State

Firstly, the contact angles (between ball and nut, and ball and screw) were varied (as specified in Table 9). The resulting maximum I_q currents are shown in Table 10 for all speed demands with 80% mechanical system efficiency.

Table 10. Maximum I_q Currents Under Varying Contact Angles for All Speeds (Healthy States).

Test Case	**Demand Speed (RPM)**	**Contact Angle (deg)**		**Max. Current (Amps)**
		BN	**BS**	
1	3000	40	40	9.61
2	3000	38	40	9.55
3	3000	38	38	9.46
4	1500	40	40	4.80
5	1500	38	40	4.78
6	1500	38	38	4.73
7	500	40	40	1.61
8	500	38	40	1.60
9	500	38	38	1.58

Table 10 shows that more I_q current is drawn with increasing severity of B-N and B-S contact angles. However, the margins become increasingly smaller between the I_q currents (for respective contact angle cases) at lower speed demands.

These cases were classified as being healthy although it could be challenging to diagnose against early stages of deterioration, especially when operating at low speeds.

The mechanical system efficiency was changed to 70% with resulting maximum I_q currents shown in Table 11. Contact angles for B-N and B-S at 40 degrees are also presented alongside the previous results with 80% efficiency. As can be seen, the variation in peak I_q current becomes larger with speed due to the velocity dependent Viscous friction coefficient.

Table 11. Maximum I_q Currents Under Varying Mechanical System Efficiencies for All Speeds (Healthy States).

Test Case	Demand Speed (RPM)	Mechanical System Efficiency (%)	Max. Current (A)
1	3000	70	10.97
2	3000	80	9.61
3	1500	70	5.49
4	1500	80	4.80
5	500	70	1.84
6	500	80	1.61

Degrading State

Larger contact angle offsets were introduced (as specified in Table 9) to represent degrading cases to further analyse the effect on the I_q currents. A sample of these cases is presented in Table 12.

Table 12. Maximum I_q Currents Under Varying Contact Angles for All Speeds (Degrading States),

Test Case	Demand Speed (RPM)	Contact Angle (deg)		Max. Current (A)
		BN	BS	
1	3000	35	43	9.84
2	3000	43	43	9.81
3	3000	35	35	9.67
4	3000	43	38	9.58
5	1500	35	43	4.92
6	1500	43	43	4.91
7	1500	35	35	4.84
8	1500	43	38	4.79
9	500	35	43	1.65
10	500	43	43	1.64
11	500	35	35	1.62
12	500	43	38	1.60

Table 12 shows the progressive nature of the ballscrew degradation where I_q currents are increasing with severity of contact angle offsets.

Variations in mechanical system efficiencies (for degrading conditions) were introduced and compared with two examples of contact angle offsets. Table 13 shows the results of this where simulations were run at 3000 RPM command speed.

Table 13. Maximum I_q Currents Under Varying Mechanical System Efficiencies at 3000 RPM (Degrading States).

Test Case	Contact Angle (deg)		Mechanical System Efficiency (%)	Max. Current (A)
	BN	BS		
1	35	43	35	22.48
2	43	38	35	21.89
3	35	43	55	14.31
4	43	38	55	13.93
5	35	43	70	11.24
6	43	38	70	10.94

Significantly higher current is drawn with reducing mechanical system efficiencies. Not only is this indicative of a severely degraded system, the risk of overcurrent becomes more probable (peak current of the PMSM rated at 28.7 A as specified in Table 7).

Faulty State

Lower values of mechanical system efficiencies were modelled to represent faulted states of the EMA. The results of which are shown in Table 14.

Table 14. Maximum I_q Currents Under Varying Contact Angles for All Speeds (Faulty States).

Test Case	Demand Speed (RPM)	Contact Angle (deg)		Max. Current (A)
		BN	BS	
1	3000	35	35	31.55
2	3000	43	43	31.41
3	3000	38	38	30.27
4	1500	35	35	15.77
5	1500	43	43	15.71
6	1500	38	38	15.14
7	500	35	35	5.26
8	500	43	43	5.23
9	500	38	38	5.04

More specifically, the onset of ballscrew jamming was modelled by reducing the relative velocities between the ball and nut, and ball and screw. Table 15 shows the resulting maximum currents of such scenarios with simulations run at 3000 RPM demand speed.

Table 15. Maximum I_q Currents for Reducing Relative Velocities (close to 0) Between Ball-Nut and Ball-Screw.

Test Case	Conditions	Max. Current (A)
1	Relative velocities close to 0 in BN and BS	61.40
2	Relative velocities close to 0 in BS	52.68
3	Relative velocities close to 0 in BN	45.98

Table 15 shows that significantly more I_q currents are drawn when relative velocities (between B-N and B-S) are set close to zero. More I_q current is drawn for ball-screw interaction especially as this is the most contentious area of friction in a ballscrew (Vahid-Araghi & Golnaraghi, 2011).

Given the simulated data presented so far, further challenges become apparent which may lead to a misclassification of a health state. This can arise from data analysis of motor current signals where information relating to loads, operating speeds and quantification of system efficiency are unknown.

A misclassification can occur during an external disturbance such as gust or aeroloads.

Table 16. Example Misclassification Between Healthy and Degrading I_q Currents at 500 RPM.

Test Case	Mechanical System Efficiency (%)	External Load	Max. Current (A)	Health State
1	70	Yes	2.20	Healthy
2	65	No	1.95	Degrading

Table 16 shows an example of where, for the same demand speed, a misclassification can occur where the healthy signal experiences a higher I_q current than the degrading one due to external load disturbances.

3.4.2 Model-based State of Health Prediction Through Supervised Learning Approach

A total of 667 I_q current datasets were generated with each set processed to obtain peak current values (from steady state ~ 2 to 20 seconds cycle time) for training towards data classification.

The datasets were 'supervised' as the response to each set of variables are known i.e. Healthy, Degrading or Faulty. A sample set of peak I_q currents at 3000 RPM were plotted against their respective health state. The results are shown in Figure 35.

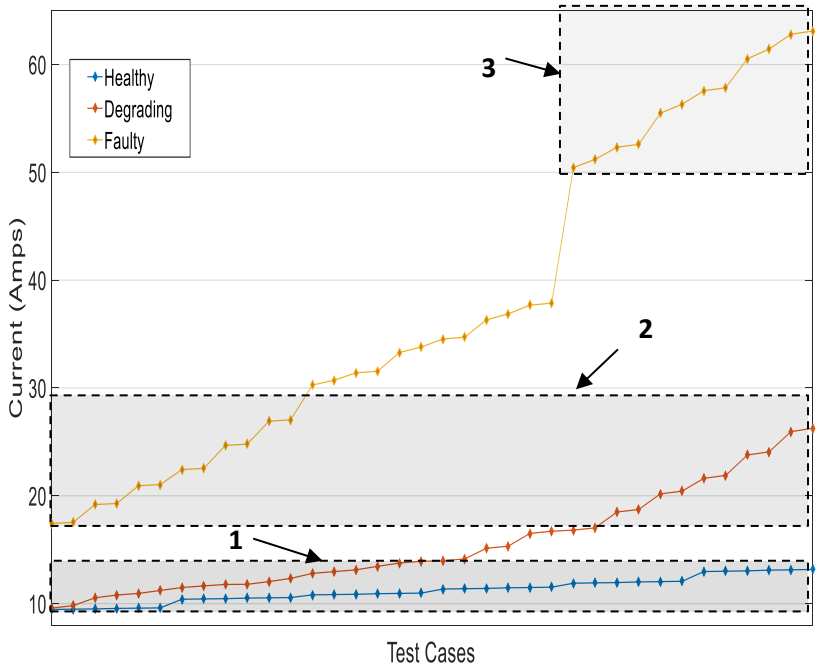

Figure 35. Sample Peak I_q Currents at 3000 RPM – Regions 1 and 2 highlights potential misclassification between Healthy and Degrading datasets respectively and Region 3 distinguishes cases where the onset of jamming could be predicted.

Here it can be seen that the risk of misclassification is much higher between healthy and degrading datasets (as can be seen from the region labelled 1) due to the overlap in observations. False results are also possible for data generated in the lower bounds of the faulty data and higher bounds of the degrading data where the observations are overlapping (as can be seen from the region labelled 2). Despite the possibility of a misclassification, the actual health state of the EMA can be distinguishable outside regions 1 and 2. In particular, the onset of jamming can be predictable with such cases highlighted as shown in the region labelled 3.

In the context of aircraft maintenance of such systems, motor current and speed may be the only parameters available for diagnosis and fault detection during scheduled checks (Isturiz et al. 2012). Therefore, all peak I_q currents and speeds were classified and plotted against their respective health state in a Confusion Matrix. The Confusion Matrix (Figure 36) was generated after training the data using k-NN classification algorithm to show the classification accuracy of these datasets given the conditions.

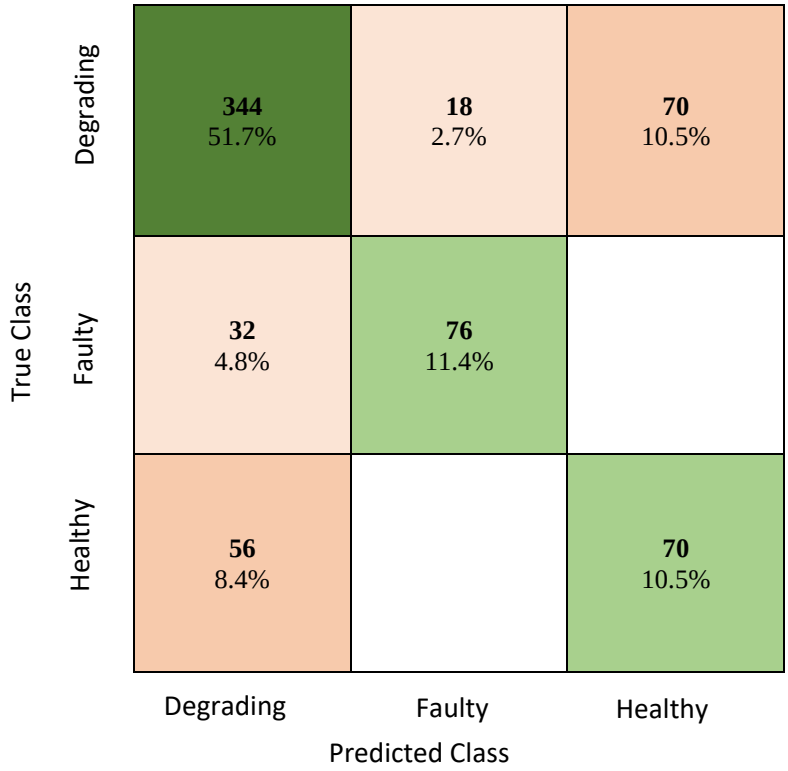

Figure 36. Confusion Matrix for Classifications with Knowledge of I_q Currents and Demand Speeds.

An overall classification accuracy of 73.6% was obtained (summation of green diagonal boxes). The red squares highlight instances of classification uncertainty from the simulated datasets. As can be seen, false results are most prevalent in cases where there is misclassification in data between Healthy and Degrading, and Degrading and Faulty states. It can also be seen that there are no misclassifications between Healthy and Faulted states.

The final step was to predict a classification (health state) based on the k-NN classifier for a new query. The queries to be evaluated were mainly based on situations where the data lies within a region of uncertainty of the trained classification. The queries to be tested are listed in Table 17.

Table 17. Queries to be Tested.

Query	**Demand Speed (RPM)**	**I_q current (A)**
1	500	2.1
2	500	2.8
3	500	4.2
4	1500	5.1
5	1500	12.3
6	1500	12.7
7	3000	10.1
8	3000	23

Query	Demand Speed (RPM)	I_q current (A)
9	1000	10
10	1850	21
11	2600	9

The first set of predictions were generated based on a k-NN classifier with a neighbourhood size of 1. The results of this are presented in Table 18.

Table 18. Predicted Classifications Using 1-NN.

Query	Demand Speed (RPM)	I_q current (A)	Predicted Classification (NN = 1)
1	500	2.1	Degrading
2	500	2.8	Degrading
3	500	4.2	Faulty
4	1500	5.1	Healthy
5	1500	12.3	Faulty
6	1500	12.7	Degrading
7	3000	10.1	Degrading
8	3000	23	Faulty
9	1000	10	Degrading
10	1850	21	Faulty
11	2600	9	Healthy

A classifier can be more robust with more neighbours (Murphy, 2012) so a new set of predictions was generated for the same queries with increasing neighbourhood size. The results of this are shown in Table 19. Classifications highlighted in bold indicate a change in classification through each change in neighbourhood size value.

Table 19. Predicted Classifications Using Different NN Values.

Query	Predicted Classification				
	NN=1	**NN=2**	**NN=3**	**NN=5**	**NN=10**
1	Degrading	Degrading	Degrading	Degrading	Degrading
2	Degrading	Degrading	Degrading	Degrading	Degrading
3	Faulty	**Degrading**	**Faulty**	**Degrading**	Degrading
4	Healthy	Healthy	Healthy	Healthy	Healthy
5	Faulty	**Degrading**	Degrading	Degrading	Degrading
6	Degrading	Degrading	Degrading	Degrading	Degrading

7	Degrading	Degrading	Degrading	**Healthy**	**Degrading**
8	Faulty	**Degrading**	**Faulty**	**Degrading**	Degrading
9	Degrading	Degrading	**Faulty**	**Degrading**	Degrading
10	Faulty	Faulty	Faulty	Faulty	Faulty
11	Healthy	Healthy	Healthy	Healthy	Healthy

As can be deduced from Table 19, some queries exhibited consistency in terms of predicted classification result i.e. queries 1, 2, 4, 6, 10 and 11.

Inconsistency in predicted classification was evident for queries 3 and 8 in particular where ascertaining the true state of health was difficult given the variation in classification of the nearest respective neighbours. Due to the uncertainty of these queries, such classifications can be deemed inconclusive as they can give rise to false predictions.

3.5 Modelling Findings

Based on the simulations, the findings of this investigation indicate that certain features of ballscrew degradation could be identified through analysing I_q currents from high fidelity modelling of dynamic behaviour of the motor and non-linearities in the ballscrew.

The PMSM peak starting current was predicted and shown to be a feature that will vary with speed and load from which could be identifiable through 3-phase and I_q currents. Gao and Kang (2014) conducted modelling and simulation of a PMSM through vector control techniques and also demonstrated this peak starting current behaviour.

The Stribeck friction effect was also modelled in the ballscrew. Through simulation, an additional peak current (due to the Stribeck effect) was identifiable during the acceleration. This condition is indicative of the transition between static and kinetic friction. Degrading features could be ascertained from analysing this peak current which could then be attributed to the presence of static friction within the contact zones in the ballscrew. Figures 30 and 31 demonstrated this effect. Experimental work previously conducted by Jeong and Cho (2002) also highlighted these frictional effects at low velocities. Therefore, the level of ballscrew stiction could be monitored through analysis of I_q currents during acceleration.

The effects of Viscous friction within the ballscrew were also modelled as was shown in Figure 33. The ballscrew mechanical efficiency could be ascertained through motor current. As evident in Figure 33, this is a velocity dependent friction component, therefore, more current was drawn at higher speeds.

Evaluation of these features can provide information regarding the overall ballscrew condition with respect to wear and degradation through service life.

The effects of load were considered to simulate the effects of external loads such as aeroloads from a real application. Given the knowledge about operating speed, load torque could also be inferred through motor current. Jeong and Cho (2002) also demonstrated this feature for a ballscrew driven milling machine as a function of varying cutting forces.

Through simulation, it was also found that analysing a time domain I_q current signal could reveal information regarding ballscrew geometry which may otherwise be challenging to detect in a 3-phase current signal (as was shown in Figure 34). Following this, data classification techniques were applied to classify simulated data of peak I_q currents in steady state conditions (after peak starting current) for different ballscrew contact angles and mechanical efficiencies using kNN classification algorithm. A classification of ~74% was achieved following simulations of 667 peak I_q currents. The performance of this was also tested with new queries. Misclassifications were apparent and increasing the dimensionality of the classifier by including peak starting current information may improve the predictive accuracy.

3.6 Conclusions

Through high fidelity modelling, it was found that it can be possible to identify and characterise dynamic friction behaviour of ballscrew EMAs through motor current.

Simulated data were generated from a high fidelity Matlab/Simulink EMA model and used for data classification using the k-NN algorithm. The EMA was modelled for speed and current control with the PMSM modelled using dq axis transform theory, which enabled analysis using I_q currents. The Stribeck model was included to evaluate friction at a local level of the ballscrew as a function of relative velocities between the ball and nut, and the ball and screw. The EMA model was able to detect changes to the ballscrew contact angles and geometry as well as variation in mechanical system efficiencies using I_q currents. The risk of misclassification was greater when simulations were run with external load disturbances added in. This can make it difficult to detect variations in contact geometry and efficiencies.

Chapter 4: EMA Test Stand Analysis

The chapter presents the findings from a series of experiments conducted on a custom made EMA test stand to validate the modelling and characterise degrading ballscrew conditions through motor current. The results from rogue ball tests are also presented with analysis.

4.1 EMA Test Stand Campaign

A linear EMA test stand was designed and developed to analyse system behaviour and to also use as a means to validate the high fidelity model developed earlier in this chapter. The test stand was also used to get a better physical understanding of how a ballscrew may fail by seeding the EMA with some common mode failures. This would enable the data features to be identified that could be utilised for such failures as well as understanding any emerging system behaviour patterns in the lead up to a failure through motor current analysis.

In addition to validation of normal system behaviour, one of the main objectives of this test stand campaign was to perform seeded failure tests. This included 'rogue ball' testing whereby an oversized ball was seeded to the ballnut to analyse the effects of ballscrew thermal expansion as described in Section 2.2.1.1.

4.1.1 EMA Test Stand Requirements

The first objective from the test campaign was to validate normal system behaviour based on the results produced during the initial modelling and simulation. Therefore, the test stand needed to be designed and developed to match the configuration and system parameters that were used for the EMA systems model (prior knowledge of the motor and ballscrew parameters to be used for testing was known for modelling). Therefore, the EMA test stand consisted of the following components:

1. Ballscrew (specification as per Table 8);

2. Ballnut (specification as per Table 8);

3. Ballnut housing;

4. Bearing blocks;

5. Linear guide assembly – a. linear guide b. bushing c. carriage;

6. Torque transducer;

7. Oldham coupling – motor shaft to torque transducer connection;

8. Bellows coupling – torque transducer to ballscrew connection;

9. Base plate – used for mount bearing blocks and linear guide, and for shaft alignment;

10. PMSM motor and bracket.

Each of these parts are shown in the EMA test stand set up illustrated in Figure 37.

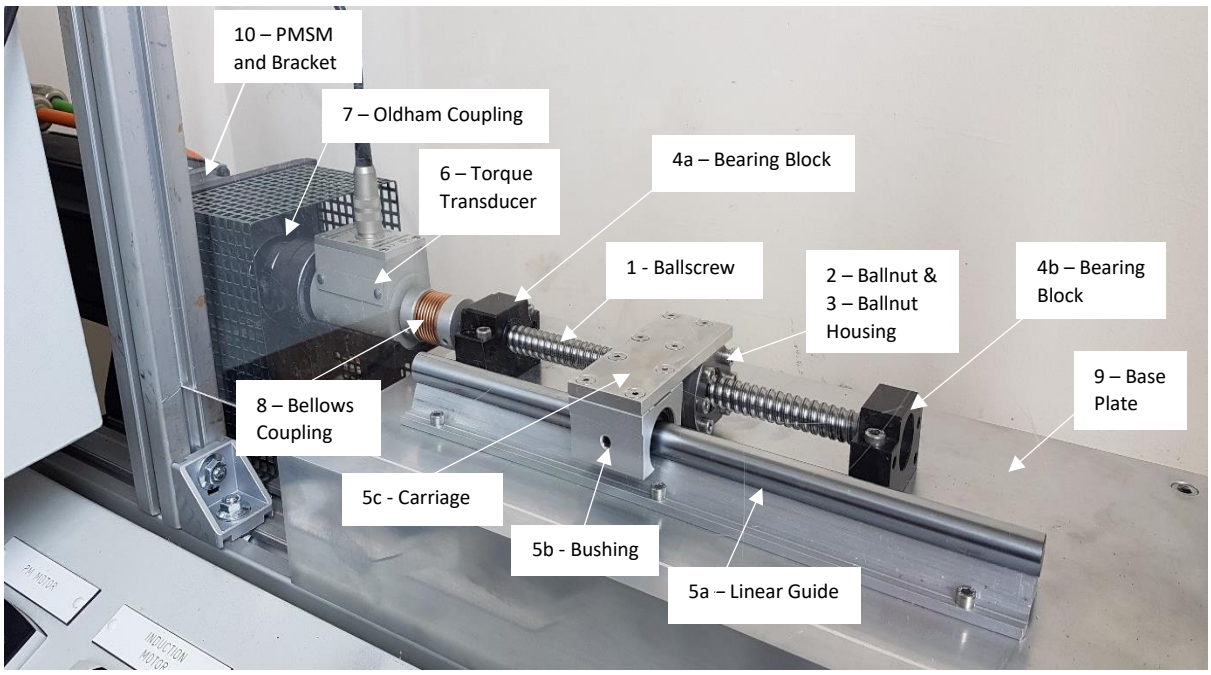

Figure 37. EMA Test Stand Layout.

4.2 EMA Test Stand Test Cases

This section describes the test cases that were performed using the EMA test stand described in Section 4.1. The test campaign was split in to three phases. A preliminary phase was added to ensure correctness and precision in experiment methodology and data analysis. A post experiment phase was also added to ensure accuracy in data reading through noise filtering and signal reconstruction. These phases are described in more detail below.

4.2.1 Preliminary Phase – Pre-experiment Procedures

Viscous friction in the bearings (motor and ballscrew assembly) is a temperature dependent feature (REF). The Viscous friction is higher during the first test run of the day or after a lengthy period. It was therefore necessary to perform a warm up run of the EMA stand prior to each experiment. Temperature readings of the motor were also recorded to ensure consistency in temperature during each experiment.

4.2.2 Phase 1 – Obtain Friction Coefficients and Model Validation

One of the main objectives of Phase 1 testing was to verify dynamic frictional behaviour within the PMSM and ballscrew under healthy conditions for feature extraction. Furthermore, the plan was to obtain values of motor current across a speed range to estimate Stribeck friction coefficients for the PMSM and the ballscrew. These friction coefficients were then updated in to the high fidelity model (described earlier in this chapter) for validation. Table 20 summarises the test plan for Phase 1.

Table 20. Phase 1 Test Plan Summary.

Test Number	**Test Stand Configuration**	**Action**	**Objective(s)**
1.1	PMSM only	Collect 3-phase currents across a speed range of 10 – 1000 RPM.	To demonstrate and verify peak starting current and steady state current behaviour for a time series signal. To demonstrate and verify the PMSM dynamic friction behaviour by analysing peak currents over the speed range. To obtain the PMSM Stribeck friction coefficients to update and validate model.
1.2	PMSM + Ballscrew Assembly	Collect 3-phase currents across a speed range of 10 – 1000 RPM.	To demonstrate and verify the ballscrew dynamic friction behaviour by analysing peak currents over the speed range. To obtain the ballscrew Stribeck friction coefficients to update and validate model.

4.2.3 Phase 2 – Demonstrate Stribeck Effects in the Ballscrew through Motor Current

The objective of Phase 2 was to demonstrate the detection in ballscrew stiction through motor current analysis using the EMA test stand. The plan was to seed the ballscrew with an oversized (rogue) ball to replicate the effects of ballscrew stiction. As previously discussed in Section 2.2.1.1, a rogue ball condition may arise due to ball thermal expansion. The diameter of a healthy ball is 3.175 mm for a

16mm diameter ballscrew. For these series of experiments, 1 healthy ball was replaced with a rogue ball of diameter 3.45 mm. Subsequent data analysis evaluated 3-phase and I_q currents to detect Stribeck behaviour at lower velocities. Table 21 summarises the test plan for Phase 2.

Table 21. Phase 2 Test Plan Summary.

Test Number	**Test Stand Configuration**	**Action**	**Objective(s)**
2.1	PMSM + Ballscrew Assembly (Healthy)	Collect 3-phase currents across a low speed range of 10 – 150 RPM.	To characterise and evaluate Stribeck behaviour through motor current at low speeds for a healthy ballscrew.
2.2	PMSM + Ballscrew Assembly (Healthy)	Collect 3-phase currents at 1000 RPM.	To characterise and evaluate Stribeck behaviour through motor current in the time domain at high speed for a healthy ballscrew.
2.3	PMSM + Ballscrew Assembly (with 1 rogue ball)	Collect 3-phase currents across a low speed range of 10 – 150 RPM.	To characterise and evaluate Stribeck behaviour through motor current at low speeds for a ballscrew with a rogue ball inserted.
2.4	PMSM + Ballscrew Assembly (with 1 rogue ball)	Collect 3-phase currents at 1000 RPM.	To characterise and evaluate Stribeck behaviour through motor current in the time domain at high speed for a ballscrew with a rogue ball inserted.

4.2.4 Post Experiment Phase – Motor Current Signal Noise Filtering and Signal Reconstruction

Due to the presence of noise from electronic switching and other white noise, it was necessary to perform Fast Fourier Transform (FFT) and, signal filtering and reconstruction of the motor current sine wave signal to obtain a cleaner signal to improve the accuracy during data analysis. Figure 38 provides a summary of the methodology in 5 stages to identify the switching frequency from the raw signal, filtering of the unwanted frequencies and reconstruction of the motor current sine wave signal.

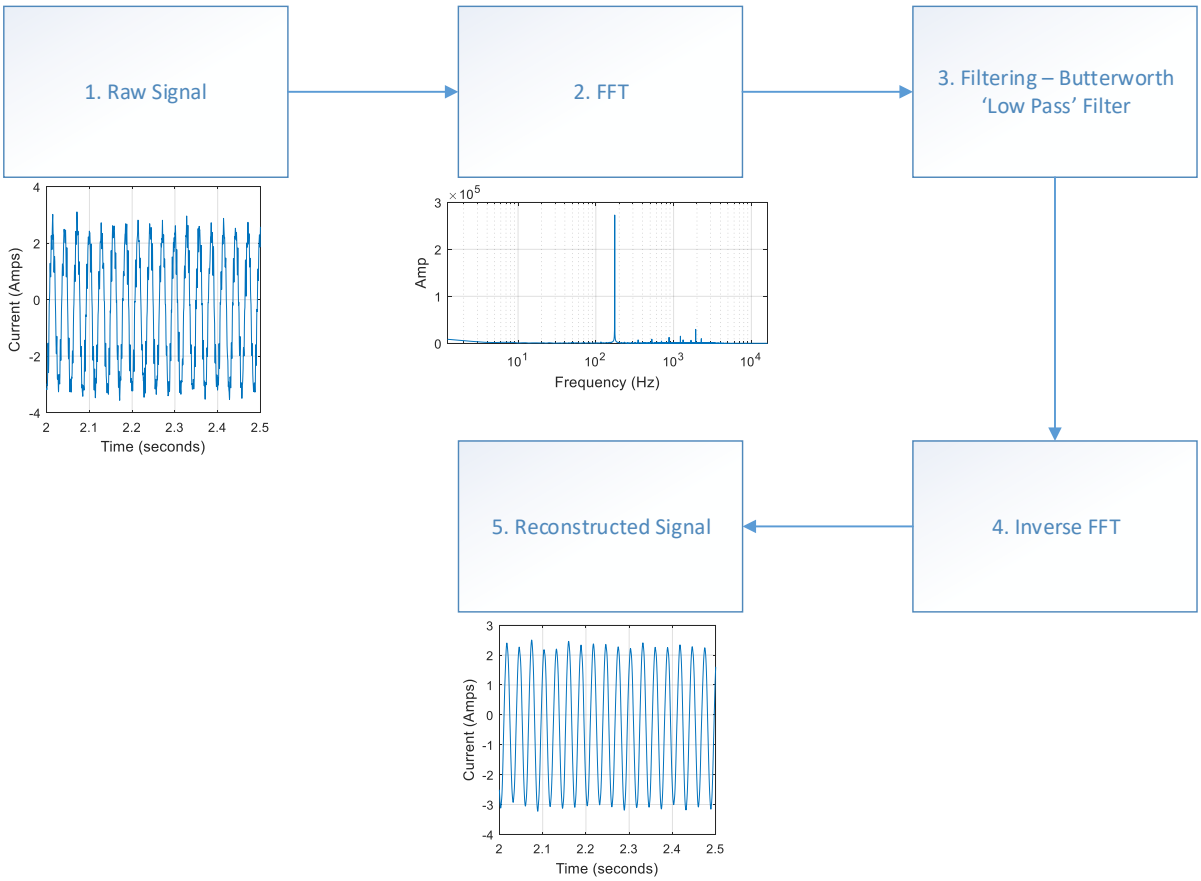

Figure 38. Motor Current Raw Signal Noise Filtering and Signal Reconstruction Methodology.

The full Matlab code used to perform these 5 stages (in Figure 38) can be found in Appendix B with further annotation and elaboration on the use of FFT and Butterworth filtering methods.

4.3 EMA Test Stand Test Results

This section presents the results of the of the EMA test stand campaign. Analysis and key outcomes are discussed based on the 3 phases of test cases that were discussed in Section 4.2.

4.3.1 Phase 1 Results

The objective of this phase of testing was to estimate values of Stribeck friction coefficients for both the PMSM and ballscrew for a healthy system.

4.3.1.1 PMSM Normal Behaviour and Friction Coefficients

Firstly, Figure 39 shows the 3-phase current signal at 1000 RPM (PMSM only) where the peak starting current due to acceleration and steady state current are demonstrated.

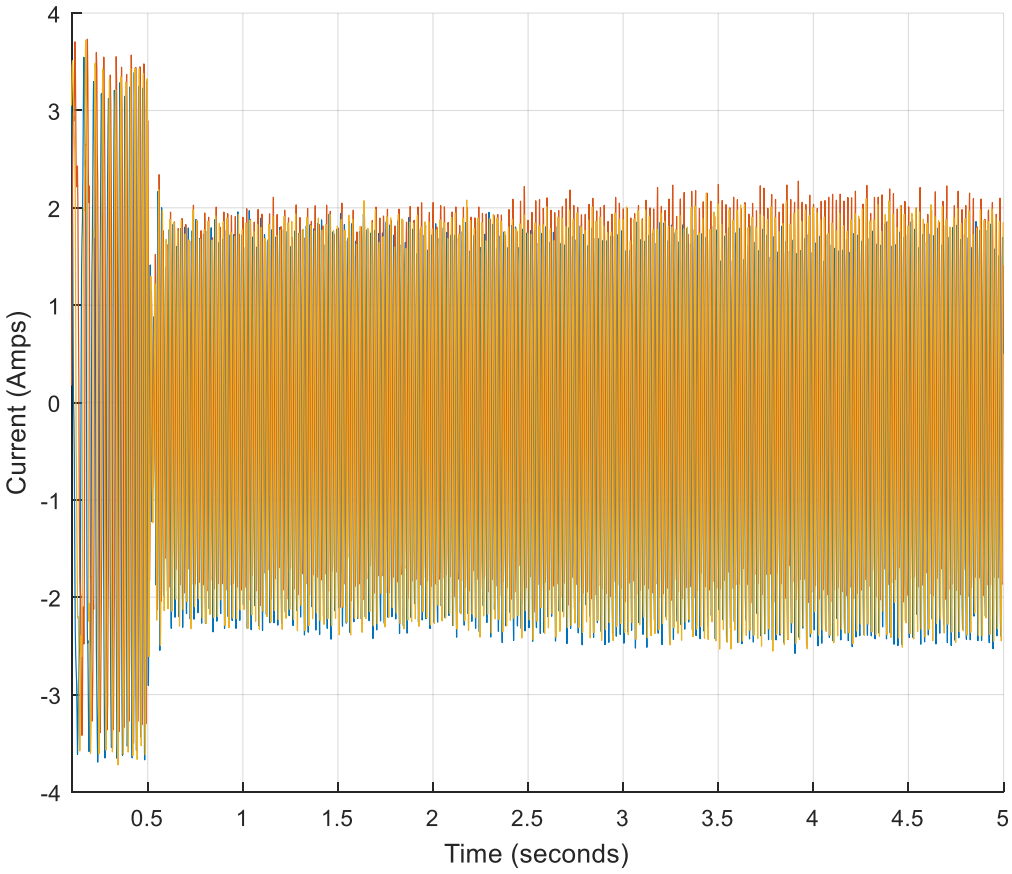

Figure 39. 3-phase Currents at 1000 RPM (PMSM only).

The corresponding I_q current signal is shown in Figure 40.

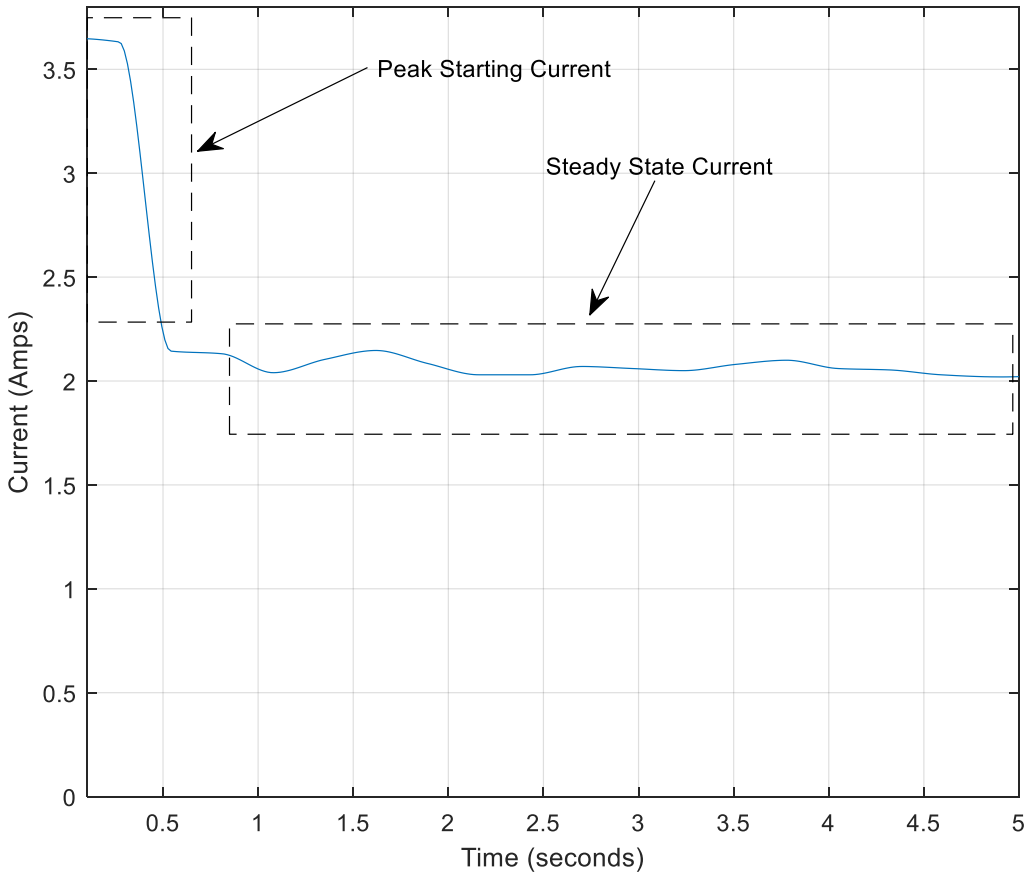

Figure 40. I_q Current at 1000 RPM (PMSM only).

The Park transformation was performed using motor speed values and integrating to get an approximation of rotor angle position. Such approach can be improved by utilising actual rotor angle position data (obtain from hall effect sensors) to minimise the effects of latency. As can be seen in the highlighted regions, the peak starting current is noticeable during the acceleration phase before settling to steady state current when target speed was reached. Figure 41 shows mean current values (during steady state operation) across a speed range of 10 – 1000 RPM for the PMSM.

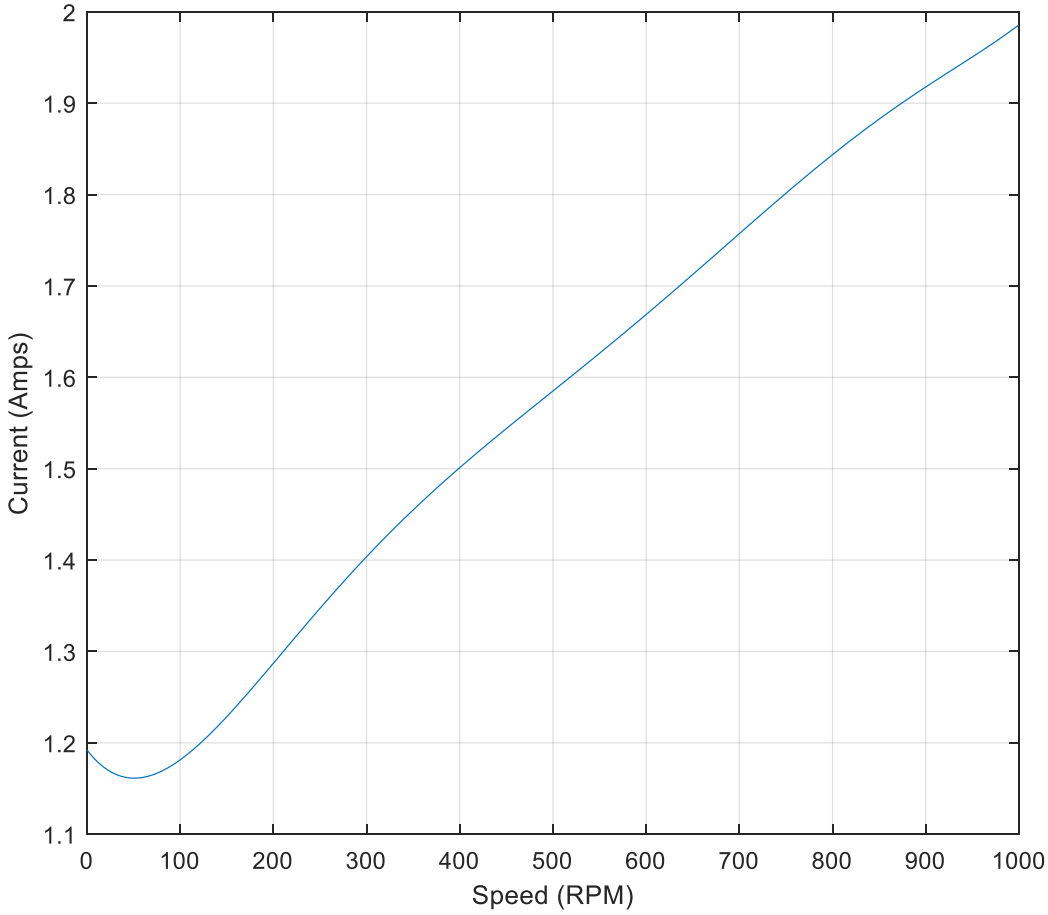

Figure 41. Current v Speed (PMSM Only).

Stribeck behaviour can be observed from the plot in Figure 41. Based on this plot, the Stribeck, Viscous and Coulomb friction coefficients for the PMSM can be estimated using the Armstrong model (Armstrong-Helouvry et al. 1994) where kinetic friction τ_{fk} is expressed by:

$$\tau_{fk}(\omega) = sign(\omega)\left(k_c + (k_s - k_c)e^{-\left|\frac{v_s}{v_0}\right|^{\delta v}}\right) + k_v\omega \quad (28)$$

where k_c, k_v and k_s are the Coulomb, Viscous and Stribeck friction coefficients, respectively.

The calculation of k_c and k_v is based on angular velocity, $\omega \neq 0$. Since it is assumed $L_d = L_q$, the electromagnetic torque can be given by:

$$T_e = \frac{3p}{4}\lambda_{af} I_q \quad (29)$$

A PMSM mechanical model to express friction can be derived by:

$$\frac{d\omega_m}{dt} = \frac{1}{J}(T_e - sign(\omega_m)k_c - k_v\omega_m - T_l + T_c) \quad (30)$$

Where T_l and T_c are the load and cogging torques respectively.

Equations (29) and (30) can be combined to give the following equation:

$$\frac{d\omega_m}{dt} = \frac{1}{J}\left(\frac{3p}{4}\lambda_{af}I_q - sign(\omega_m)k_c - k_v\omega_m + T_l + T_c\right) \quad (31)$$

At constant speed, $d\omega_m/dt = 0$. With PMSM running without load ($T_l = 0$), and cogging torque assumed negligible for this analysis ($T_c = 0$) therefore:

$$0 = \frac{1}{J}\left(\frac{3p}{4}\lambda_{af}I_q - sign(\omega_m)k_c - k_v\omega_m\right) \quad (32)$$

Using Equation (32) and linear data interpolation from Figure 41, values for k_c and k_v were estimated. A value for k_s was also estimated using the shape parameter (δ_v) in Equation (28). The estimated values for PMSM Stribeck, Coulomb and Viscous friction coefficients are shown in Table 22.

Table 22. Estimated PMSM Friction Coefficients.

PMSM Friction Coefficient	**Value**
Viscous	0.083 kgm^2/s
Coulomb	1.86 Nm
Stribeck	1.92 Nm

The estimated PMSM Stribeck friction coefficients were then updated in to the high fidelity model used in Section 3.3 for validation. Using the PMSM model alone, mean current values (during steady state operation) were simulated across a speed range of 10 – 1000 RPM and were evaluated against the results shown in Figure 41 from the test stand. Figure 42 illustrates both sets of results in one graph.

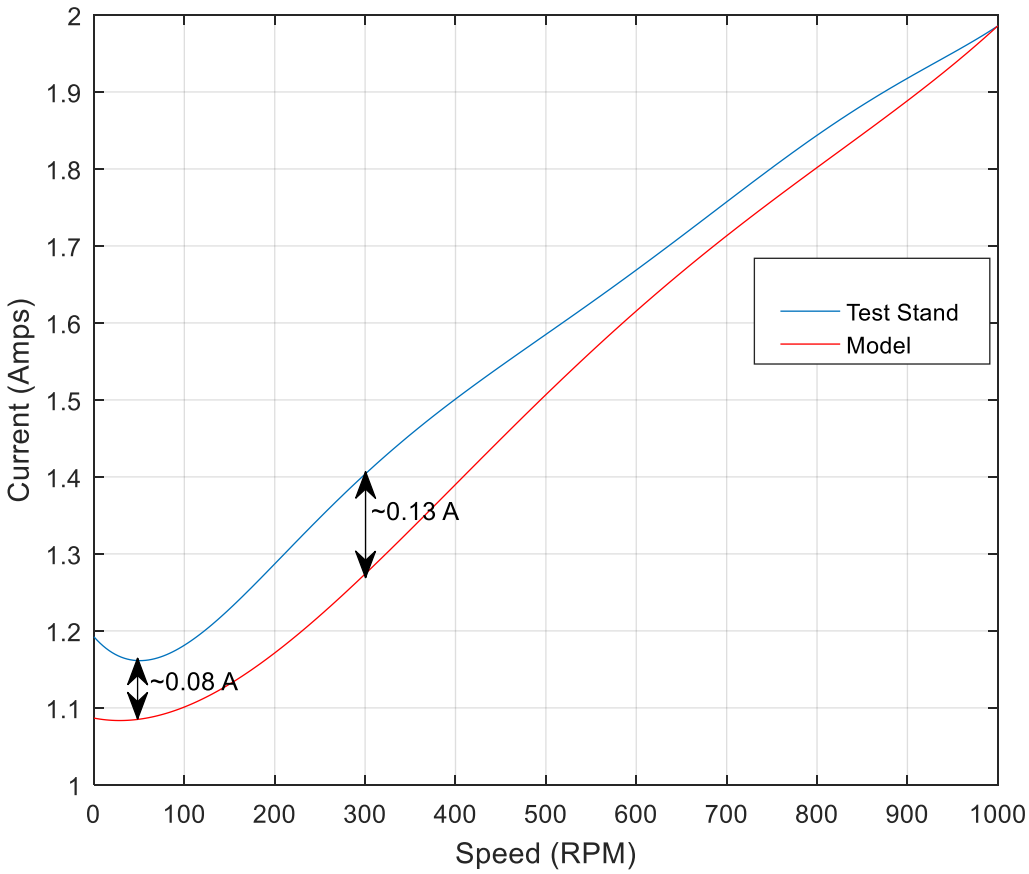

Figure 42. Comparison of PMSM Current v Speed Graphs between Test Stand and Model (with updated PMSM Stribeck Friction Coefficients).

As can be observed from Figure 42, there is satisfactory agreement between the PMSM model and the PMSM used for the EMA test stand. Slight discrepancies are apparent at lower velocities which could be attributed to other non-linear effects from the PMSM. There are also slight discrepancies in Viscous friction which may be attributed to temperature changes during testing.

4.3.1.2 PMSM + Ballscrew Assembly Normal Behaviour and Ballscrew Friction Coefficients

The ballscrew assembly was fitted to the PMSM drive (to complete the full EMA assembly as depicted in Figure 37) with the objective to demonstrate dynamic friction behaviour through motor current for feature extraction and to obtain ballscrew Stribeck friction coefficients accordingly. The ballscrew assembly was new with adequate lubrication on the screw thread and bearings and it was therefore deemed to be in a healthy condition. Figure 43 shows a time series signal for I_q current during start up and steady state operation at demand speed of 1000 RPM.

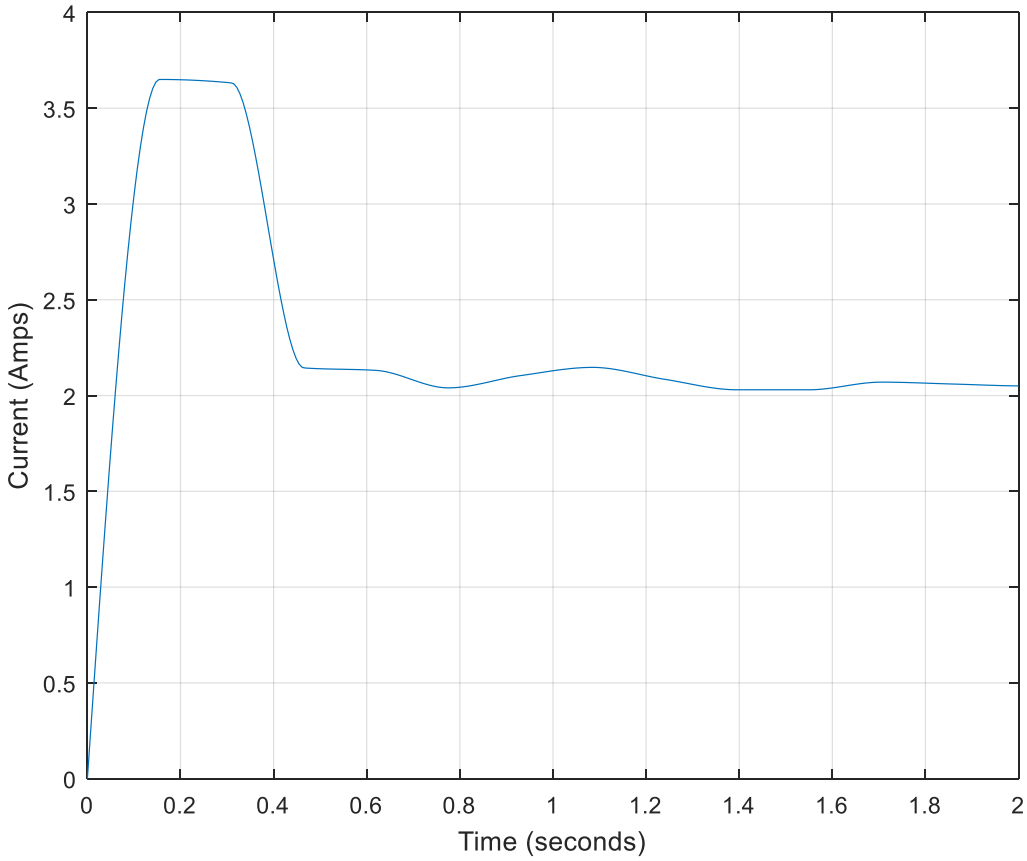

Figure 43. I_q Current at 1000 RPM (PMSM + Ballscrew Assembly).

As expected, the peak starting current due to acceleration is observed as well as the settling current during steady state operation once the demand speed was reached.

Figure 44 shows the mean current value (during steady state operation) across a speed range of 10-1000 RPM. These data were plotted alongside the mean current values generated for the system with PMSM running without the ballscrew assembly to show the variation in motor current due to the additional ballscrew stiction and Viscous loads.

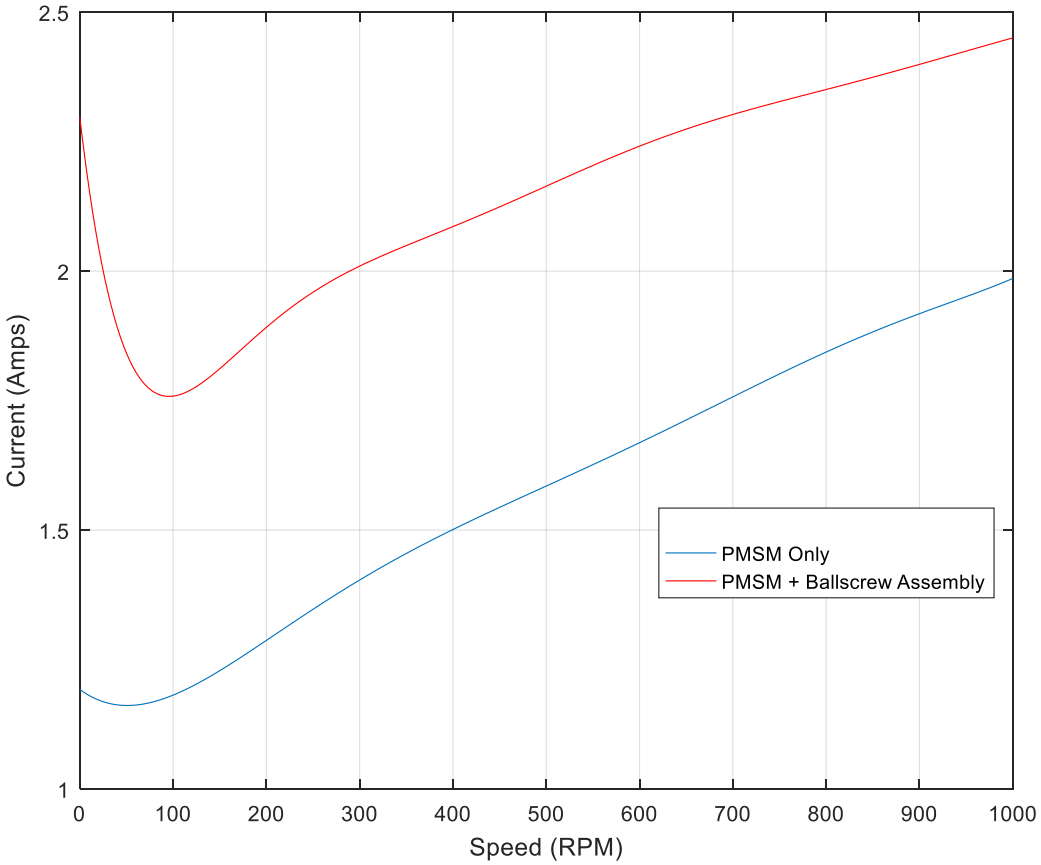

Figure 44. Current v Speed Comparison between PMSM and PMSM + Ballscrew Assembly.

As can be seen from Figure 44, there is more current drawn at lower velocities with the ballscrew assembly due to the added stiction in the system. Subsequently there is also more Viscous friction at higher velocities from the increased load torque.

Using equations (28)-(32), the ballscrew Stribeck friction coefficients were estimated and are shown in Table 23.

Table 23. Estimated Ballscrew Friction Coefficients.

Friction Coefficient	**Value**
Viscous	0.025 kgm^2/s
Coulomb	1.05 Nm
Stribeck	1.68 Nm

The friction coefficients in Table 23 were updated into the high fidelity EMA model for validation. Figure 45 shows a comparison between the model and test stand results for mean currents values in steady state operation across a speed range of 10 – 1000 RPM.

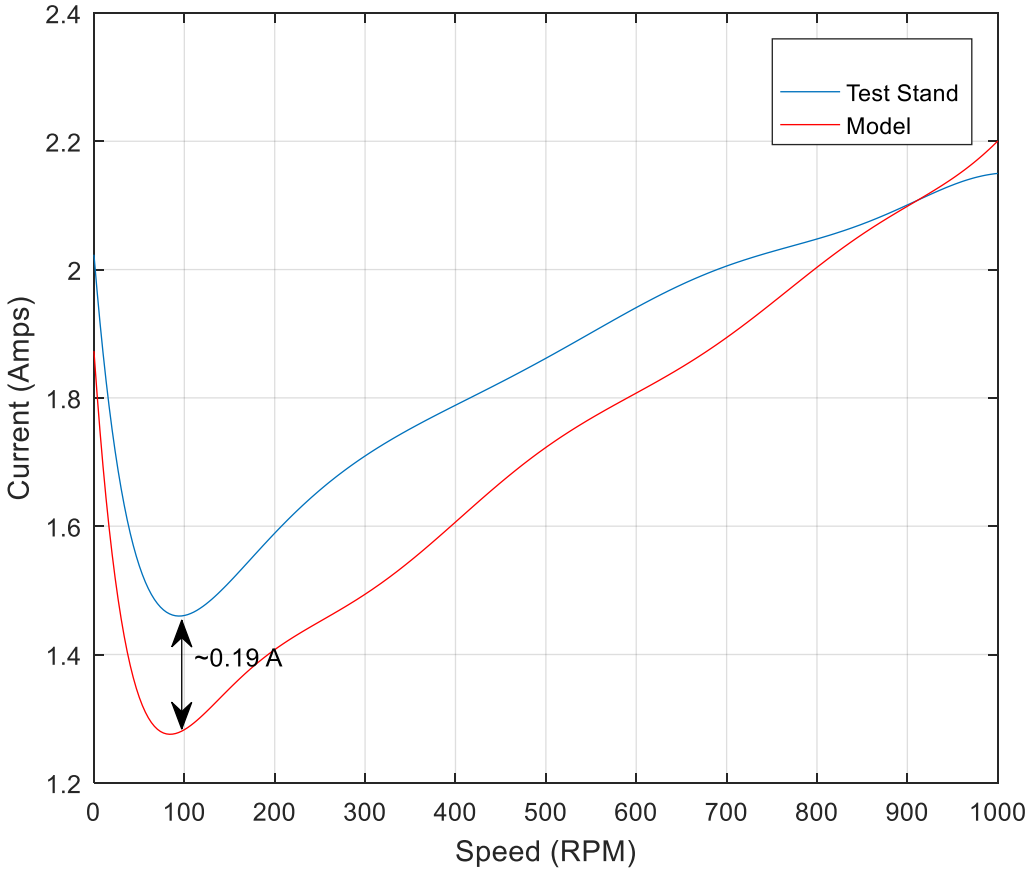

Figure 45. Comparison of EMA Current v Speed Graphs between Test Stand and Model Data.

A few discrepancies can be observed when comparing current v speed between the EMA test stand and the modelled system as can be seen in Figure 45. Firstly, at lower velocities, the Stribeck effect is more apparent in the test stand. The additional stiction could be attributed to the fact that the measurement accounts for stiction in the whole system including the couplings and bearings whereas the model considers the PMSM and ballscrew alone. The modelled system shows a steeper gradient in more current drawn compared to the test stand (that is more noticeable at higher speeds). This could be as a result of thermal effects on the motor whereby the Viscous friction becomes less at higher speeds.

4.3.2 Phase 2 Results

This section presents the results of Phase 2 of the EMA test stand campaign. The objective was to demonstrate ballscrew Stribeck behaviour through motor current for a degrading ballscrew EMA. This was achieved by replacing a healthy ball with a rogue/oversized ball inside the ball nut to simulate a stick-slip condition that could lead to ballscrew jamming.

4.3.2.1 Analysing the Effect of Rogue Ball on Ballscrew Stribeck Behaviour at Lower Speeds

Firstly, mean currents during steady state operation were collected at lower speeds (10 – 150 RPM) for a healthy ballscrew. A rogue/oversized ball was then seeded in to the ballscrew (replacing a healthy ball). Using the ballscrew with rogue ball, these tests were repeated with mean steady state currents collected at lower speeds (10 – 150 RPM). Figure 46 compares the resulting mean motor currents for both these conditions during state operation at lower speeds.

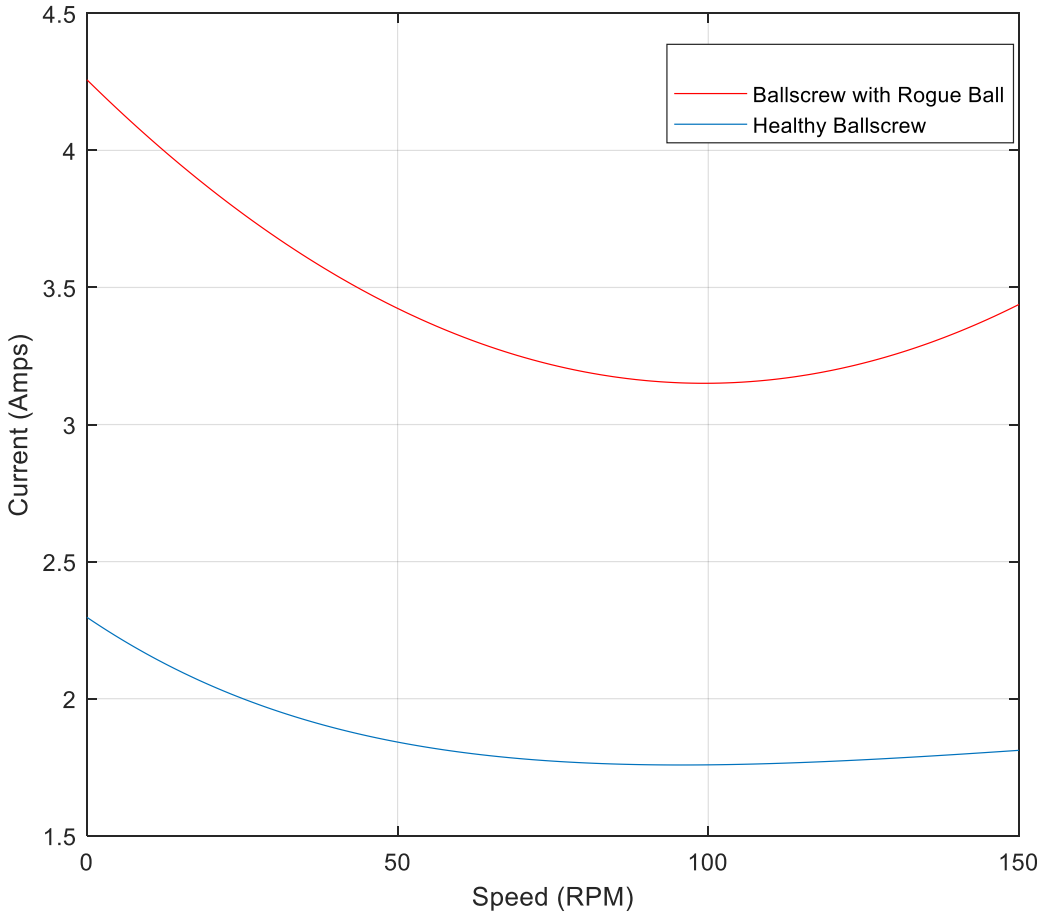

Figure 46. Current v Speed Comparison between a Healthy Ballscrew EMA and a Ballscrew with a Rogue Ball.

As can be seen from Figure 46, there is a significant disparity in motor current at lower speed demands between the healthy EMA and EMA with rogue ball. The Stribeck effect is therefore greater due to the higher stiction caused by the increased contact between the ball and nut and, ball and screw.

4.3.2.2 Identifying Dynamic Friction Behaviour due to Rogue Ball over a Time Series Motor Current Signal

Secondly, it was necessary to analyse the Stribeck effect due to the rogue ball at a higher speed over a time series I_q current signal. Figure 47 shows a time series I_q current signal for a demand speed of 1000 RPM for both healthy ballscrew EMA and ballscrew EMA with a rogue ball.

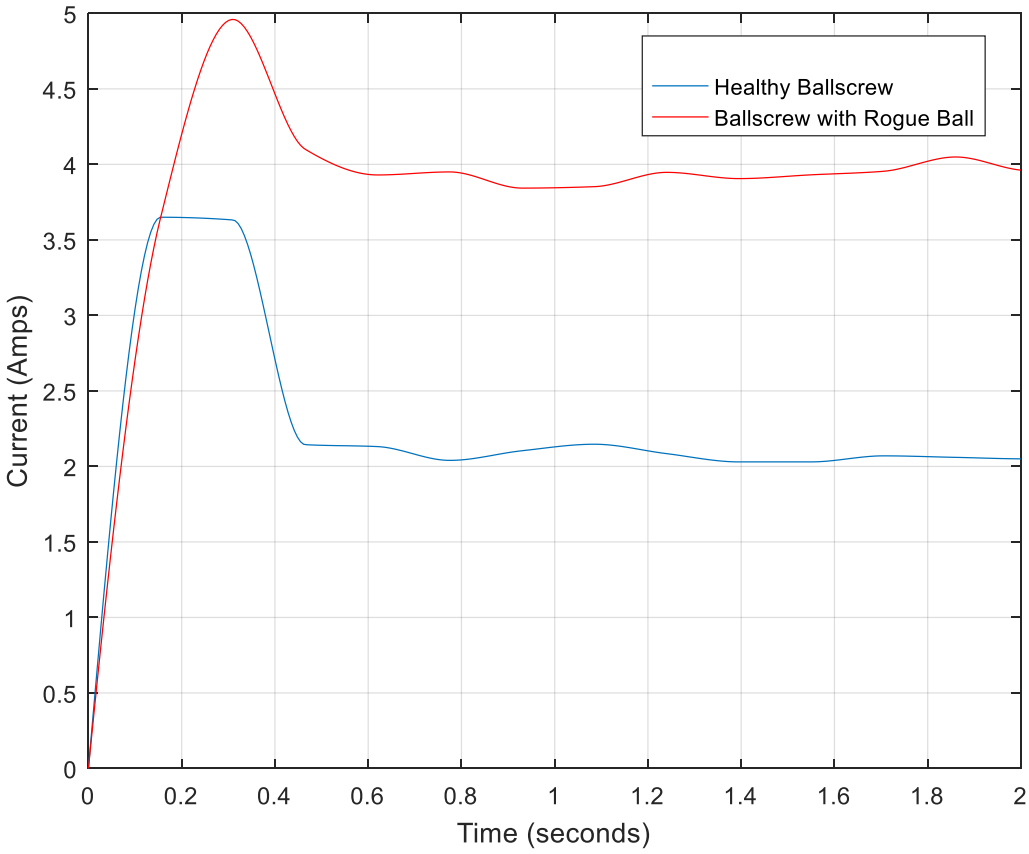

Figure 47. I_q Current Comparison Between a Healthy Ballscrew and a Ballscrew with a Rogue Ball accelerating from 0 - 1000 RPM.

As can be seen from the time series I_q current signals in Figure 47, the Stribeck effect is more apparent and distinguishable in the ballscrew with the rogue ball during acceleration. During steady state operation, the load current consumption is significantly higher (~2A) for the ballscrew with rogue ball compared to the healthy ballscrew. This was attributed to the recirculating rogue ball in the ball nut which caused more Viscous friction which therefore resulted in the additional Viscous loads.

4.4 Conclusions

The EMA test stand campaign was used to validate the high fidelity EMA modelling (from Chapter 3). The Stribeck friction coefficients were estimated and updated in to the model for validation. The results

showed satisfactory agreement with discrepancies apparent due to Viscous friction from temperature variations. There was also variation in stiction which can be attributed to the test stand Stribeck friction estimation accounting for overall system stiction, whereas the model considers the PMSM and ballscrew stiction only.

Rogue ball testing was also conducted on the EMA test stand whereby a slightly oversized was replaced by a healthy ball in the ballscrew. The results showed that the additional stiction can be detected at the beginning of the cycle during acceleration of the EMA through motor current. During steady state operation, the presence of the rogue ball resulted in increased Viscous loads. These features can provide an indication of an impending jamming case in the EMA ballscrew system.

Chapter 5: Aircraft Landing Gear Extension-Retraction System Study

This chapter presents a case study based on an Airbus A320 Nose Landing Gear (NLG) extension-retraction system. This includes a remodelled gear driven actuation system with real A320 NLG extension-retraction end loads data included. The simulations demonstrate feature extraction of dynamic friction behaviour in the system through motor current signals whilst factoring in NLG extension-behaviour and aerodynamic loads.

5.1 Background and Objectives

5.1.1 Background Summary

As mentioned in Chapter 1, this EngD research was motivated by a need in the aerospace industry to replace existing hydro-mechanical systems for EMAs for safety critical actuation applications to achieve MEA. These safety critical applications include the retraction actuator for landing gear extension-retraction systems. Figure 48 shows the location of the retraction actuator as part of a Main Landing Gear (MLG) system.

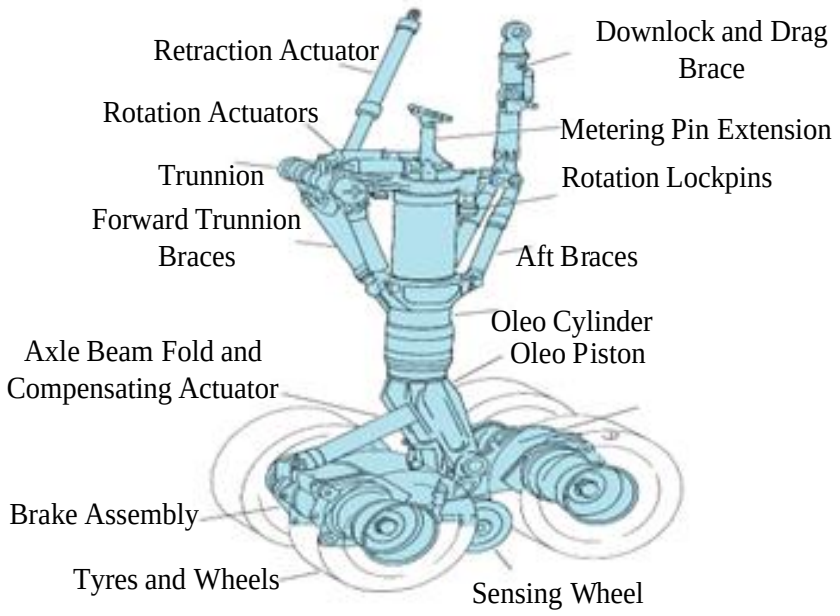

Figure 48. Main Landing Gear (Mouritz, 2012). *Reproduced by permission of Elsevier*.

As previously discussed, concerns in reliability and the need to mitigate ballscrew jamming have resulted in consideration of applying fault diagnostics techniques to identify the onset of jamming using

motor current alone. However, the presence of aeroloads during landing gear extension-retraction makes it further challenging to isolate faults within the drivetrain. Aircraft manufacturers are also reluctant to add more sensors due to added weight implications (Donald et al. 2004) and reduced reliability, hence PHM designers are required to rely on motor current alone to detect the onset of ballscrew jamming.

5.1.2 Previously Published Work

Phillips (2012) conducted a model-based fault analysis of a gear driven EMA system for an A320 NLG retraction actuator. This involved modelling and simulation of the dynamic characteristics in the actuation system by using published information relating to actuator loads to get a truer representation of load torque and inertia through an extension-retraction profile. Faults were simulated by modelling changes to physical parameters such as the frictional coefficient, torque constants and motor resistance to isolate and characterise faults in the EMA drivetrain. Changes to these parameters were reflected through simulated responses in current, torque and speed. During the simulations, some of the seeded faults were not distinguishable from one another thus making certain faults challenging to characterise for applying fault diagnostics. Phillips (2012) commented that rapid extension-retraction can cause control difficulties at the end of the actuation cycle risking potential damage to landing gear structures and bay. Therefore, speed control should be an important factor in the actuator design of such systems.

5.1.3 Objectives

The analysis in Chapter 3 demonstrated that dynamic frictional behaviour could be characterised for a ballscrew in a linear direct drive EMA system through motor current. Bearing in mind the main objective of the EngD, this chapter aims to present an extended analysis for an aerospace safety critical application through modelling and simulation. The A320 NLG extension-retraction system was chosen with the actuator load data from the research conducted by Philips (2012) to be re-used and modelled as part of this study with the aim to see if ballscrew dynamic friction can be evaluated in the presence of aeroloads for feature extraction for use in hybrid fault diagnostics.

5.2 Landing Gear Systems Modelling

The methodology is centred around high fidelity modelling and simulation of a gear driven EMA for a NLG extension-retraction system for an A320 aircraft. Figure 49 provides an overview of the system to be modelled. This consists of a PMSM with speed and current controller, gearbox, ballscrew system and NLG retraction actuator with external aerodynamic forces, F_{ex}.

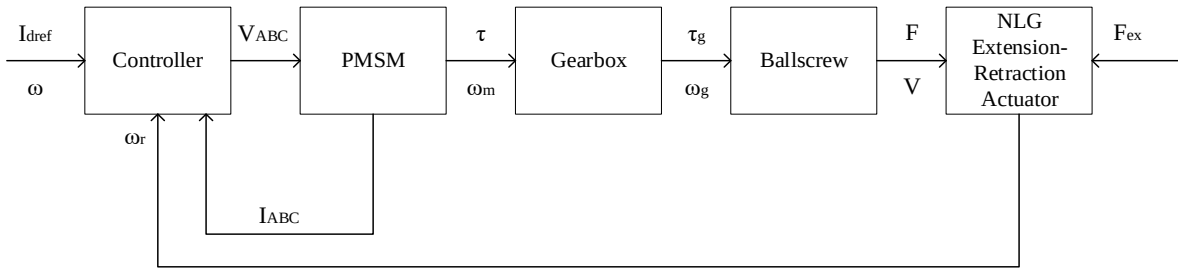

Figure 49. Block Diagram for A320 Nose Landing Gear Extension-Retraction EMA System.

5.2.1 Motor and Motor Controller Modelling

The PMSM was modelled in the same way as was in Chapter 3, whereby the Park's transform was used to reduced 3-phase AC quantities to 2-phase DC quantities. As previously demonstrated, this enabled simplified analysis of the DC quantities which provided in-depth understanding of motor dynamics for condition monitoring and fault detection within the EMA drivetrain.

The motor controller was modelled for speed and current control to enable real time control of torque variation demand, mechanical speed and regulation of the phase currents, thus reducing the occurrence of current spikes during transient operation.

The modelling of both the PMSM and controller was modelled using the same equations (Equations (1) to (12)) from Chapter 3.

5.2.2 Ballscrew Modelling

Given that the build-up of friction was identified as a pre-cursor to EMA ballscrew jamming (Balaban et al., 2009b) and the objective of this study was to evaluate dynamic friction through motor current, a high-fidelity approach was required to model the ballscrew kinematics to capture the main sources of friction (ball and nut, and ball and screw). The ballscrew was therefore modelled using the same methods as in Chapter 3 by considering the contact mechanics of the ball and nut, and ball and screw. This then enabled the calculation of the sliding velocities in these areas to calculate velocity dependent friction using the Stribeck model. The dynamic friction components of the Stribeck model were varied to evaluate ballscrew degradation through motor current.

The modelling of the ballscrew kinematics and Stribeck friction components were modelled using the same equations (Equations (13) to (26)) from Chapter 3.

5.2.3 A320 NLG Retraction Actuator Loads Modelling

The A320 NLG load profiles were modelled using static and aerodynamic load data generated from landing gear kinematic models by Messier-Dowty (Phillips, 2012). The Messier-Dowty models accounts for the kinematic relationship between EMA and the landing gear leg during extension - retraction. For a NLG, the NLG rotation (during extension - retraction) is actuated by the EMA acting on the NLG structure. The load transferred to the EMA during extension-retraction accounts for the NLG weight, the aerodynamic forces on the NLG as well as any acceleration effects during manoeuvres and extension – retraction. There are three different load profiles to consider for NLG extension.

- Load Case 1: 0 knots airspeed, 1g load factor
- Load Case 2: 170 knots airspeed, 1.1g load factor
- Load Case 3: 250 knots airspeed, 1.3g load factor

Load case 1 defines a case where the landing actuator has no aerodynamic loads acting on it. Load case 2 is more representative of a nominal case and load case 3 is an extreme operation envelope case. Figure 50 shows the load profiles for load cases 2 and 3 during NLG extension. These loads include the effects of snubbing and therefore has damping near the end of the extension cycle.

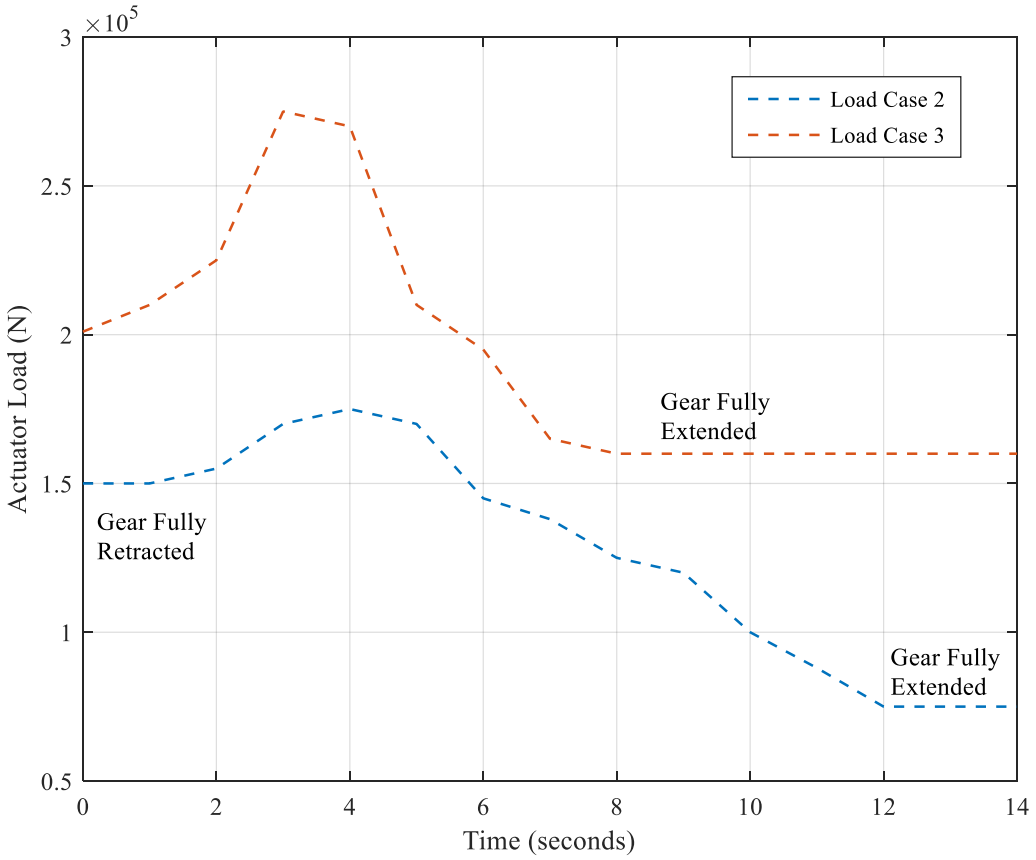

Figure 50. NLG Actuator Loads During Extension.

When the NLG is fully retracted, the actuator should be at a fully extended position. During NLG extension, the actuator pulls against a lever arm which acts about a pivot to lower the NLG. The applied loading drives the NLG motion downwards. For NLG retraction, the actuator extends and pushes against the lever arm and so the applied load works against the NLG which therefore results in higher load generation. At higher loads, the applied load drives the extension motion thus pushing the gear down with the additional loads resulting in a faster extension time.

Failure to extend a landing gear can lead to a catastrophic aircraft condition, therefore, for this study, only NLG extension loads were used for the modelling. The loads were converted to motor load torques and were fed back in to the PMSM torque model to be processed for motor current values. The reflected load inertia to the motor was modelled using equation (13).

5.2.4 Gearbox Modelling

Given the high load torque requirement, a gear driven EMA system model was necessary. The gearing reduces the motor speed at the ballscrew and deliver an increased torque to meet the required load torque values.

5.2.5 Model Parameters

Phillips (2012) used following ballscrew parameters as listed in Table 24.

Table 24. Ballscrew Parameters from Previous Study (Phillips, 2012).

Parameter	**Value**
Ballscrew Lead	6 mm
Actuator Full Extension Stroke	0.234 m

The same ballscrew parameters were used for this case study. Using Equation 20, a lead angle, β of ~5.5° was calculated assuming a ballscrew diameter of 20mm.

Philips (2012) used a Brushless DC (BLDC) Motor with the following parameters listed in Table 25.

Table 25. Motor Parameters from Previous Study (Phillips, 2012).

Parameter	**Value**
Inductance	$1.2x10^{-3}$ H
Supply Voltage	540 V
Motor Resistance	0.395 Ω
EMF Constant	0.221 $Vrad^{-1}s^{-1}$
Torque Constant	0.221 NmA^{-1}
Motor Inertia	$1.02x10^{-3}$ kgm^2
Motor Viscous Load	$2.21x10^{-4}$ $Nmsrad^{-1}$

The same motor specification was used for this study with the exception that a surface mounted PMSM would be used instead. It was assumed that the inductances would be equal on both d and q axes.

5.3 Simulations and Feature Extraction

As mentioned previously, the main emphasis of this study was to determine whether dynamic friction features of the ballscrew could be extracted and analysed through motor current in the presence of high aerodynamic and static loads for a NLG actuator during extension.

5.3.1 EMA System Simulation without NLG loads

The first simulation shows the motor currents without the NLG loads to demonstrate the steady state behaviour of the EMA system using nominal friction values. A ballscrew efficiency of 90% was used which therefore corresponded to a Viscous friction coefficient of 0.01 using Figure 26. A trapezoidal speed profile was used with motor speed demand of 2700 RPM. Figure 51 also shows the resulting 3-phase and I_q currents.

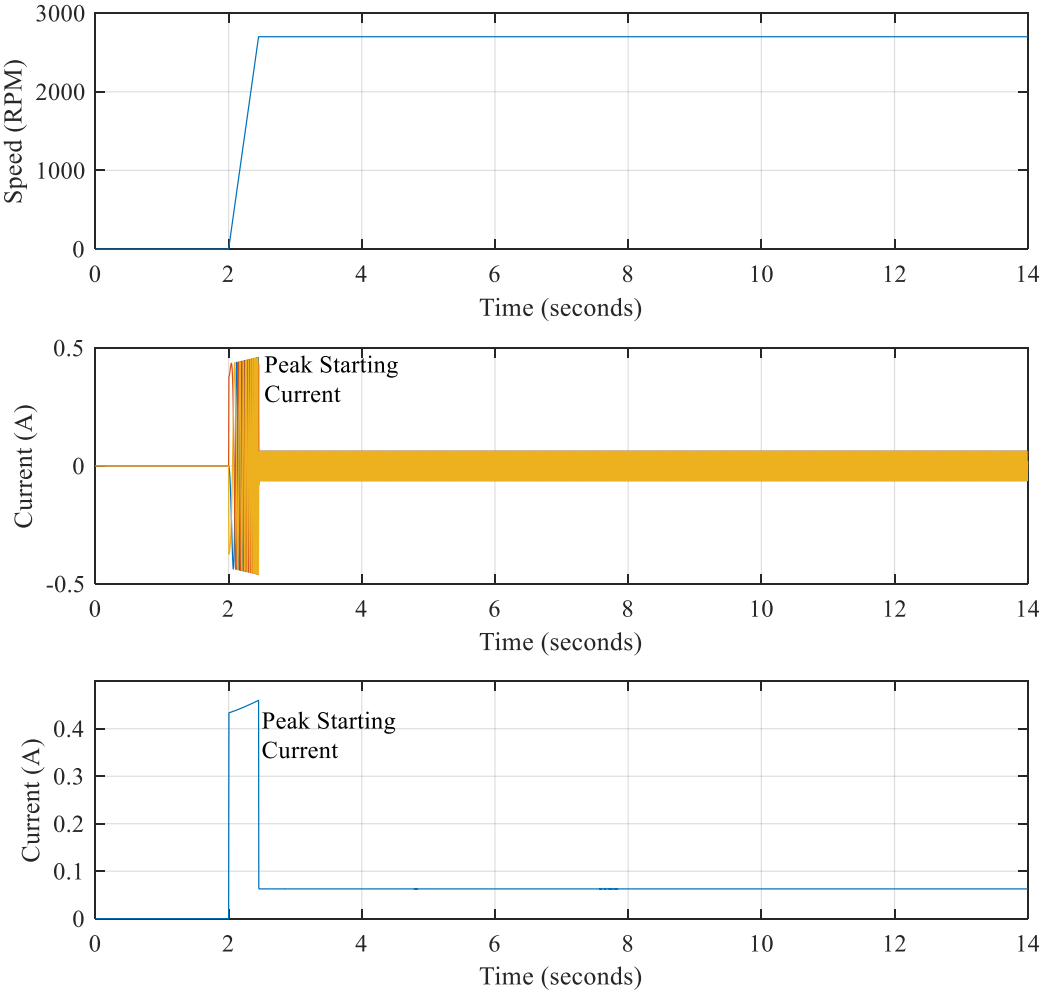

Figure 51. 3-phase and I_q Currents for Speed Profile without NLG Actuator Loads.

As can be seen from Figure 51, the peak currents are noticeable at the transient period of the simulation due to acceleration. Steady state current is then achieved once the command speed has been reached.

5.3.2 EMA System Simulation with NLG Loads

This section introduces the effect of load case 2 to the EMA system. As described in the previous section, load case 2 is the nominal case for the NLG extension-retraction operation during flight. Figure 52 shows the corresponding speed profile and motor currents for this load case with nominal friction values as used in the previous simulation.

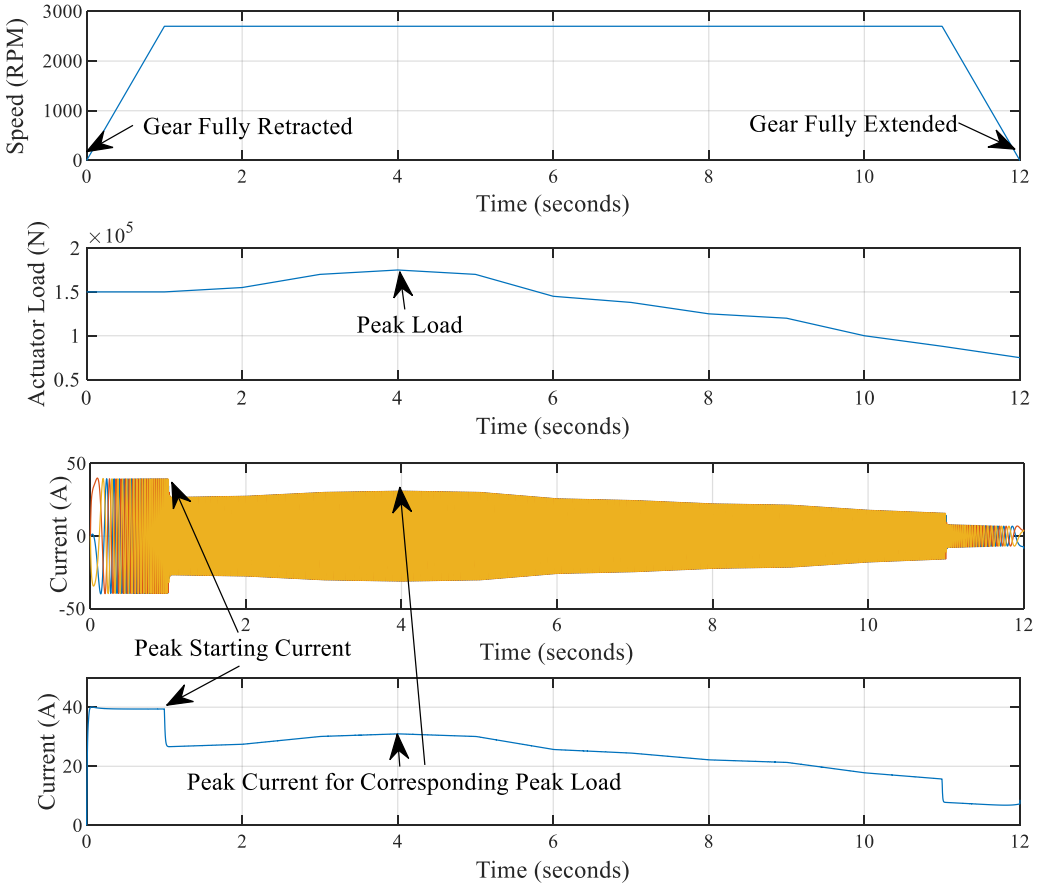

Figure 52. 3-phase and I_q Currents for Speed Profile with Nominal Case NLG Actuator Loads and Ballscrew Friction.

As can be noticed form these simulations, the NLG actuator loads can be inferred through motor current making it possible for feature extraction during NLG extension, in particular for identifying the peak loads as shown in Figure 52.

5.3.3 EMA System Simulations on Nominal case NLG Loads with Ballscrew Stribeck Behaviour

This section modelled the effect of the ballscrew Stribeck behaviour with data from load case 2 utilised again. Increasing values of Stribeck friction were modelled to analyse whether the additional peak starting current feature could be identified as previously demonstrated in Chapter 3. Figure 53 shows the corresponding I_q currents for these simulations.

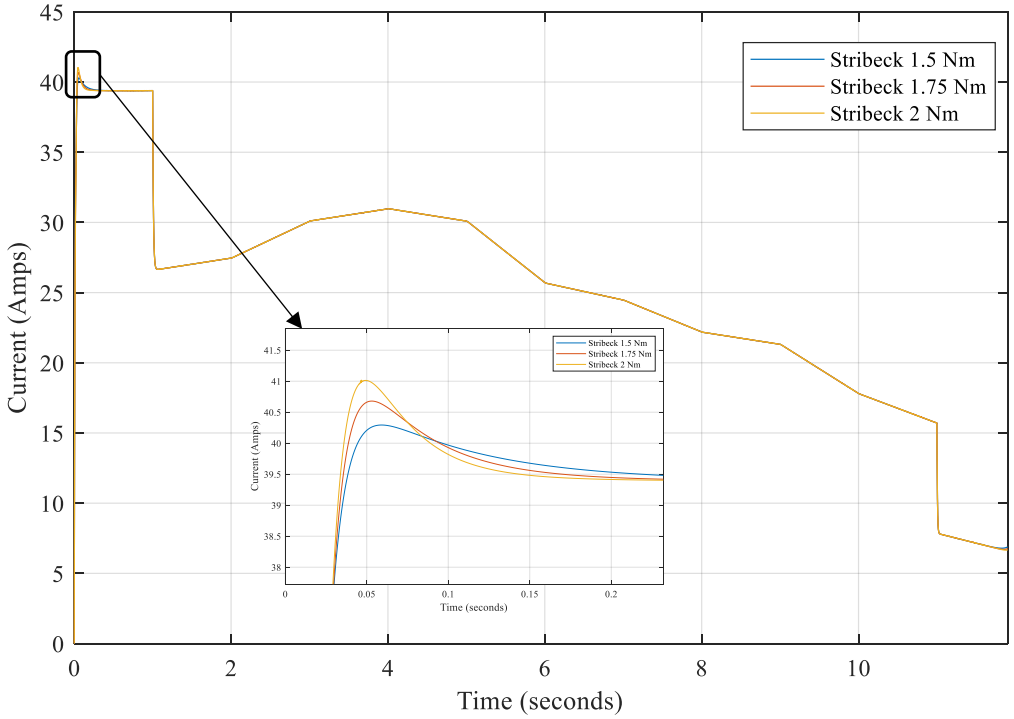

Figure 53. I_q Currents for Speed Profile with Nominal Case NLG Actuator Loads and varying Ballscrew Stribeck Friction Behaviour.

From the zoomed view in the I_q currents, the current spike corresponding to Stribeck behaviour is more apparent with increased severity. As expected, this is occurring at low velocities just as the motor has started to accelerate. These current spikes are characterisable through magnitude and Stribeck effect whereby the maximum peak point indicates the static region between the interacting surfaces within the ballscrew before transitioning to partial and full fluid lubrication as the velocities become high enough for separation.

Therefore, based on these simulations, it may be possible to identify ballscrew stiction at the beginning of the actuation cycle using I_q currents for feature extraction.

5.3.4 EMA System Simulations on Nominal Case NLG Loads with Ballscrew Viscous Friction Behaviour

In Chapter 3, the effects of Viscous friction were simulated to represent a degrading and faulty ballscrew. It was demonstrated that this speed dependent feature could be detected through motor current where increases in I_q were noticeable with increasing values of Viscous friction. This section aims to demonstrate these effects with the presence of high actuator aeroloads.

Figure 54 shows the corresponding I_q currents (for load case 2), for two different Viscous friction cases - healthy (~90% efficiency) and faulty (~50% efficiency).

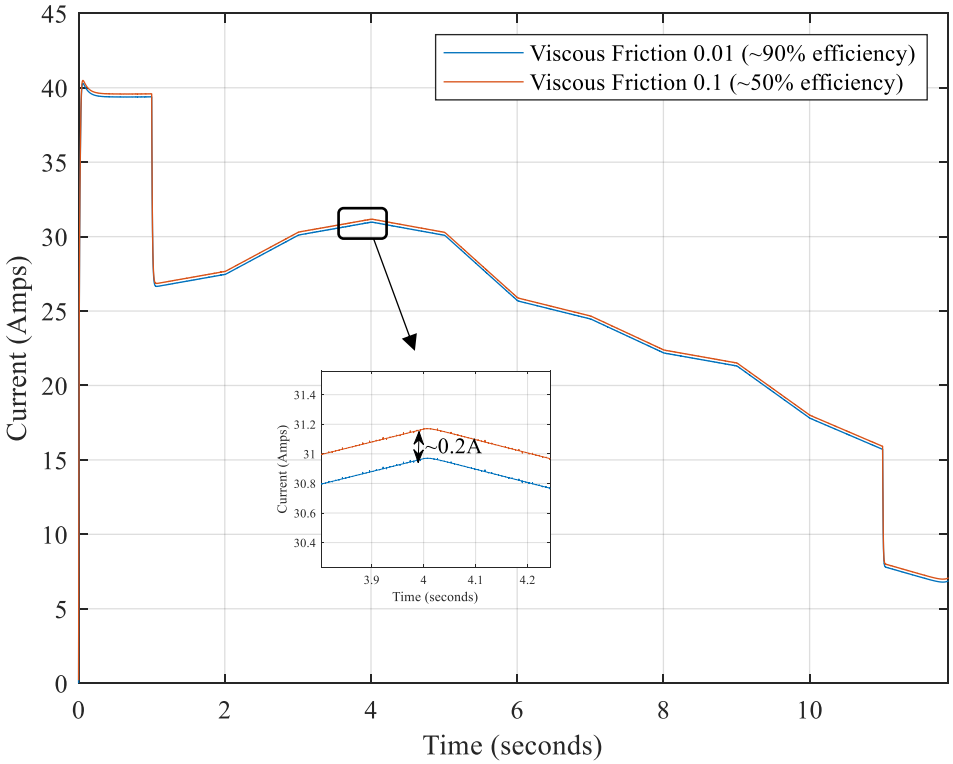

Figure 54. I_q Currents for Nominal Case NLG Actuator Loads and Ballscrew Viscous Friction Behaviour.

From the zoomed view in Figure 54, there is very little discrepancy in motor current magnitudes between healthy and faulty state conditions. This can be attributed to the high load inertia in the system thus making it challenging to characterise ballscrew wear based on motor current alone.

Therefore, it may not be possible to identify the gradual wear of the ballscrew especially in the presence of higher aeroloads during NLG extension which contributes to higher load currents. This problem becomes accentuated for data extracted from a real system, whereby load current could be impacted by other factors. This includes effects of Viscous friction within the motor bearings. For the majority of the time, the landing gear is extended during the descent of an aircraft after a few hours of flight. During cruise level flight, the aircraft system components become cooler including the inactive landing gear system components. Therefore, this could give rise to higher Viscous friction coefficients within the motor bearings for the landing gear extension-retraction EMA systems.

5.4 Conclusions

The main objectives of this chapter were to ascertain whether ballscrew EMA dynamic friction could be analysed through motor current in the presence of aerodynamic loads from an A320 NLG extension-retraction system. High fidelity modelling techniques for an EMA system were applied in the context

of an A320 NLG extension-retraction actuation system. Real aerodynamic loads were used to replicate actuator forces for landing gear extension.

The study found that feature extraction of ballscrew stiction through motor current could be possible at the beginning of the extension-retraction cycle. This could provide aircraft maintenance teams useful information regarding the state of health of the ballscrew as it can be an early indicator for the onset of ballscrew jamming. Ballscrew wear was also simulated to analyse the effect of Viscous friction through motor current signals. It was found that this may not be possible to characterise worsening ballscrew Viscous friction cases as the increased current consumption was seen to be negligible and could be attributed to other factors such as Viscous friction in the motor bearings.

The model used for this case study included a gearbox. In the future, faults associated to gearbox failure should be simulated in order to characterise and distinguish such faults from other parts of the EMA drivetrain. As discussed previously in Section 2.2.2.1, losses in gear systems are primarily attributed to gear tooth friction and lubrication churning losses (Schlegel, Hösl & Diel, 2009).

Chapter 6: Summary and Discussion - Towards a Feature Driven Algorithm to Detect EMA Ballscrew Jamming

This chapter brings together the key outcomes from this thesis towards designing a feature extraction based algorithm to detect EMA ballscrew jamming for an aircraft NLG extension-retraction system. The proposed algorithm design was based around a top-level approach to use hybrid fault diagnostics in which motor current data were extracted and analysed through high fidelity modelling and testing to identify dynamic friction within EMA ballscrews in the context of an A320 NLG extension-retraction system.

6.1 Algorithm Inputs

The outcomes from the previous chapters of this thesis were considered as key inputs towards the proposed algorithm design for monitoring EMA ballscrew dynamic friction through motor current alone. Therefore, this section summarises the fault diagnostics philosophy, EMA availability and cost benefit through hybrid fault diagnostics, and the findings from EMA ballscrew failure analysis from high fidelity modelling and the test stand campaign.

6.1.1 Hybrid Fault Diagnostics Philosophy and Standardisation

Based on a review of literature (Chapter 2), it was decided that a hybrid approach to fault diagnostics would be the optimal top-level approach to mitigate EMA ballscrew jamming. By this, a combination of a high fidelity EMA model and extraction of relevant test stand data were proposed as the ideal approach in performing fault diagnostics for identifying EMA ballscrew jamming (Hussain Y. M, et al. 2018b). As presented previously in Section 2.1.2.3, Figure 55 provides the proposed hybrid approach to hybrid fault diagnostics for EMA ballscrews.

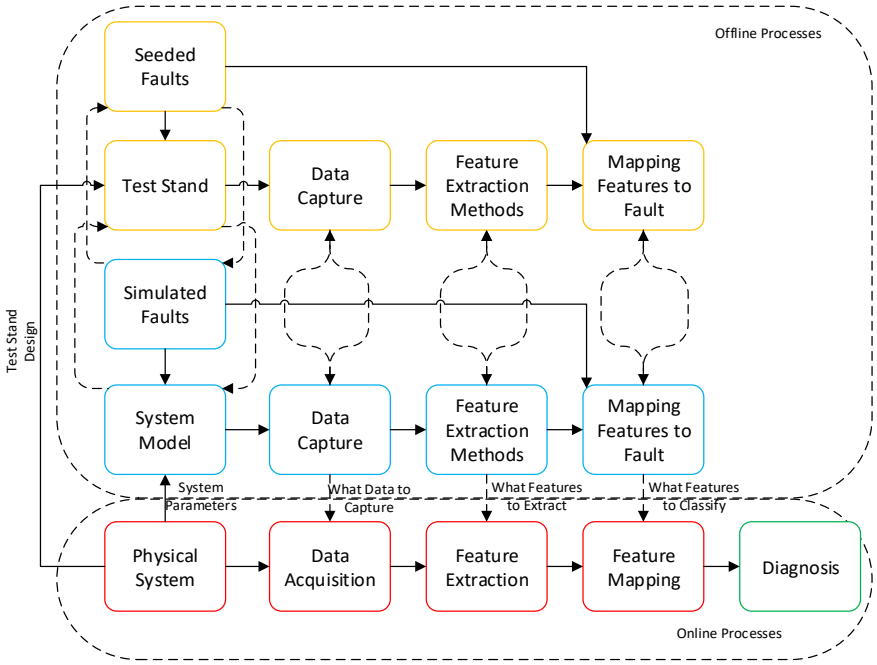

Figure 55. Hybrid Approach to EMA Fault Diagnostics.

The proposed approach considers amalgamating data from a high fidelity system model, test stand as well as from the physical system itself for feature extraction and diagnosis. Since the algorithm is being designed for an actual aircraft system, it was also important to consider the standardisation of the health monitoring holistically in terms of data management, state detection, advisory and decision making by maintenance and operation teams. Jennions (2012) proposed the key components of online and offline health monitoring for CBM as part of Integrated Vehicle Health Management (IVHM) philosophy. These included: Data Acquisition (DA), Data Manipulation (DM), State Detection (SD), Health Assessment (HA), Prognosis Assessment (PA) & Advisory Generation (AG). Bearing in mind that the target application is an aerospace safety critical system, it is necessary to apply certain regulations and standards in conjunction with the algorithm design. Table 26 provides a list of possible regulations and standards.

Table 26. List of Standards for Algorithm Design.

Standard	**Description**
ARP4754A (Guidelines for Development of Civil Aircraft and Systems)	Deals with the development processes which support certification of aircraft systems (Aerospace Recommended Practice, 2010).
DO-178 (Software Considerations in Airborne Systems and Equipment Certification)	Guideline for implementing safety critical software for airborne systems.
ARP 6461 (Guidance on Structural Health	Applicable to civil and military aerospace airframe applications for guidance on the development and certification of Structural Health Monitoring (SHM)

Standard	Description
Monitoring for Aerospace Applications)	technologies. It is also recognised that many stakeholders (such as regulatory agencies, airlines, OEMs, academia, and equipment suppliers) are interested in the Safety and IVHM process of certifying SHM solutions. To that end, a common language, framework, and recommended practices are needed to promote fruitful and efficient technology development (Jennions, 2012).

The intended algorithm was designed assuming that no additional on-board hardware would be required, as the hybrid fault diagnostics approach intends to re-use existing sensors and parameters (motor current, loads profiles) therefore DO-254 (Design Assurance Guidance for Airborne Electronic Hardware) is not required and should be considered for implementation of airborne electronic systems where necessary.

6.1.2 Determining the Frequency of Hybrid Fault Diagnostics Algorithm for Aircraft Maintenance

A case study (separate to this thesis) was conducted to evaluate the effectiveness of fault diagnostics (through CBM) for improving component availability (Hussain Y. , Burrow, Henson, & Keogh, 2016). As captured in Chapter 2, the study involved analysing reliability data for EMAs which revealed an improvement in reliability over time where there were significantly less unscheduled removals of EMAs from commercial aircraft (Quanterion, 2016). Through Systems Dynamics simulation, it was shown that with the latest reliability figures, a rigorous CBM strategy would only see a slight improvement in component availability against a non-CBM approach. However, it was still deeemed necessary to implement a fault diagnostics based CBM strategy (for safety) as a means to mitigate the single point of failure (EMA ballscrew jamming) and prevent a catastrophic aircraft condition. Therefore, implementing a CBM a based strategy (through hybrid fault diagnostics) on a once per week schedule was deemed sufficient.

6.1.3 Characterisation and Feature Extraction of EMA Ballscrew Friction through Motor Current

A major part of the algorithm design shall be to extract indicative features to determine the state of health of the EMA ballscrew to make informed decisions about component and systems maintainability.

In Chapters 3 and 4, extensive analysis was conducted through high fidelity modelling and testing of an EMA test stand to understand whether dynamic friction behaviour of the ballscrew could be captured through motor current alone. The results showed that it can be possible to extract ballscrew Stribeck behaviour through I_q current analysis. Further simulations demonstrated the ability to detect ballscrew defects (such ballscrew contact angle misalignment) through analysing I_q current spikes over a time series signal. Rogue ball analysis was conducted on the EMA test stand to simulate a condition that could result in ballscrew jamming. The results of which demonstrated the increased Stribeck effect further at lower velocities as well as increased viscous friction during steady state operation.

The high fidelity modelling was extended in the context of an A320 NLG extension-retraction system loads case study (Chapter 5). This study demonstrated further the ability to identify ballscrew stiction in the presence of different operating conditions (loads and airspeeds) during NLG extension. However, ballscrew wear cases were seen to be more challenging to extract from I_q currents with worsening mechanical efficiencies showing a variation of ~0.2A which could lend itself to misclassification when determining the state of health.

The simulations were also classified and trained using the k-NN algorithm (a supervised machine learning methodology) to make predictions for ballscrew state of health based on motor current and speed values. Given the A320 NLG load case study, the proposed algorithm design shall utilise NLG loads and airspeed information (obtained from the flight computer) in addition to motor current and speed data to improve state of health prediction accuracy when using the k-NN machine learning approach.

6.2 Algorithm Design and Description

Given the inputs from the previous section, the proposed algorithm was based on determining the state of health (based on dynamic friction) for an EMA ballscrew for an A320 NLG retraction actuator during the extension phase. The algorithm was designed using a ‘decision tree’ based approach through data acquisition, signal processing, utilisation of the key parameters (motor current, motor speed, NLG loads, aircraft airspeed) and data analysis to enable key decisions for maintenance recommendations following analysis for Stribeck behaviour, Viscous friction (mechanical efficiency) and ballscrew mechanical defects. The proposed algorithm design description can be found in Section 6.2.1 and diagram in Appendix D.

6.2.1 Algorithm Description

This section provides further description about the key stages within the algorithm that are presented in Appendix D.

6.2.1.1 Stage 1 – Data Acquisition from Physical System

The first stage was to extract data from the system being monitored. In this study, this was raw motor current data from the PMSM driving the NLG retraction actuator (during extension) for an A320 aircraft.

6.2.1.2 Stage 2 – Signal Processing

Signal processing is required in order remove unwanted frequencies due to electronic switching and white noise to obtain a cleaner signal to improve the accuracy during data analysis to be performed in the subsequent stages of the algorithm. In Section 4.2.4, a series of procedures was conducted to mitigate the frequencies due to electronic switching and white noise through FFT analysis and low pass filtering. Inverse FFT was then applied to reconstruct a clearer signal. This process is illustrated in Figure 56 and can be utilised as part of the algorithm design.

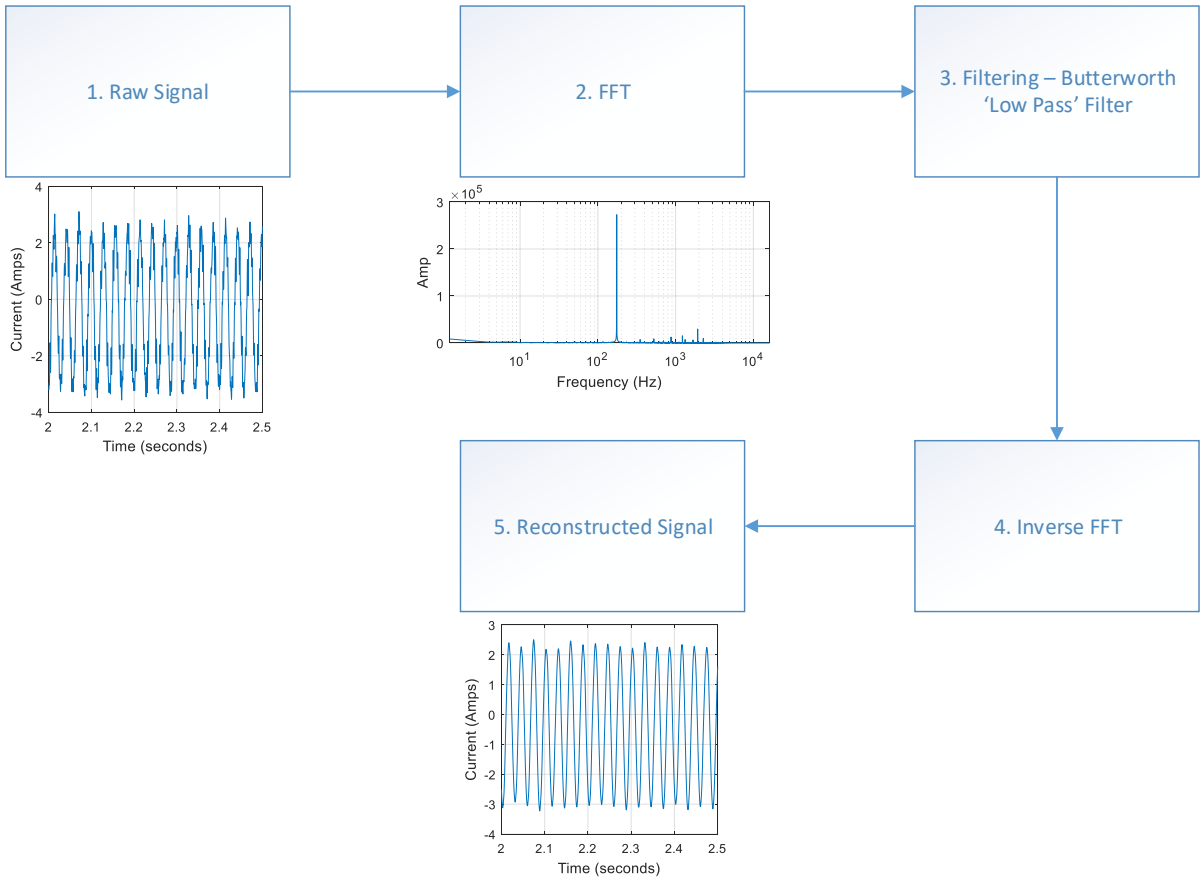

Figure 56. Motor Current Raw Signal Noise Filtering and Signal Reconstruction Methodology.

It should be noted that real-time experience would be required to determine the actual harmonics of the system being monitored from the aircraft for more accurate signal processing.

6.2.1.3 Stage 3 – Parks Transform of Reconstructed Signal

This stage would involve performing Parks transform to the 3-phase current signals to obtain I_q currents which would be utilised for analysis. As demonstrated in Chapters 3-5, this will enable simplified analysis of DC quantities and will provide in-depth motor understanding for condition monitoring and fault detection in the subsequent stages.

6.2.1.4 Stage 4 – Flight Computer Data Input

In this stage, data from the flight computer can be obtained to provide information about the aerodynamic loads and airspeed experienced on the NLG extension-retraction actuator during retraction. Knowledge about these parameters will aid condition based feature extraction through model-based analysis.

6.2.1.5 Stage 5 – Model-based Analysis

Given that the parameter (motor command speed) and operating conditions (NLG loads and airspeed) are now known, a simulation can be performed using the high fidelity modelling approach (as demonstrated in Chapter 5) for a healthy condition using the above inputs. This will enable the end user to obtain a motor current signal that can be analysed against the actual system out for discrepancies.

6.2.1.6 Stage 6 – I_q Current Analysis

By analysing the I_q current signal generated from the model (Stage 5), and from the reconstructed signal from the application (Stage 3), a more in-depth feature extraction based analysis can be performed by looking for anomalies due to ballscrew stiction, wear and other mechanical faults. This is explained further in Stages 7, 8 and 9.

6.2.1.7 Stage 7 – Stribeck Behaviour Analysis

The first part of the state of health detection is to analyse the time series I_q signals during acceleration for ballscrew stiction. As demonstrated in Chapters 3 – 5, the Stribeck peak can be identified as the motor begins to accelerate which can provide an indication on the level of stiction (and therefore jamming) within the ballscrew. Based on the analysis conducted in Section 5.3.3, a threshold was estimated such that should the Stribeck peak exceed 1A from a healthy case, this should be alerted to line maintenance for further investigation. As can be seen from Figure 57 (Appendix D), a prompt is

given to conduct reactive maintenance which would involve workshop level inspection of the EMA drivetrain to identify the source of stiction. Otherwise, the fault diagnostics engineer should proceed with the next stage to analyse for other faults.

6.2.1.8 Stage 8 – Viscous Friction and Mechanical Efficiency Analysis

This stage evaluates the steady state part of the I_q current signal where the level of viscous friction and therefore ballscrew mechanical efficiency can be estimated to provide an indication of ballscrew wear. The recorded data would be compared against modelling, test stand and previous in-flight data as part of a supervised learning approach through use of k-NN algorithm. Recommendations for maintenance is raised if the ballscrew is estimated to be less than 80% efficient which is below the threshold of a healthy system.

6.2.1.9 Stage 9 – Identification of Current Spikes during Steady State Operation

This stage analyses the time series I_q current signal for any spikes during steady state operation. As demonstrated in Section 3.4, current peaks could appear due to the misalignment in ballscrew (ball and nut, and ball and screw) contact angles. Maximum and minimum values would be collected and be analysed through a supervised machine learning approach (k-NN algorithm) to determine the state of health. The k-NN algorithm would be trained based on previous flight data experience as well as model-based and test stand data. Should a peak I_q current exceed a discrepancy of 1A, a fault would be alerted to maintenance for further workshop level inspection and potentially replacement of the EMA ballscrew.

6.2.1.10 Stages 10 and 11 – No Fault Found and Repeat Process

Reaching Stage 10 indicates that the fault detection and diagnostics has shown that the EMA ballscrew is in a healthy and airworthy condition with no fault found. Following this, the process should be repeated once per week (or every 15 flight cycles) to provide efficient and regular fault diagnostics and condition monitoring of the EMA ballscrew for the NLG extension-retraction actuator.

6.3 Conclusions

Given the inputs and key findings from the research, a flowchart and decision tree based algorithm was proposed for diagnosing EMA ballscrew jamming and potentially other faults for an A320 NLG extension-retraction actuator. The algorithm design was based around performing offline maintenance checks on accumulated flight data (motor current signals) on a weekly basis. The diagnostics were based on extracting dynamic friction features of the EMA ballscrew through I_q currents which also involved

a comparative analysis (hybrid approach) against previous flight data, high fidelity model-based data as well as test stand data.

The proposed algorithm will need further work in terms of validation. This would include improving the accuracy of the thresholds which would improve the efficacy and technical maturity of the algorithm. This would however, need to be considered on a case by case basis for other systems. A formalised process defining the steps to industrialisation would also need to be completed in order to demonstrate compliance to the standards listed in Section 6.1.1.

Chapter 7: Conclusions

This chapter reflects on the research problem stated at the beginning of the thesis along with the methodologies employed to solve the problem. The key findings and contributions to knowledge are summarised as well as the impacts to Stirling Dynamics and industry. The limitations of the research are addressed with suggestions for further work listed.

7.1 Summary of Key Findings

This investigation was focused around the topic of MEA. One of the key targets to achieving MEA is to introduce EMAs in place of traditional hydromechanical systems for use in safety critical applications such as landing gear and primary flight control systems.

However, as addressed in Chapter 1, the technical challenge for EMA implementation is the risk of EMA ballscrew jamming which could lead to failure to extend the landing gear or the loss of flight control functionality. This formed the basis of the investigation.

In Chapter 2, it was found that existing fault tolerant designs of EMAs could mitigate ballscrew jamming, however, they may add complexity which could therefore impact the system reliability and maintainability. Health monitoring of such systems was also considered as a methodology to mitigate jamming whereby previous investigations and case studies employed the use of model-based analysis, experimentation through use of a representative test stand and a combination of both. A challenge for applying health monitoring in the context of aerospace safety critical actuation systems is that sensing is limited to using motor current only. It was therefore decided to opt for a health monitoring based methodology through a hybrid approach to fault diagnostics with focus on extracting physical features from motor current signals to ascertain the state of health of the ballscrew which would also improve the understanding of the ballscrew physics of failure.

The hybrid approach relied on the development of a high fidelity model of the system to begin with. As documented in Chapter 3, a high fidelity model of a direct drive linear EMA system was developed with speed and current control. The model was utilised for simulations and was able to demonstrate the feature extraction of ballscrew dynamic friction and ballscrew faults through I_q current analysis.

In Chapter 4, a representative EMA test stand was designed and built based around the high fidelity model from Chapter 3 for validation of the EMA dynamic behaviour and also to update the motor and

ballscrew friction coefficients in to the model. The model showed satisfactory agreement with the test stand following friction coefficient updates with some discrepancies recorded due to temperature and other motor losses (copper and stray loads). There were also other discrepancies due to the approximated Stribeck friction coefficient (from the test stand) accounting for overall stiction in the EMA drivetrain. The EMA test stand was also utilised to conduct rogue ball testing to simulate a potential ballscrew jamming case. As a result, a more severe Stribeck peak was observed as well as additional Viscous loads. Therefore, based on these results, it would be possible to identify the onset of ballscrew jamming through I_q current signals.

In Chapter 5, the high fidelity modelling was extended and remodelled with gearing for a case study for an A320 NLG extension-retraction system which utilised loads and speed profiles. The modelling analysis showed that it was possible to identify the onset of ballscrew jamming by evaluating stiction at the beginning of the extension cycle through I_q current signals in the presence of different NLG load and speed profiles. It was found that this may not be possible to characterise worsening ballscrew Viscous friction cases as the increased current consumption was seen to be negligible and could be attributed to other factors such as Viscous friction in other parts of the EMA drivetrain.

Chapter 6 detailed the proposed algorithm towards a hybrid fault diagnostics approach for mitigating EMA ballscrew jamming for an A320 NLG extension-retraction system (using the model from Chapter 5). The algorithm was flowchart and decision tree based whereby the design was based upon performing offline maintenance checks on accumulated flight data (motor current signals) on a weekly basis. The diagnostics were based on extracting dynamic friction features of the EMA ballscrew through I_q currents which also involved a comparative analysis (hybrid approach) against previous flight data, high fidelity model-based data as well as test stand data.

7.2 Relevance of Research to Stirling Dynamics and Industry

This EngD research was conducted in collaboration with Stirling Dynamics. The long-term objective at Stirling Dynamics was to develop health monitoring functionality for their simulation products that use EMAs. The technical objective for Stirling Dynamics was to utilise health monitoring technology and algorithms to reduce downtime due to unscheduled maintenance. The research presented in this thesis focused on using health monitoring to mitigate the onset of EMA ballscrew jamming for aerospace safety critical applications. It is therefore envisaged that the key findings from this research could be applied as part of an integrated health monitoring solution for one of Stirling Dynamics'

products. This could include the use of motor current signals to extract information about ballscrew/rollerscrew dynamic friction.

One of the main points raised from the semi-structured interviews with ballscrew users (as captured in Section 2.4), was the problem of the electrical drives electronically masking the faults in the mechanical part of the drivetrain. Through the analysis in Chapters 3-5 of this thesis, it has been demonstrated that dynamic friction behaviour could be detected through motor current by analysing stiction during transient operation and Viscous loads during steady state operation. Excessive stiction may indicate an impending jamming condition or ballscrew wear, from which could allow the user to perform CBM through a feature driven approach that is customised for the application.

7.3 Limitations of Research and Recommendations for Future Work

This section addresses the limitations of the research as well as provide recommendations for future work. These are discussed concurrently in the following subsections.

7.3.1 Benefits Analysis through System Dynamics Case Study: Limitations and Recommendations for Future Work

The benefits analysis through SD case study (captured as part of EngD but separate to this thesis – see Appendix A) provided a trade-off between two maintenance policies to demonstrate the efficacy of CBM in terms of component availability in an aerospace operations environment. Whilst the analysis was deemed to be a proof of concept based on previous in-service failure rate data and experience, more fidelity could be added to model the impacts of resource management to get a more global perspective and understanding from an airline maintenance and operations point of view and thus improve the business case for CBM. Furthermore, assumptions were made in terms of reduction in reactive and scheduled maintenance from varying CBM frequencies. This requires validation through systems integration to develop a more accurate and realistic model of traditional maintenance impacts due to offline based CBM and subsequently derive in to a cost model.

7.3.2 High Fidelity Modelling: Limitations and Recommendations for Future Work

Dynamic friction behaviour through motor current in the EMA ballscrew was demonstrated through high fidelity modelling of the main contact areas within the ballscrew. Through the case study based on an A320 NLG extension-retraction actuator, it therefore may be possible to detect identify ballscrew

stiction during acceleration through feature extraction of motor current at lower velocities and during acceleration. However, to improve the characterisation of the various types of impending failure features and failure classification accuracy, high fidelity modelling of contact areas within the gearing mechanism (for gear driven EMAs) could be conducted since this could also be a major source of static and dynamic friction.

7.3.3 EMA Test Stand Analysis: Limitations and Recommendations for Future Work

The EMA test stand analysis validated the dynamic behaviour of the ballscrew through motor current analysis. Estimations were made in calculating the friction coefficients in the PMSM as well as the ballscrew. Assumptions were made during the estimation of the ballscrew friction coefficients whereby the calculations included the whole of the mechanical drivetrain. Although deemed negligible, to obtain a more accurate estimation of the ballscrew friction experimentally, it is recommended to approximate the friction coefficients of each item (bearings, couplings etc.) separately to ascertain the decomposition of frictional losses in the mechanical side of the EMA.

With reference to the semi-structured interviews and failure analysis in Chapter 2, it was highlighted that excessive lubrication of the ballscrew could lead to a faulty condition including jamming. It is therefore recommended through EMA test stand analysis to investigate the effects of excessive or loss of ballscrew lubrication to identify and characterise features of such conditions through motor current to supplement the algorithm design.

7.3.4 Algorithm Design: Limitations and Recommendations for Future Work

Assumptions were made when assigning failure detection thresholds based on motor currents during the proposed algorithm design. As addressed in Section 6.3, this would require validation based on more test stand and in-service experience to improve the robustness of the supervised machine learning approach and to also ensure a more accurate state of health estimation for specific applications.

The proposed fault diagnostics algorithm would also require a check to ensure compliance to standards with a view to achieving full implementation and industrialisation.

7.3.5 Recommendations for Future Work to Achieve Full Prognostics Functionality

The high fidelity modelling demonstrated the ability to extract EMA ballscrew faults and dynamic friction features through I_q current signals. Stribeck behaviour was further validated through EMA test stand analysis. Therefore, it can be concluded that whilst progress has been made in the fault diagnostics of ballscrew safety critical faults (through use of offline algorithms), further analysis can be conducted in achieving a full prognostics functionality in terms of determining the remaining useful life of the component.

If considering an offline prognostics functionality that relies on motor current alone, a robust wear model (inferred through motor current) would need to be developed as a key input for deriving the time to failure. This would require additional data and experience primarily from test stand experiments (through characterisable run-to-failure tests) to enable accurate parameterisation of high fidelity models of the EMA system.

Alternatively, for future aircraft, integrated health monitoring solutions may be considered. This could be advantageous through utilising additional sensing such as wear or temperature to supplement the use of motor current signals to improve the reliability of fault isolation and prediction. This is assuming future aircraft systems strive towards weight saving initiatives to therefore consider additional sensing for integrated health monitoring. 'Time to failure' prognostics based functionality could benefit the end user in terms of predictive maintenance to save costs associated to aircraft downtime. Therefore, this functionality could be developed with the business case as a priority for non-safety critical items to begin with to gain experience before moving towards safety critical systems.

References

Abssac. (2020). *Trapezoidal Carbon Steel C45 POWER screw TRC45*. Retrieved from Abssac Precision Motion: https://www.abssac.co.uk/p/Power+Lead+Screws/Trapezoidal+Carbon+Steel+C45+POWER+screw+TRC45/113/#.Xl-CxUrLc2w

Ackert, S. P. (2010, October 1). Basics of Aircraft Maintenance Programs for Financiers. *Evaluation & Insights of Commercial Aircraft Maintenance Programs*.

Adams, C. (2001, October 1). A380 'More Electric Aircraft'. *Avionics Magazine*.

Aerospace Recommended Practice. (2010). *Guidelines for Development of Civil Aircraft and Systems, ARP 4754.* SAE Aerospace.

AIR5713. (2008). *In-service Reliability Data of Continuously Active Ballscrew and Geared Flight Control Actuation Systems*. SAE.

Airbus. (1998). *A319/A320/A321 Flight deck and systems briefing for pilots.* Airbus.

Airlines for America. (2014). *Per-Minute Cost of Delays to U.S. Airlines*. Retrieved December 2015, from Airlines for America: http://airlines.org/data/per-minute-cost-of-delays-to-u-s-airlines/

Armstrong-Helouvry, B., Dupont, P., & De Wit, C. (1994). A Survey of Models, Analysis Tools and Compensation Methods for the Control of Machines with Friction. *Automatica, 30*, 1083-1138.

Balaban, E., Bansal, P., Stoelting, P., Saxena, A., Goebel, K., & Curran, S. (2009a). A Diagnostic Approach for Electro-Mechanical Actuators in Aerospace Systems. *IEEE Aerospace*.

Balaban, E., Saxena, A., Goebel, K., Byington, C., Watson, M., Bharadwaj, S., & Smith, M. (2009b). Experimental Data Collection and Modelling for Nominal and Fault Conditions on Electromechanical Actuators. *IJPHM*.

Balaban, E., Saxena, A., Narasimhan, S., Roychoudhury, I., & Goebel, K. (2011). Experimental Validation of a Prognostic Health Management System for Electro-Mechanical Actuators. *American Institute of Aeronautics and Astronautics*.

Balaban, E., Saxena, A., Narasimhan, S., Roychoudhury, I., Goebel, K., & Koopmans, M. (2010). Airborne Electro-Mechanical Actuator Test Stand for Development of Prognostic Health Management Systems. *Annual Conference of the Prognostics and Health Management Society 2010.* PHM.

Balaban, E., Saxena, A., Narasimhan, S., Roychoudhury, I., Koopmans, M., Ott, C., & Goebel, K. (2015). Prognostic Health-Management System Development for Electromechanical Actuators. *Journal of Aerospace Information Systems*, 329-344.

Ballscrew Services Limited. (2015). Retrieved from Ballscrew Services Limited: http://www.ballscrewservices.co.uk/

Bartos, B. (2016). *Mastering Ball Screws Pt. 1: Steel Ball Recirculation System and Characteristics*. Retrieved from Misumi MechLab: http://blog.misumiusa.com/ball-screw-steel-ball-recirculation/

Bennett, J. (2010). *Fault Tolerant Electromechanical Actuators for Aircraft.* Doctoral Dissertation, Newcastle University, Newcastle, United Kingdom. Retrieved from https://theses.ncl.ac.uk/dspace/handle/10443/990

Bennett, J., Mecrow, B., Atkinson, D., & Atkinson, G. (2011). Safety-critical Design of Electromechanical Actuation Systems in Commercial Aircraft. *IET Electric Power Applications*, 37-47.

Bivona, E., & Montemaggiore, G. (2005). Evaluating Fleet and Maintenance Management Strategies through System Dynamics Model in a City Bus Company. *The 23rd International Conference of the System Dynamics Society.* Boston.

Bodden, D. S., Clements, S., Schley, B., & Jenney, G. (2007). Seeded Failure Testing and Analysis of an Electromechanical Actuator. *Aerospace Conference IEEE*, 1-8.

Bodden, D., Clements, S., Schley, B., & Jenney, G. (2007). Seeded Failure Testing and Analysis of an Electromechanical Actuator. *Aerospace Conference* (pp. 1-8). IEEE.

Boeing. (1994). *757 Operations Manual.* Seattle: The Boeing Company.

Bowden, F., & Tabor, D. (1950). *The Friction and Lubrication of Solids.* Oxford: Oxford University Press.

Byington, C., & Stoelting, P. (2004). A Model-Based Approach to Prognostics and Health Management for Flight Control Actuators. *2004 IEEE Aerospace Conference* (pp. 3551-3562). IEEE.

Checkland, P., & Poulter, J. (2007). *Learning for Action: A Short Definitive Account of Soft Systems Methodology, and itsd use for Practitioners, Teachers and Students.* John Wiley.

Chumai, R. (2009). System Dynamic Modeling of Plant Maintenance Strategy in Thailand. *The 27th International Conference of the System Dynamics Society.* Albuquerque.

Churn, P., Maxwell, C., Schofield, N., Howe, D., & Powell, D. (1998). Electro-hydraulic Actuation of Primary Flight Control Surfaces. *IEE Colloquium on All Electric Aircraft*, (pp. 3/1-3/5).

Collins, A., & Sunstrand, H. (2004). *USA Patent No. US 6776376 B2.*

Collins, D. (2017). *What is back driving and why is it important?* Retrieved from THK: https://www.linearmotiontips.com/what-is-back-driving-and-why-is-it-important/

Cooper, M. (2014). *Simulating Actuator Energy Demands of an Aircraft in Flight.* Cranfield University.

Croke, S., & Herrenschmidt, J. (1994). More Electric Initiative - Power by Wire Actuation Alternatives. *IEEE Proceedings of the National Aerospace and Electronics Conference* (pp. 1338-1346). IEEE.

Cronin, M. (1985). *USA Patent No. US 4530271A.*

Design World. (2015, August). Design World. *2015 Motion Systems Handbook*, p. 30.

Dixon, M. (2006). *The Maintenance Costs of Aging Aircraft.* RAND.

Donald, S., Garg, S., Hunter, G., Guo, T., & Semega, K. (2004). *Sensor Needs for Control and Health Management of Intelligent Aircraft Engines.* NASA.

Edwards, R., & Holland, J. (2013). *What is Qualitative Interviewing?* . Bloomsbury.

Exlar. (2014). Retrieved from Exlar Actuator: http://exlar.com/content/uploads/2014/09/GSX-Catalog-Section.pdf

Federal Aviation Administration. (1997). *Maintenance Review Board Procedures.* Advisory Circular AC 121-22A.

Feldman, A., Kurtoglu, T., Narasimham, S., Poll, S., Garcia, D., Kleer, J., . . . Gemund, A. (2010). Empirical Evaluation of Diagnostic Algorithm Performance Using a Generic Framework. *International Journal of Prognostics and Health Management*.

FMEA-FMECA. (2006). *FMEA-FMECA.* Retrieved from FMEA RPN: http://www.fmea-fmeca.com/fmea-rpn.html

Forrestor, J. W. (1961). *Industrial Dynamics.* Cambridge, MA: The M.I.T Press.

Gao, J., & Kang, J. (2014). Modelling and Simulation of Permanent Magnet Synchronous Motor Vector Control. *Information Technology Control Journal*, 578-582.

Gerada, C., & Bradley, K. (2008). Integrated PM Machine Design for and Aircraft EMA. *IEEE Transactions on Industrial Electronics*, 3300-3306.

Hoffman, A., Hansen, I., Beach, R., Plencner, R., Dengler, R., Jefferies, K., & Frye, R. (1985). *Advanced Secondary Power System for Transport Aircraft.* NASA.

Hussain, Y. M., Burrow, S., Keogh, P. S., & Henson, L. (2018a). A High Fidelity Model Based Approach to Identify Dynamic Friction in Electromechanical Actuator Ballscrews using Motor Current. *International Journal of Prognostics and Health Management*.

Hussain, Y. M., Burrow, S., Keogh, P. S., & Henson, L. (2018b). A Review of Techniques to Mitigate Jamming in Electromechanical Actuators for Safety Critical Applications. *International Journal of Prognostics and Health Management*.

Hussain, Y., Burrow, S., Henson, L., & Keogh, P. (2016). Benefits of Prognostics & Health Monitoring for Aircraft Maintenance using System Dynamics. *3rd European Conference of the Prognostics & Health Management Society* . Bilbao: SAE.

IATA. (2018). *Maintenance Costs for Aging Aircraft.* IATA.

Ismail, A., Balaban, E., & Spangenberg, H. (2016). Fault Detection and Classification for Flight Control Electromechanical Actuators. *Aerospace Conference.* IEEE.

Isturiz, A., Vinals, J., Manuel, A., & Aitzol, I. (2012). Health Monitoring Strategy for Electromechanical Actuator Systems and Components, Screw Backlash and Fatigue Estimation. *Recent Advances in Aerospace Actuation Systems and Components.*

Item Software. (2017). *Reliability Prediction Basics*. Retrieved from Reliability Education: http://www.reliabilityeducation.com/ReliabilityPredictionBasics.pdf

Jabar, B. H. (2003). Plant Maintenance Strategy: Key for Enhancing Profitability.

Jennions, I. (2012). *Integrated Vehicle Health Management: Business Case Theory and Practice.* SAE International.

Jeong, S., & Park, J. (1992). Thermal Expansion Analysis of the Ball Screw System by Finite Difference Methods. *Journal of the Korean Society for Precision Engineering*, 44-57.

Jeong, Y., & Cho, D. (2002). Estimating Cutting Force from Rotating and Stationary Feed Motor Currents on a Milling Machine. *International Journal of Machine Tools and Manufacture*, 1559-1566.

Jiang, H., Song, X., Xu, X., Tang, W., Zhang, C., & Han, Y. (2010). Multibody Dynamics Simulation of Balls Impact-contact Mechanics in Ball Screw Mechanism. *International Conference on Electrical and Control Engineering* (pp. 1320-1323). IEEE.

Jin, W., Chen, Y., & Lee, J. (2013). Methodology for Ball Screw Component Health Assessment and Failure Analysis. *International Manufacturing Science and Engineering Conference.* Wisconsin.

Jokinen, T., Ylén , P., & Pyötsiä, J. (2011). Dynamic Model for Estimating the Added Value of Maintenance Services. *The 29th International Conference of the System Dynamics Society.* Washington DC.

Jones, R. I. (1999). The More Electric Aircraft: The Past and the Future? *IEE Colloqium on Electrical Machines and Systems for the More Electric Aircraft*, 1/1-1/4.

Karpenko, M., & Sepehri, N. (2003). Robust Position Control of an Electrohydraulic Actuator With a Faulty Actuator Piston Seal. *Journal of Dynamic Systems, Measurement, and Control*, 413-423.

Karter, J. (2016). *Machine Learning, Design of Experiments and Statistical Process Control Using Matlab.* Create Space Independent Publishing Platform.

Knotts, R. M. (1999). Civil Aircraft Maintenance and Support Fault Diagnosis from a Business Perspective. *Journal of Quality in Maintenance Engineering*, 335-348.

Kugel Motion Limited. (2018). Retrieved from Kugel Motion Ballscrew Products: http://www.kugelmotion.co.uk/

Landing Gear parts. (2015). Retrieved from Pininterest: https://uk.pinterest.com/pin/488359153317845635/

Lee, W., Lee, J., Hong, M., Nam, S., Jeon, Y., & Lee, M. (2015). Failure Diagnosis System for a Ball-Screw by Using Vibration Signals. *Hindawi Shock and Vibration*.

Leonard, J. (1984). All-Electric Fighter Airplane Flight Conrol Issues, Capabilities and Projections. *IEEE Transactions on Aerospace and Electronics Systems*, 234-242.

Li, L., Wang, Z., Liu, Z., & Bu, S. (2014). Trend Prognosis of Aero-Engine Abrupt Failure Based on Affinity Propagation. *First Symposium on Aviation Maintenance*, 13-22.

Maggiore, P., Vedova, M., Pace, L., & Desando, A. (2014). Definition of Parametric Methods for Fault Analysis applied to an Electromechanical Servomechanism affected by Multiple Failures. *European Conference of the Prognostics and Health Management Society 2014.* PHM.

Mare, J. (2016). *Aerospace Actuators 1: Needs, Reliability and Hydraulic Power Solutions.* Wiley-ISTE.

McNier, T. (2016). *Specifying, Selecting and Applying Linear Ball Screw Drives.* Thomson.

Min, B., Park, C., & Chung, S. (2016). Thermal Analysis of Ballscrew Systems by Explicit Finite Difference Method. *Transactions of the Korean Society of Mechanical Engineers, Volume 40*, 41-51.

Moir, I., & Seabridge, A. (2008). *Aircraft Systems: Mechanical, electrical, and avionics subsystems integration.* John Wiley and Sons, Ltd.

Motion Control Tips. (2011, October). *What are ballscrews? Summary for design engineers*. Retrieved from Motion Control Tips: https://www.motioncontroltips.com/ballscrews/

Mouritz, A. (2012). *Introduction to Aerospace Materials.* Elsevier.

Murphy, K. (2012). *Machine Learning, A Probabalistic Perspective.* The MIT Press.

Narasimhan, S., Roychoudhury, I., Balaban, E., & Saxena, A. (2010). Combining Model-Based and Feature-Driven Diagnosis Approaches - A Case Study on Electromechanical Actuators. *21st International Workshop on Principles of Diagnosis.*

Nguyen, D., Behar, B., & Mckay, T. (2014). *USA Patent No. US 8794084 B2.*

Ninomiya, M., & Miyaguchi, K. (1998). Recent Technical Trends in Ball Screws. *NSK Technical Journal: Motion Control*, 1-3.

Park, R. (1929). Two Reaction Theory of Synchronous Machines. *AIEE Transactions 48*, 716-730.

Phillips, P. A. (2012). *Health Monitoring of Electrical Actuators for Landing Gears.* Doctoral Submission, University of Manchester, Manchester. Retrieved from https://www.research.manchester.ac.uk/portal/files/54520238/FULL_TEXT.PDF

Pidd, M. (2004). *Systems Modelling: Theory and Practice.*

Prokopenko, J., & North, K. (1997). Productivity and Quality Management. In *Productivity by Maintenance.*

Qantas. (2016, July). *The A, C and D of aircraft maintenance*. Retrieved from Qantas Newsroom: https://www.qantasnewsroom.com.au/roo-tales/the-a-c-and-d-of-aircraft-maintenance/

Quanterion. (2016). *Nonelectronic Parts Reliability Data.* New York: Reliabiity Databook Series.

Radzicki, M. J., & Robert, T. A. (2008). Origin of System Dynamics: Jay W. Forrester and the History of System Dynamics. *U.S. Department of Energy's Introduction to System Dynamics*.

Rea, J. (1993, August). Boeing 777 High Lift Control System. *IEEE AES Systems Magazine*, pp. 15-21.

RK Bearings. (2015). Retrieved from RK Bearings: http://rkbearings.in/wp-content/uploads/2015/08/Lead-Screw.pdf

Robelin, O. (2010, January). *Maintenance Review Board Process (MRB) and Instructions for Continuied Airworthiness.* Retrieved from EASA: https://www.easa.europa.eu/system/files/dfu/ws_prod-g-doc-Events-2010-jan-19-Ref-9.-MRB-process.pdf

Saltoğlu, R., Humaira, N., & İnalhan, G. (2016). Aircraft Scheduled Airframe Maintenance and Downtime Integrated Cost Model. *Advances in Operations Research, Volume 2016*.

Saxena, A. (2010). Prognostics, The Science of Prediction. Portland.

Schlegel, C., Hösl , A., & Diel, S. (2009). Detailed Loss Modelling of Vehicle Gearboxes. *Proceedings 7th Modelica Conference.* Como: The Modelica Association.

Şenturk, C. (2010). Optimization of Aircraft Utilization by Reducing Scheduled Maintenance Downtime. *10th AIAA Aviation Technology, Integration and Operations (ATIO).* Fort Worth, Texas.

Shelton, G. (2010). *Roller Screw Actuators: Benefits, Selection and Maintenance*. Retrieved from Design World Online: https://www.designworldonline.com/roller-screw-actuators-benefits-selection-and-maintenance/

Song, X., Jian, L., Zhao-tan, W., Xian-yin, L., & Bao-min, L. (2005). Research and Development of Test System of Combination Property of High Speed Ball Screw Unit. *Tool Engineering*, 34-36.

Spohrer, J., & Maglio, P. (2010). Service Science: Toward a Smarter Planet. *ntroduction to Service Engineering*, 3-30.

Sterman, J. D. (2000). *Business Dynamics: Systems Thinking and Modeling for a Complex World.* Jeffrey J. Shelstad.

Stirling Dynamics. (2018). Retrieved from Stirling Dynamics: https://www.stirling-dynamics.com/about/

Stridsberg, L. (2005). *Low Weight, Highly Reliable Anti-Jamming Device for Electromechanical Actuators.* Texas: SAE Technical Paper Series.

Tako, A. A., & Robinson, S. (2008). Model Building in System Dynamics and Discrete Event Simulation: a quantitative comparison. *The 2008 International Conference of the System Dynamics Society*. Athens.

The Ballscrew Company. (2017). Retrieved from The Ballscrew Co Ltd: http://www.theballscrewco.uk/

Todeschi, M. (2011). Airbus - EMAs for Flight Controls Actuation System - An Important Step Achieved in 2011. *SAE International*.

Triumph Actuation Systems - U.K, Ltd. (2015). *High Availability Redundant Actuation Systems - HARAS*. Retrieved from Gateway to Research: http://gtr.rcuk.ac.uk/projects?ref=102374

Vahid-Araghi, O., & Golnaraghi, F. (2011). *Friction Induced Vibration in Lead Screw Drives.* Springer.

Vas, P. (1996). *Electrical Machines and Drives: A Space Vector Theory Approach.* Oxford.

Ventana Systems. (2015). *Vensim*. Retrieved from https://vensim.com/

Wei, C., & Lin, J. (2004). Kinematic Analysis of the Ball Screw Mechanism Considering Variable Contact Angles and Elastic Deformations. *AMSE Journal of Mechanical Design*, 717-733.

Weiss, J. (2014). Control Actuation Reliability and Redundancy for Long Duration Underwater Vehicle Missions with High Value Payloads. *Underwater Intervention*.

Westminister, E. b. (2008). *"Innovative cooperative actions of R&D in EUROCONTROL programme CARE INO III", Technical Discussion Document 9.0.* Retrieved from https://www.eurocontrol.int/eec/gallery/content/public/documents/projects/CARE/CARE_INO_III/DCI_TDD9-0_Airline_maintenance_marginal_delay_costs.pdf.

Wheeler, K. R., Kurtoglu, T., & Poll, S. D. (2010). A Survey of Health Management User Objectives Related to. *International Journal of Prognostics and Health Management*.

Xu, S., Yao, Z., Sun, Y., & Shen, H. (2014). Load Distribution of Ball Screw With Consideration of Contact Angle Variation and Geometry Errors. *International Mechanical Engineering Congress and Exposition.* ASME.

Appendix A: ‘A System Dynamics Approach to Evaluate Component Availability under Condition Based Maintenance’ Journal paper

A System Dynamics Approach to Evaluate Component Availability under Condition Based Maintenance

Yameen M. Hussain[1], Stephen Burrow[2], Leigh Henson[3], Patrick Keogh[4]

[1,2]*University of Bristol, Bristol, BS8 1TR, United Kingdom*
yameen.hussain@bristol.ac.uk
Stephen.Burrow@bristol.ac.uk

[3]*Stirling Dynamics Ltd, Bristol, BS8 4HG, United Kingdom*
Leigh.Henson@stirling-dynamics.com

[4]*University of Bath, Bath, BA2 7AY, United Kingdom*
p.s.keogh@bath.ac.uk

ABSTRACT

In this paper System Dynamics (SD) is used to evaluate component availability under Condition Based Maintenance (CBM). CBM is implemented via Prognostics and Health Monitoring (PHM): a key motivation of which is to increase aircraft availability by reducing unscheduled removals and downtime, ultimately reducing Direct Maintenance Costs (DMC). The benefits of CBM to aircraft maintenance were tested by modelling two maintenance philosophies using SD: the traditional approach driven by scheduled and reactive maintenance; and CBM through PHM. The study was focused at an aircraft component level with the target application being Electromechanical Actuators (EMA). A fleet of 100 aircraft over an 8-year maintenance overhaul period was modelled using real failure rate data from in-service history. The results indicated there were fewer unscheduled removals as a result of CBM in comparison to the traditional approach. The cost effectiveness of CBM as a was demonstrated through DMC accumulation for various commercial aircraft types. For example, in the case of a B747-400, it was found that CBM is no longer cost-beneficial when over 73% of the component life has been used. Overall, the SD models provided an enhanced level of systems understanding of the causalities that are inherent within the two maintenance policies. The utilization of real failure rate data from in-service history in the SD model meant that it be considered a useful methodology in terms of forecasting component availability and cost effectiveness of differing maintenance regimes.

Keywords—Prognostics; Health Monitoring; Aerospace; Condition Based Maintenance; System Dynamics; Electromechanical Actuators

1. INTRODUCTION

The stringent requirement of safety alongside the increasing complexity of technology and cost pressures on aircraft operations have led to an increasing interest in the implementation of PHM functionality within the Aerospace industry. To make a robust case for PHM it is necessary to quantify the benefits and challenges associated with its implementation and application: there are many benefits and drawbacks to account for when considering all stakeholders associated with PHM. Only if it is possible to capture all of these benefits and drawbacks, will PHM become acceptable to the Aerospace industry and to fulfil the objective to improve aircraft availability by reducing equipment downtime through enhanced understanding of health (Wheeler, Kurtoglu, & Poll, 2010).

1.1 Aircraft Maintenance

When PHM is employed in aerospace applications the aim is to increase equipment availability, optimise cross-fleet maintenance to reduce Direct Maintenance Costs (DMC), and to reduce costs associated with unscheduled maintenance (Jennions, 2012). Therefore, the impact of PHM on aircraft line maintenance actions is a key area of study when analysing the benefits.

Aircraft maintenance forms a significant part of an aircraft's airworthiness criteria, with the objectives to ensure a fully serviced, operational and safe aircraft (Ackert, 2010). Poor maintenance can have a variety of impacts on an aircraft, its crew and its passengers. For example: delays to aircraft dispatch time could cause a financial impact to the airline (runway charges) and customer dissatisfaction. In more severe cases, poor maintenance could lead to passenger or crew discomfort, injury or, in the worst case, a safety critical situation. It is useful to consider the different types of maintenance activities with respect to time as shown in Figure 1. It is desirable for airlines to have maximum operability, or 'up time', through minimisation of the 'down time' activities (Şenturk, 2010).

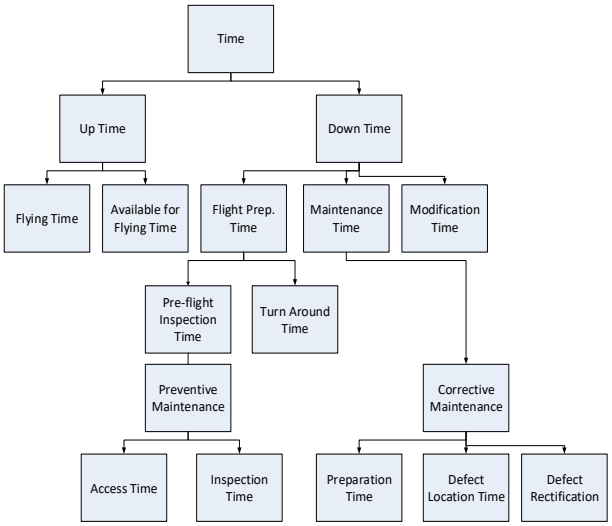

Figure 1. Maintenance Time Relationships (Knotts, 1999).

Aircraft maintenance regimes can be classified as comprising of activities stemming from preventive, corrective and design-out maintenance. These forms of maintenance are illustrated in Figure 2.

'Corrective maintenance' is often described as unplanned or reactive and is a form of maintenance based on troubleshooting equipment when it operates under undesirable conditions or fails, resulting in loss of operation.

'Design-out maintenance' is a means to improve equipment operability and reliability through a process of studies, construction and testing and may serve as part of an iterative design improvement of the equipment being maintained. An example of this is where later generations of a component or part have improved design.

'Preventive maintenance' describes a maintenance intervention before failure. It can be broken down into Scheduled maintenance, where equipment is serviced at periodic intervals and Condition-Based Maintenance (CBM) where continuous monitoring of a component with a PHM system is used to determines its health during normal aircraft operations.

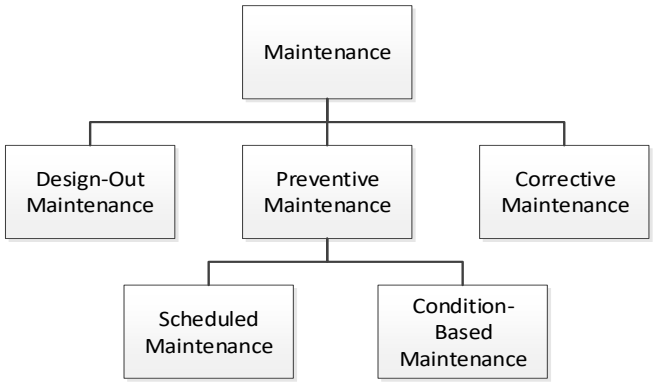

Figure 2. Maintenance Categories (Prokopenko & North, 1997).

Currently, most aircraft maintenance regimes are based around a series of scheduled maintenance tasks for each respective sub-system and components. These generally comprise of periodic inspections, which are classified into A, B, C and D checks with A and B checks conducted more frequently. A and B checks generally consist of visual inspections and general servicing often at a regular airport, whereas C and D checks are more extensive with checks requiring increased man-hours (Federal Aviation Administration, 1997) and performed at a specilist maintenace facility. The D check is the least frequent but the most comprehensive and is factored as an overhaul of the whole aircraft. Table 1 summarises what these checks may consist of as well as the duration.

Table 1. Typical Maintenance Checks (Westminister, 2008).

Check	Description	Duration
Line	Daily (before first flight checks). Visual inspection; fluid levels; tires and brakes; emergency equipment	~1 hour
A	Routine light maintenance; engine inspection	~10 hours
B	Similar to A check but with different tasks	~10 hours to 1 day
C	Structural inspection of airframe, opening access panels; routine and non-routine maintenance; run-in tests	~3 days to 1 week
D	Major structural inspection of the airframe after paint removal; engines, landing gear and flaps removed; instruments, electronic and electrical equipment removed; interior fittings removed; hydraulic and pneumatic components removed	~1 month

Table 2 shows the typical intervals of these maintenance checks for various commercial aircraft types. B-checks are often incorporated into successive A-checks (Qantas, 2016), therefore have been omitted from this table.

Table 2. Typical Maintenance Check Intervals for Various Commercial Aircraft Types (Saltoğlu, Humaira & İnalhan, 2016).

Aircraft	A Check	C Check	D Check
B737-800	500 FH	4000 – 6000 FH	96-144 Months

Aircraft	A Check	C Check	D Check
B757-200	500-600 FH	18 Months	72 Months
B767-300ER	600 FH	18 Months	72 Months
B747-400	600 FH	18 Months/7500 FH	72 Months
A319	600 FH	6000 FH	72 Months
A320	600 FH	6000 FH	72 Months
A321	600 FH	6000 FH	72 Months

In addition to the main scheduled maintenance experienced by a commercial aircraft, corrective maintenance will arise due to faults that cannot be detected during, or arise in the period in between, inspections. Existing aircraft systems also incorporate some CBM in the form of BITE (Built In Test Equipment), found in electrical subsystems (Ackert, 2010).

1.2 Origins of System Dynamics

System Dynamics (SD) is a methodology used to aid the understanding of complex processes over time through the use of Stock & Flow diagrams and internal feedback loops stemming from Causal Loop Diagrams (CLD) (Radzicki & Robert, 2008). Historically, SD came into prominence in the mid-1950s from Professor Jay Forrestor through an ambition to understand the core issues which define the success or failure of organisational processes (Forrestor, 1961).

SD seeks to integrate several disciplines such as economics, law, management sciences, and management of information systems within a single analysis tool (Spohrer & Maglio, 2010).

Complexity within a system is generally defined in terms of the number of components or processes within it or the number of combinations and scenarios to aid decision making which is termed ‘combinatorial complexity’ (Sterman, 2000). It is often assumed such complexity could arise in a system through additive combinations however, complexity may arise in simpler systems with low combinatorial complexity (Sterman, 2000) as dynamic complexity results from the combination of interactions amongst system elements through time.

1.3 Published System Dynamics Applications

SD techniques have been applied sparsely as a methodology in demonstrating PHM qualitative and quantitative benefits to aircraft maintenance in general. This section reviews previously published SD research from other applications.

Several case studies have been carried out to explore the dynamics of maintenance strategies within production plants with the view to reduce overall plant operation cost and increase uptime (Jabar, 2003), e.g. work conducted by Chumai (2009) included a SD model of plant maintenance systems to simulate plant maintenance behaviour. The results suggest that industrial plants should reduce preventive maintenance practice in a move towards CBM to increse plant uptime and keep maintenance costs to a minimum. The SD modelling presented a bespoke and detailed representation of the production plant in question from the perspective of the modeller, however it was noted that consolidation of this model may be required in order to present it in a format mutually understood amongst other practitioners (in the same field).

A dynamic model for estimating the added value of maintenance services was developed using SD techniques for a production plant (Jokinen, Ylén & Pyötsiä, 2011). It included modelling various maintenance systems to facilitate the service provider’s understanding of its customer’s business as a communication tool and of the added value of services in the hope that it would enhance value propositions. The SD modelling served its initial purpose of providing visualisation of the intricacies of the maintenance system behaviour as a means to identify robust policies and isolate critical areas within the system. However, estimations of quantitative output data were seen as unreliable due to uncertainty in the input data.

SD was also applied to evaluate fleet and maintenance strategies in a bus company (Bivona & Montemaggiore, 2005). The objective was to demonstrate how SD could be used to support key decision makers in designing and evaluating their maintenance strategies with reflection on their company performance. Results showed that CBM would provide benefit over scheduled maintenance in terms of optimisation of maintenance personnel and reducing equipment downtime (Bivona & Montemaggiore, 2005).

1.4 Aims and Objectives

The purpose of this paper is to quantify the impact of PHM on aircraft operations by using SD techniques. To achieve this two maintenance strategies will be modelled and results compared:

1. A traditional approach driven by scheduled and reactive maintenance;

2. Condition Based Maintenance (CBM) implemnted via PHM.

The aim is to capture any benefits of CBM through rigorous SD modelling, and also to exploring the sensitivity of any benefits derived from CBM to variations in performance, for example as components age. A further benefit that can be derived as consequence of employing SD is to reveal the interconnectedness of the sub-system elements of the two maintenance policies.

The paper is structured as follows: Section 2 describes the target aircraft application to be used for this study. This also includes key failure rate data used for the analysis; Section 3 presents SD methodology contextually with Causal Loop Diagrams (CLD) and Stock and Flow diagrams presented. Section 4 shows results of the simulations with focus on component availability and cost effectiveness as a result of CBM using SD modelling. Section 5 provides conclusions with an overview of key findings and suggestions for future work.

2. TARGET APPLICATION: EMA

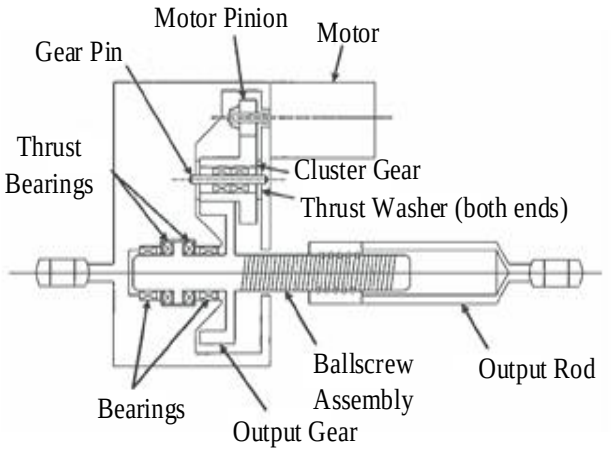

Figure 3. EMA System (Bodden et al. 2007).

Despite their inherent advantages over other technologies, Electro-Mechanical Actuators (EMA) have seen little use to date in safety critical aircraft applications due to the potential for jamming, creating a single point of failure even when configured in parallel redundant formats (Balaban, et al. 2011). It has however been widely suggested that the next generation of fly-by-wire aircraft could benefit from EMA technology if PHM could be successfully incorporated (Balaban, et al. 2011).

The EMA considered in this study is a linear ballscrew that provides linear motion when driven by a rotary electric motor. Figure 3 shows a typical schematic of the system, consisting of a single actuator assembly driven by a brushless DC motor via a single stage gearbox with the motor mating with a single pinion in the ballscrew assembly (Bodden et al. 2007). EMA ballscrew actuator failures are often a result of gradual degradation of the ballscrew surface through metal to metal contact of the re-circulating balls to the hardened metal surface of the ball screw shaft, eventually leading to jamming (Jin et al. 2013). Typical PHM schemes measure a parameter correlated with degradation (feature extraction) and then map this to a damage state through a diagnostic algorithm. In keeping with the modelling capability of SD, in this paper a particular PHM scheme is not considered, instead the perfromance of a PHM scheme is expressed as a false positive/negative rate and used as a variable in the SD modelling to determine the sensitive of cost benefits to PHM performance.

In this paper, SD is used to model component availability across a maintenance overhaul period, considering an airline operating 100 aircraft over an 8 year period (D Check). To better constrain the model historical in-service EMA failure data is used from the 'Non Electronic Parts Reliability Database' (NPRD). The NPRD intends to provide a comprehensive database of field failure rate data on a variety of electrical, mechanical and electromechanical parts and assemblies to assist in reliability analyses and assessments (Quanterion, 2016). The NPRD has been publishing since the early 1970s with a cumulative compilation of data at each up-issue every 5-6 years.

The 2016 edition added an extra 138,000 parts and 370 billion part hours, representing a 400% increase in data compared to the previous edition in 2011 (Quanterion, 2016). Table 3 compares failure rate data for linear EMAs between data published in 1991 and in 2016.

Table 3. Linear EMA failure, NPRD data (Quanterion, 2016).

Years	Part	Total Failed	Operating Hours 10^6	Failures per 10^6 Hours
~1970-1991	Linear EMA	460	0.5256	875.2
~1970-2016	Linear EMA	1725	100.6478	17.14

It can be seen from the data collected in Table 3, the rate of failure was much higher between the early 1970s and 1991 than compared to between early 1970s and 2016. This may be attributed to improvements in actuator design for safety and reliability as well as improvements in maintenance. Usage profiles are not made apparent within the NPRD and so the nature of how the failures occurred is unclear. The failure rate data for 2016 can be further decomposed to show the rates for each application environment, these are shown in Table 4.

Table 4. Linear EMA failure by application, NPRD 2016 (Quanterion, 2016).

Application Environment	Total Failed	Operating Hours (10^6)	Failures per 10^6 Hours
Airborne Attack (AA)	806	3.3384	241.43
Airborne Uninhabited Attack (AUA)	229	2.1928	104.43
Airborne Inhabited Attack (AIA)	10	0.3655	27.36
Airborne Commercial (AC)	680	94.7512	7.18

Given the data in Table 4, a clear distinction can be made in failure rates between applications on military and commercial platforms. For military aircraft, there are a higher number of removals which can be attributed to the fact that military aircraft are generally designed for enhanced performance and operate beyond the performance envelope of a commercial aircraft.

It is challenging for aircraft operators and maintenance teams using CBM when the component degrades at a faster rate (Li et al. 2014). Early stage abrupt failures could arise from actuator misalignment leading to mechanical seizure of the ballscrew assembly (Balaban et al. 2015). Failures exhibiting a gradual degradation initially before experiencing a jam can be attributed to abrupt seizures in the bearings of the screw from a build-up of debris or loss of lubrication (Balaban et al. 2015).

3. SD METHODOLOGY

SD methodology consists of a series of procedures and equations to develop the finalised SD model. The modelling includes CLD modelling to provide the initial visualisation of the maintenance strategies by modelling the key attributes and parameters through a Stock and Flow model. The modelling was conducted using 'Vensim' which is an industrial software specialised for SD simulations (Ventana Systems, 2015).

CLDs represent a simplistic map of the system being modelled encompassing all the system elements and interactions. CLDs also capture feedback loops which in turn enable better understanding of the system. Each link is given a positive or negative causal relationship: for a pair of connected nodes, a positive causal link means they are changing in the same direction and a negative causal link means they change in opposite directions. Feedback loops consist of either Reinforcing (+) or Balancing (-) loops. Reinforcing loops are often associated with exponential increases or decreases whereas Balancing loops infer a plateauing effect. Derived from the CLD, a 'Uses tree' provide a logic-based understanding of the causalities.

The 'Stock and Flow' diagram provides a detailed impression of the CLD allowing the user to analyse the system in a more quantitative manner. A 'Stock' (state variable) depicts any entity in the system which can accrue or lessen over time and a 'Flow' (state change) is the rate of change of a Stock.

3.1 Causal Loop Diagram for aircraft maintenance

The CLD presented in Figure 4 provides an initial visualisation of the processes involved in the traditional maintenance approach driven by scheduled & reactive maintenance for an EMA in a commercial aircraft.

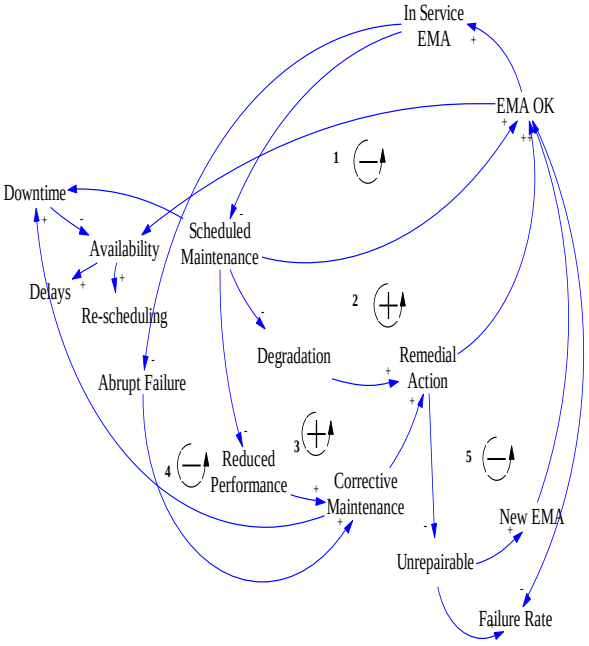

Figure 4. Scheduled & Reactive Maintenance processes CLD.

A Uses Tree is shown in Figure 5, showing the in-service component to be subjected to Scheduled maintenance at a defined period with failures occuring sporadically. Five feedback loops were identified in the CLD and these are described in detail in Table 9 of the appendix.

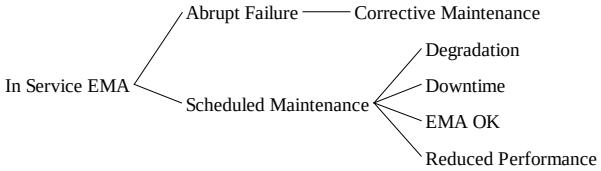

Figure 5. Scheduled & Reactive Maintenance Uses Tree.

The same process was followed for modelling the CBM approach with the corresponding CLD shown in Figure 6.

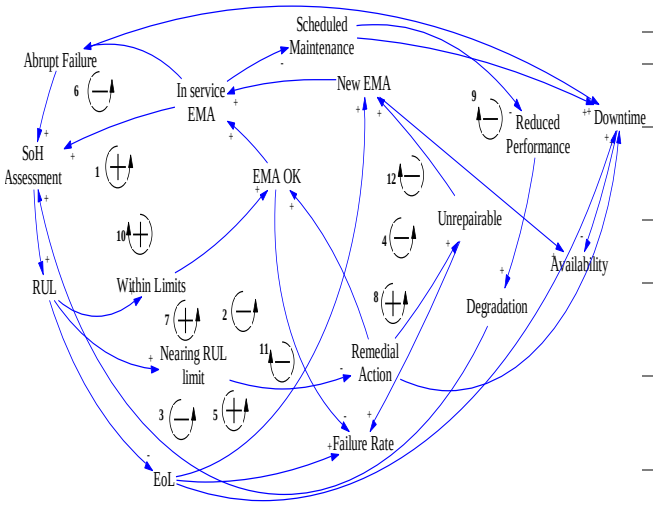

Figure 6. CBM processes CLD (RUL – Remaining Useful Life).

The additional steps relating to PHM processes were included in the CLD by adding loops related to a 'State of Health' (SoH) assessment. As shown in the Uses Tree in Figure 7, the SoH is a sequential step as it is something intended to be performed offline (at a frequent interval) and becomes a dominant feature within CBM.

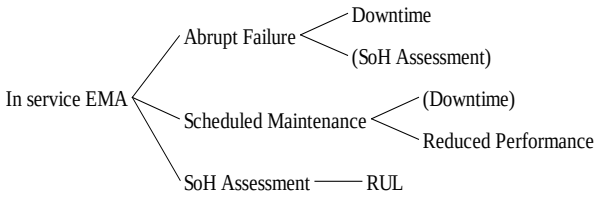

Figure 7. CBM Uses Tree.

There were considerably more feedback loops in the CLD model with PHM processes included. The feedback loops were broken down into 3 groups as shown in the appendix Tables 10-12.

3.2 Stock and Flow Diagram for aircraft maintenance

The CLDs provide an initial overview of the system with the relationship between top-level processes involved in maintenance elucidated. The next stage in SD modelling is to build a detailed sub-system model through Stock and Flow diagrams.

Table 5. State Variables.

Stocks	Definition
Working EMAs	EMAs that are fully operable and functioning for safe intended purpose.
Degrading EMAs	EMAs that are starting to lose efficiency as a result of mechanical wear.
Working EMAs to undergo CBM	EMAs that are subject to PHM.
Degrading EMAs to undergo CBM	Queue for EMAs to undergo CBM.
EMAs under Scheduled Maintenance	All EMAs are subject to system level periodic checks.
Failed EMAs	EMAs that have failed to operate at design operating conditions.
EMAs failed prematurely	EMAs that have failed before MTBF.
EMAs under remedial action	Failed EMAs at workshop for repair.
Direct Maintenance Costs	Incurred costs as a result of scheduled or unscheduled maintenance activities.

Table 6. State Changes.

Flows	Definition
Failure Rate	The frequency at which the EMA fails.
Premature Failure Rate	The frequency at which the EMA fails before the MTBF.
Failure Rate (following CBM)	The frequency at which the EMA fails post-CBM.
Repair Rate	The frequency at which remedial action is conducted by workshop engineers.
False PHM Rate	The frequency at which False Positives/Negatives occur.
Rate of Detected Failures	The frequency at which failures are detected through CBM.
CBM Work Rate	The frequency at which PHM is performed.

Many sub-system models can be developed from the CLD; however, for the purpose of this paper the objective was to build a Stock and Flow diagram of a sub-system evaluating EMA maintenance and availability. The goal was to investigate the ability of PHM to reduce corrective maintenance and how advanced prediction in the onset of a degrading failure can reduce unscheduled removals and thus boost availability. Prior to modelling the Stock and Flow diagram of the sub-system, it was necessary to define the stocks (state variables) and flows (state changes) necessary to model the sub-system. These are listed in Tables 5 and 6 respectively. Based on these Stock and Flow attributes and system level information from the CLD modelling in section 3.1, a Stock & Flow diagram was constructed and is presented in Figure 8.

To draw-out the time dependence of availability on CBM, the model assumed CBM is be applied at discrete time steps (rather than continuously) from no CBM, through monthly, weekly and finally daily application, and would be conducted offline, therefore no additional downtime is incurred for each CBM check.

It can be seen from Figure 8, that multiple parameterised attributes impact each stock and flow, adding granularity of the model and can reveal causality. The 'Rate of Wear' value is derived from the historical in-service failure rates as shown previously in Tables 3 and 4.

4. Results and Discussion

The analysis was based on two metrics: (1) EMA availability (i.e. the probability of an EMA being in an operable state at the beginning of a flight), (2) Evaluation of cost effectiveness by considering DMC accumulation through EMA life. The SD analysis conducted is based on a continuous simulation of discrete events as is the case for most SD simulations (Tako & Robinson, 2008).

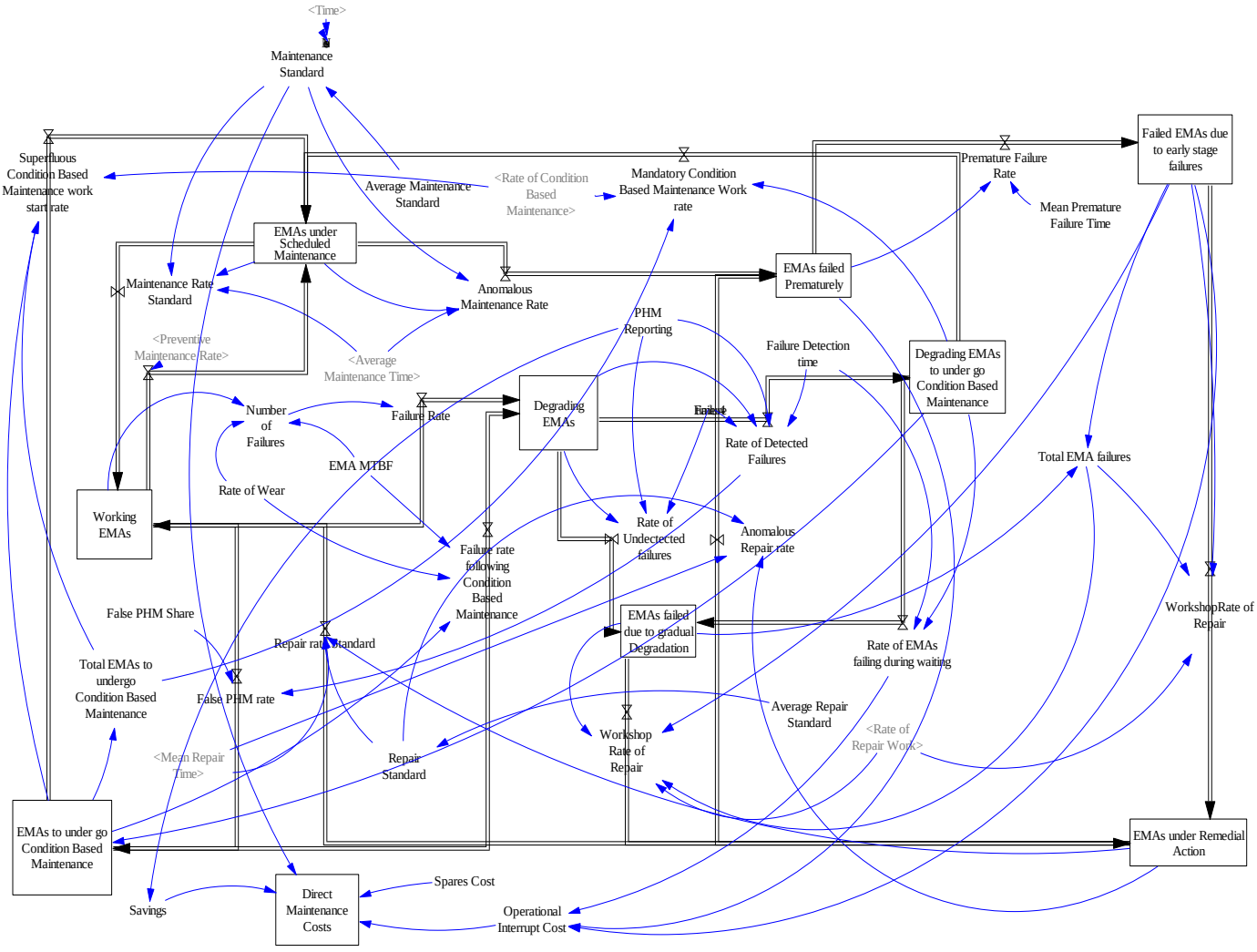

Figure 8. Stock and Flow Diagram of EMA Maintenance Sub-system.

4.1 EMA Availability

EMA availability can be derived from the Mean Time Before Failure (MTBF) divided by MTBF plus the Mean Time To Repair (MTTR) (Item Software, 2017). The MTTR is defined as the total amount of time spent performing corrective or preventive maintenance repairs (Item Software, 2017). For this study, MTTR was treated as Mean Downtime (MD) which includes mean time taken for reactive and scheduled maintenance across the overhaul period of 8 years (not including the time for the D-check itself). Thus EMA availability is described by equation 1.

$$EMA\ Availability = \frac{MTBF}{MTBF+MD} \quad (1)$$

From the data presented in Tables 1 and 2, an approximate value of MD over the maintenance overhaul period was calculated: An A-check should be conducted every 200 FC (600 FH) which corresponds to every 100 days (assuming 2 FC/day). The duration of the check is 10 hours therefore the total downtime due to A checks is estimated to be 290 hours. A C check should be conducted every 18 months with duration of each check being ~7 days. This corresponds to 896 hours of scheduled downtime. The modelling also assumed 200 hours of downtime due to reactive maintenance during the overhaul period. Therefore, total downtime was estimated to be 1386 hours.

The next step is to introduce the effect of PHM by varying the frequency of CBM. Differing CBM schedules were devised to result in a progressive range of values for MD:

1. No CBM. *Therefore, the MD during overhaul period was assumed to be 1386 hours.*
2. CBM at the end of every month – *This was modelled with the assumption that reactive maintenance would be eliminated completely. Therefore, the MD during overhaul period was assumed to be 1186 hours.*
3. CBM at the end of every month, reduced C check duration. *This case was modelled with the assumption that the C check duration would be reduced from 7 to 3 days. Therefore, the MD during overhaul period was assumed to be 874 hours.*
4. CBM at the end of every week, with reduction in frequency of C-checks. *This case was modelled with the period of the C check would be increased from 18 to 36 months. Therefore, the MD during the overhaul period was assumed to be 682 hours.*
5. CBM at the end of every day, with no C-check. *This case was modelled with the elimination of C-checks entirely, the MD during the overhaul period was thus 290 hours.*

Analysis was conducted on the failure rate data from the 1991 data set as well as the 2016 AC (Aircraft Commercial), representing the extremes of mean availability of the datasets. Figure 9 shows the variation in EMA availability for each MD of the 5 considered CBM schedules, applied to the 1991 failure rate data.

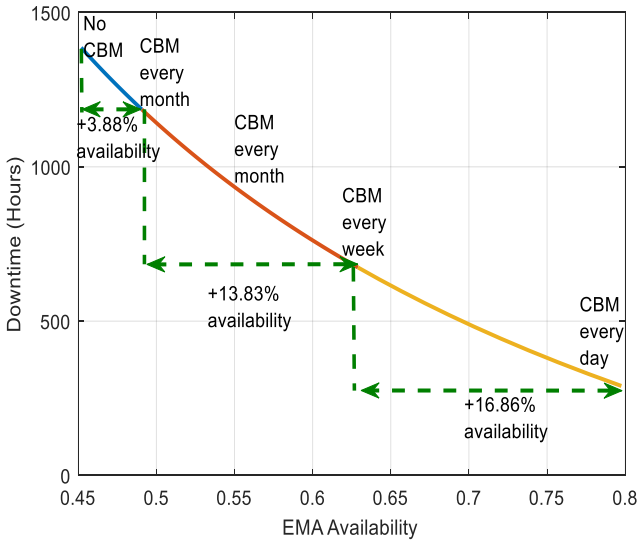

Figure 9. EMA Availability Probability Values against Mean Downtime corresponding to differing CBM schedules (1991 Failure Rate Dataset)

As expected, increasing the frequency of CBM increases the availability of EMA's due to the reduction in MD across the overhaul period. EMA availability could increase by 34.57% with CBM checks be applied every day.

The same analysis was conducted for the 2016 NPRD data. The AC data was chosen in isolation given the size of the sample and also has the lowest failure rate. Figure 10 shows the variation in EMA availability for differing MD for this dataset.

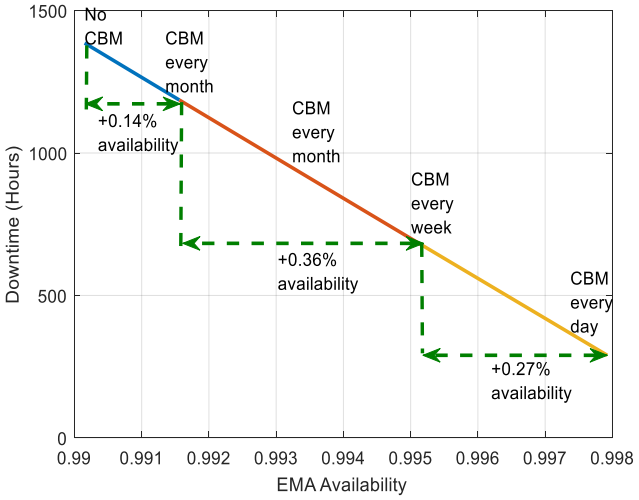

Figure 10. EMA Availability Probability Values against Mean Downtime corresponding to differing CBM schedules (2016 (AC) Dataset).

As can be seen from Figure 10, the EMA availability improves slightly with the frequency of CBM actions. This low rate of improvement can be attributed to the low failure rate from in-service history. CBM may not bring about a significant change in improving availability when eliminating reactive maintenance, however, it can be beneficial in reducing scheduled maintenance actions (C-checks) and therefore improve uptime.

The benefits of applying CBM can be observed, however, a question remains on whether a cost benefit can be realised, given the already high reliability of the component without CBM. CBM on a weekly basis could be considered to reduce scheduled maintenance actions as well as the benefit of PHM improving safety.

4.2 Cost Effectiveness of PHM

The occurrence of 'False Positive/Negative' readings is a common issue encountered when considering the economics of CBM through PHM (Feldman et al. 2010). False positive readings can hide the occurrence of an impending fault which can lead to equipment being operated whilst degrading. Subsequently, this can lead to additional DMCs.

This section evaluates the DMC impact False Positives may have due to delayed detection of faults through CBM. The analysis assumed that minimal costs would be incurred at the early detection of the onset of a failure through PHM (Dixon, 2006).

The analysis considered maintenance costs for various types of commercial aircraft. The data was initially collected in 2008 (Westminister, 2008) which includes the per block hour cost including labour cost in Euros. For the purposes of this analysis, the data was updated with conversion to Pound Sterling (1 EUR = 0.912 GBP) with an inflation rate of 2.6% per year factored in to get an approximation of today's unit maintenance costs. These are shown in Table 7.

Table 7. Maintenance Costs per Block Hour

Aircraft	Low (£)	Base (£)	High (£)
B737-800	550.68	594.74	737.91
B767-300ER	1024.27	1068.32	1409.74
B747-400	1585.96	1652.04	2125.63
A319	638.79	693.86	881.09
A321	726.90	792.98	1002.24

It should be noted that the values in Table 7 are a mixture of line, base, component and engine maintenance cost (Saltoğlu et al. 2016). Therefore, 'low' unit cost values were used in the Stock and Flow diagram for this analysis.

For a traditional maintenance approach (driven by scheduled and reactive maintenance), a fault would lead to an unscheduled replacement which would incur costs due to Operational Interrupts (OI) and DMCs. Since this analysis is modelled for a CBM approach, OI costs were deemed negligible as it was assumed that the onset of a failure can be predicted, therefore, maintenance can be planned thus mitigating unscheduled downtime. The accumulation of DMC was modelled assuming the minimum maintenance cost per block hour (from Table 7) would be accrued should CBM detect the onset of a fault immediately. The value of DMC increases in the event of a delay in fault detection (due to False Positive readings) which is modelled by an exponential function whereby the costs significantly rise with equipment deterioration (IATA, 2018).

$$DMC = e^{0.1x} + DMC_{base} \quad (2)$$

Where: DMC_Base is the minimum DMC cost and x is the percentage component life used.

The DMC accumulation for an A319 aircraft was plotted as a function of EMA percentage remaining life as shown in Figure 11. The corresponding overall savings (OI – DMC) are also shown to indicate where PHM predictions would start to incur a loss over the EMA life.

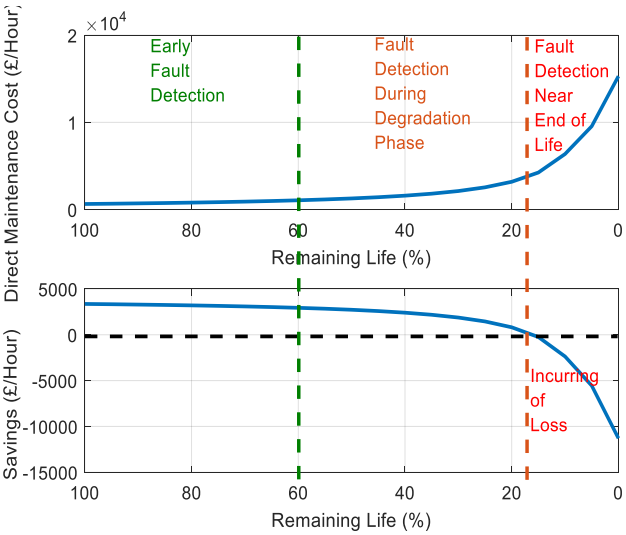

Figure 11. DMC Accumulation (top) and Savings due to PHM (bottom) through Component Life for A319.

Figure 11 illustrates the trend in which DMCs are accumulated through overall EMA life for the A319 aircraft. It was ascertained that if PHM were to identify the onset of failure at an early stage, minimal DMCs would be incurred (spares cost for replacement remains constant throughout maintenance overhaul period). An exponential rise in DMCs follows as failure detection occurs towards the end of component life. This was attributed to the degradation becoming more prevalent over time and therefore it costs more to repair. Using the data from DMC accumulation, the overall savings were deduced, and it enabled the calculation of where the PHM predictions would start to incur a loss. As can be seen from the bottom graph in Figure, PHM starts to become no longer cost beneficial if more than ~89% of the EMA life has been used.

Figure 12 shows the accumulated DMCs and Savings per PHM interval for the other commercial aircraft listed in Table 7. Figure indicates that early replacement detectable through PHM starts to become no longer cost beneficial if more than 73% of the EMA life has been used for a B747-400 and 91% for B737-800. Table 8 summarises the percentage EMA life at which PHM becomes no longer cost beneficial for all the aircraft types analysed in this study.

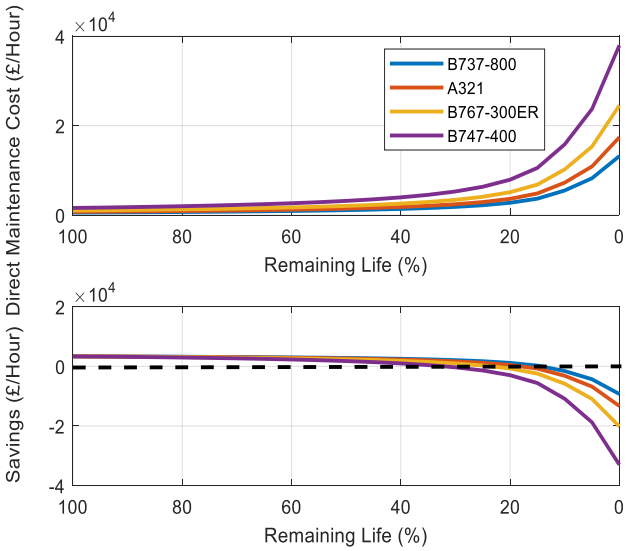

Figure 12. DMC Accumulation (top) and Savings due to PHM (bottom) through Component Life for all Aircraft.

Table 8. PHM Interval at which PHM Becomes no Longer a Cost Benefit.

Aircraft	EMA Life
B737-800	91%
B767-300ER	82%
B747-400	73%
A319	89%
A321	87%

5. CONCLUSIONS

Two maintenance policies were modelled and analysed through SD to demonstrate the potential qualitative and quantitative benefits to aircraft maintenance of using CBM.

CBM was added into the SD model to evaluate the impact on EMA availability based on historic failure datasets. The failure rate data between the early 1970s and 1991 showed significant improvements in EMA availability with increasing frequency of CBM. However, when applied to the failure rate data spanning early 1970s and 2016, it was observed that whilst an improvement in availability was noticeable, the reliability of the component was already deemed quite high from which additional CBM may incur further maintenance costs unless scheduled maintenance is reduced. However, there is scope to reduce scheduled maintenance actions as a result of CBM.

The cost effectiveness of PHM was also modelled, whereby, maintenance cost per hour data for various aircraft was used to evaluate DMC accumulation over EMA life. From this, it was ascertained that CBM

becomes no longer cost beneficial when over 73% of the EMA life has been used on a B747-400. This value becomes higher for smaller aircraft.

Overall, the SD models presented an enhanced level of systems understanding and can be seen as a useful forecasting tool for equipment availability as long as model fidelity is continually increased.

ACKNOWLEDGEMENT

This work was supported by the Systems Centre and the EPSRC funded Industrial Doctorate Centre in Systems (Grant EP/G037353/1) and Stirling Dynamics.

REFERENCES

Ackert, S. P. (2010, October 1). Basics of Aircraft Maintenance Programs for Financiers. *Evaluation & Insights of Commercial Aircraft Maintenance Programs*.

Airlines for America. (2014). *Per-Minute Cost of Delays to U.S. Airlines*. Retrieved December 2015, from Airlines for America: http://airlines.org/data/per-minute-cost-of-delays-to-u-s-airlines/

Balaban, E., Saxena, A., Narasimhan, S., Roychoudhury, I., & Goebel, K. (2011). Experimental Validation of a Prognostic Health Management System for Electro-Mechanical Actuators. *American Institute of Aeronautics and Astronautics*.

Balaban, E., Saxena, A., Narasimhan, S., Roychoudhury, I., Koopmans, M., Ott, C., & Goebel, K. (2015). Prognostic Health-Management System Development for Electromechanical Actuators. *Journal of Aerospace Information Systems*, 329-344.

Bivona, E., & Montemaggiore, G. (2005). Evaluating Fleet and Maintenance Management Strategies through System Dynamics Model in a City Bus Company. *The 23rd International Conference of the System Dynamics Society.* Boston.

Bodden, D. S., Clements, S., Schley, B., & Jenney, G. (2007). Seeded Failure Testing and Analysis of an Electromechanical Actuator. *Aerospace Conference IEEE*, 1-8.

Chumai, R. (2009). System Dynamic Modeling of Plant Maintenance Strategy in Thailand. *The 27th International Conference of the System Dynamics Society.* Albuquerque.

Dixon, M. (2006). *The Maintenance Costs of Aging Aircraft.* RAND.

Federal Aviation Administration. (1997). *Maintenance Review Board Procedures.* Advisory Circular AC 121-22A.

Feldman, A., Kurtoglu, T., Narasimham, S., Poll, S., Garcia, D., Kleer, J., . . . Gemund, A. (2010). Empirical Evaluation of Diagnostic Algorithm Performance Using a Generic Framework. *International Journal of Prognostics and Health Management*.

Forrestor, J. W. (1961). *Industrial Dynamics.* Cambridge, MA: The M.I.T Press.

IATA. (2018). *Maintenance Costs for Aging Aircraft.* IATA.

Item Software. (2017). *Reliability Prediction Basics*. Retrieved from Reliability Education: http://www.reliabilityeducation.com/ReliabilityPredictionBasics.pdf

Jabar, B. H. (2003). Plant Maintenance Strategy: Key for Enhancing Profitability.

Jennions, I. (2012). *Integrated Vehicle Health Management: Business Case Theory and Practice.* SAE International.

Jin, W., Chen, Y., & Lee, J. (2013). Methodology for Ball Screw Component Health Assessment and Failure Analysis. *International Manufacturing Science and Engineering Conference.* Wisconsin.

Jokinen, T., Ylén , P., & Pyötsiä, J. (2011). Dynamic Model for Estimating the Added Value of Maintenance Services. *The 29th International Conference of the System Dynamics Society.* Washington DC.

Knotts, R. M. (1999). Civil Aircraft Maintenance and Support Fault Diagnosis from a Business Perspective. *Journal of Quality in Maintenance Engineering*, 335-348.

Li, L., Wang, Z., Liu, Z., & Bu, S. (2014). Trend Prognosis of Aero-Engine Abrupt Failure Based on Affinity Propagation. *First Symposium on Aviation Maintenance*, 13-22.

Prokopenko, J., & North, K. (1997). Productivity and Quality Management. In *Productivity by Maintenance.*

Qantas. (2016, July). *The A, C and D of aircraft maintenance*. Retrieved from Qantas Newsroom: https://www.qantasnewsroom.com.au/roo-tales/the-a-c-and-d-of-aircraft-maintenance/

Quanterion. (2016). *Nonelectronic Parts Reliability Data.* New York: Reliabiity Databook Series.

Radzicki, M. J., & Robert, T. A. (2008). Origin of System Dynamics: Jay W. Forrester and the History of System Dynamics. *U.S. Department of Energy's Introduction to System Dynamics*.

Saltoğlu, R., Humaira, N., & İnalhan, G. (2016). Aircraft Scheduled Airframe Maintenance and Downtime Integrated Cost Model. *Advances in Operations Research, Volume 2016*.

Şenturk, C. (2010). Optimization of Aircraft Utilization by Reducing Scheduled Maintenance Downtime. *10th AIAA Aviation Technology, Integration and Operations (ATIO).* Fort Worth, Texas.

Spohrer, J., & Maglio, P. (2010). Service Science: Toward a Smarter Planet. *ntroduction to Service Engineering*, 3-30.

Sterman, J. D. (2000). *Business Dynamics: Systems Thinking and Modeling for a Complex World.* Jeffrey J. Shelstad.

Tako, A. A., & Robinson, S. (2008). Model Building in System Dynamics and Discrete Event Simulation: a quantitative comparison. *The 2008 International Conference of the System Dynamics Society*. Athens.

Ventana Systems. (2015). *Vensim*. Retrieved from https://vensim.com/

Weiss, J. (2014). Control Actuation Reliability and Redundancy for Long Duration Underwater Vehicle Missions with High Value Payloads. *Underwater Intervention*.

Westminister, E. b. (2008). *"Innovative cooperative actions of R&D in EUROCONTROL programme CARE INO III", Technical Discussion Document 9.0.* Retrieved from https://www.eurocontrol.int/eec/gallery/content/public/documents/projects/CARE/CARE_INO_III/DCI_TDD9-0_Airline_maintenance_marginal_delay_costs.pdf.

Wheeler, K. R., Kurtoglu, T., & Poll, S. D. (2010). A Survey of Health Management User Objectives Related to. *International Journal of Prognostics and Health Management*.

BIOGRAPHIES

Yameen Monsur Hussain received a BEng (Hons) in Aviation Engineering from Brunel University, London in 2010 and MSc in Fluid Power Systems from the University of Bath in 2011. He is currently an Engineering Doctorate (EngD) student at the University of Bristol studying Health Monitoring of Electrical Actuation Systems in collaboration with Stirling Dynamics Ltd. His current research interests are prognostics and health management techniques, reliability, electromechanical actuation, tribology and optimisation of maintenance scheduling.

Stephen G Burrow received the MEng and PhD degrees in electrical engineering from the University of Bristol in 1998 and 2002, respectively. He is currently a Reader in the Department of Aerospace Engineering, University of Bristol. His current research encompasses power electronics, machines and energy harvesting, and environmental sensing.

Leigh Henson received a BEng (Hons) degree in Mechanical Engineering from the University of Huddersfield in 2002 following successful completion of a four year course including a twelve month industrial placement at Agusta Westland Helicopters (now Leonardo). Awarded Chartered Engineer (CEng) status as a member of the Institute of Mechanical Engineers (IMechE) in 2006 after four years post graduate experience in the civil aerospace industry with Airbus. Working for Stirling Dynamics has built extensive experience in Landing Gear Systems covering research and technology, new aircraft/equipment development and qualification including: requirements capture, V&V process, first flight, flight test, certification, entry into service (EIS) and continuous product development (CPD).

Patrick Keogh received degrees from the universities of Nottingham and Manchester. He was a Research Technologist at the Engineering Research Centre, GEC Alstom (now Alstom). In 1990, he joined the Department of Mechanical Engineering, University of Bath, U.K. His current research interests include rotor dynamics, magnetic bearing systems, active vibration control, modern optimal control for multivariable systems, contact dynamics, and associated thermal behaviour of bearings.

APPENDIX

Table 9. Feedback Loops for Scheduled and Reactive Maintenance CLD.

Loop	*Inference*
1:In-service EMA →Scheduled Maintenance→EMA OK→In-service EMA	This is a 'balancing' feedback loop where the behavioural pattern of the loop suggests a temporary null in operation due to the EMA experiencing downtime due to mandatory maintenance.
2:In-service EMA→Scheduled Maintenance →Degradation→ Remedial Action→EMA OK→In-service EMA	This is a 'reinforcing' feedback loop due to the gradual wear that occurs within the EMA.
3:In-service EMA →Scheduled Maintenance→ Reduced Performance→ Corrective Maintenance→ Remedial Action→ EMA OK→In-service EMA	This is a 'reinforcing' feedback loop like loop 2 due to the attributes associated to gradual wear within the EMA.
4:In-service EMA→Abrupt Failure→Corrective Maintenance→ Remedial Action →EMA OK→In-service EMA	This is a 'balancing' feedback loop as abrupt failures would lead to reactive maintenance due to more severe degradation trends within the EMA system.
5:In-service EMA→Scheduled Maintenance→Degradation→Remedial Action→Unrepairable→New EMA→EMA OK	This feedback requires the need for EMA replacement as a result of the workshop deeming the component unrepairable. It was envisaged that the majority of these outcomes would arise from abrupt failures and so this was a deemed a 'reinforcing' loop.

Table 10. Feedback Loops for SoH assessment within CBM-CLD.

Loop	*Inference*
1:In-service EMA→SoH Assessment→RUL→Within Limits→EMA OK	This is a 'reinforcing' feedback loop due to the principal nature in which the SoH assessment is performed at a frequent interval as a mandated process in which there is no disruption or reduction in aircraft availability.
2:In-service EMA→SoH Assessment→RUL→Nearing RUL Limit→Remedial Action→EMA OK	This is a 'balancing' feedback loop due to the SoH assessment bringing about need for remedial action and therefore prompting the aircraft to go out of service momentarily.
3:In-service EMA→SoH Assessment→RUL→EoL (End of Life)→ New EMA	This feedback loop is similar to Loop 2 in that this has a 'balancing' feedback loop where the EMA has reached the end of its useful life and therefore a replacement is prompted.
4:In-service EMA→SoH Assessment→Nearing RUL limit→Unrepairable→New EMA	This is a 'balancing' feedback loop attributed from the aircraft experiencing downtime due to EMA replacement.

Table 11. Feedback Loops for Abrupt failures within CBM-CLD.

Loop	*Inference*
5:In-service EMA→Abrupt Failure→SoH Assessment→RUL→EoL →Remedial Action→New EMA	This was deemed to be a 'reinforcing' feedback loop due to the equipment being forced out of service prior to the SoH check thus subsequently leading to a replacement.
6:In-service EMA→Abrupt Failure→SoH Assessment→RUL→ Within Limits→LG EMA OK	This is a 'balancing' feedback loop because the abrupt failure may not be applicable to the EMA itself and therefore there is no resulting effect on parts inventory with the EMA showing satisfactory health.
7:In-service EMA→Abrupt Failure→SoH Assessment→RUL→Nearing RUL Limit→Remedial Action→EMA OK	This process is similar to loop 6 however there is a need for prolonged downtime with the EMA deemed repairable and this was deemed to be a 'balancing' feedback loop. This is the same for loop 8 where the EMA is declared unrepairable following remedial action.

Table 12. Feedback Loops for Scheduled Maintenance within CBM-CLD.

Loop	*Inference*
9:In-service EMA→Scheduled Maintenance→Degradation→SoH Assessment→RUL→ EoL→New EMA	This is a 'balancing' feedback loop due to the planned downtime for Scheduled Maintenance with poor health reading giving rise to EMA replacement. The same applies for loops 11 & 12 where the outcome of SoH check lead to remedial action and possible replacement.
10:In-service EMA→Scheduled Maintenance→Degradation→SoH Assessment→RUL→Within Limits→EMA OK	This is a 'reinforcing' feedback loop because the EMA is deemed to be in satisfactory condition for continued service. This is assumed to be the majority case scenario.

Appendix B: Matlab Code for kNN Classifier

```
load simulateddata
X = meas; %all motor current and speed data
Y = responses %corresponding state of health of each simulation
mdl = ClassificationKNN.fit(X,Y); %k-NN classification
mdl.NumNeighbours = 1; %set number of nearest neighours, default
value is 1
% Predict the classification for a new query
query1 = [500 2.2]; %example query for 500 RPM and 2.2A
query1Class= predict(mdl,query1); %class prediction
```

Appendix C: Matlab Code for FFT, Butterworth Noise Filtering and Signal Reconstruction

```
%plot raw signal
plot (I)

y = fft(I); %computes discrete Fourier transform of I using FFT
algorithm

f = (0:length(y)-1)*249899/length(y);
plot(f,abs(y)) %the plot also shows a mirror copy of the frequency
spectrum, which correspond to the signal's negative frequencies

%these commands perform a zero-centred circular shift on the
transform
n = length(I);
fshift = (-n/2:n/2-1)*(249899/n);
yshift = fftshift(y);
plot(fshift, abs(yshift))

%these commands normalise the frequencies
b = abs(y)
num_bins = length(b);
plot([0:1/(num_bins/2 -1):1], b(1:num_bins/2))

[b a] = butter(b, a, 'low') %b is filter order and a is cutoff
frequency and 'low' for low pass filtering
H = freqz(b,a, floor (num_bins/2));
hold on
plot ([0:1/(num_bins/2 -1):1], abs(H), 'r');

x_filtered = filter(b,a,I); %origigal signal filtered using
butterworth constants
plot(x_filtered, 'r') %plots reconstructed signal
```

Appendix D: Proposed Algorithm Design

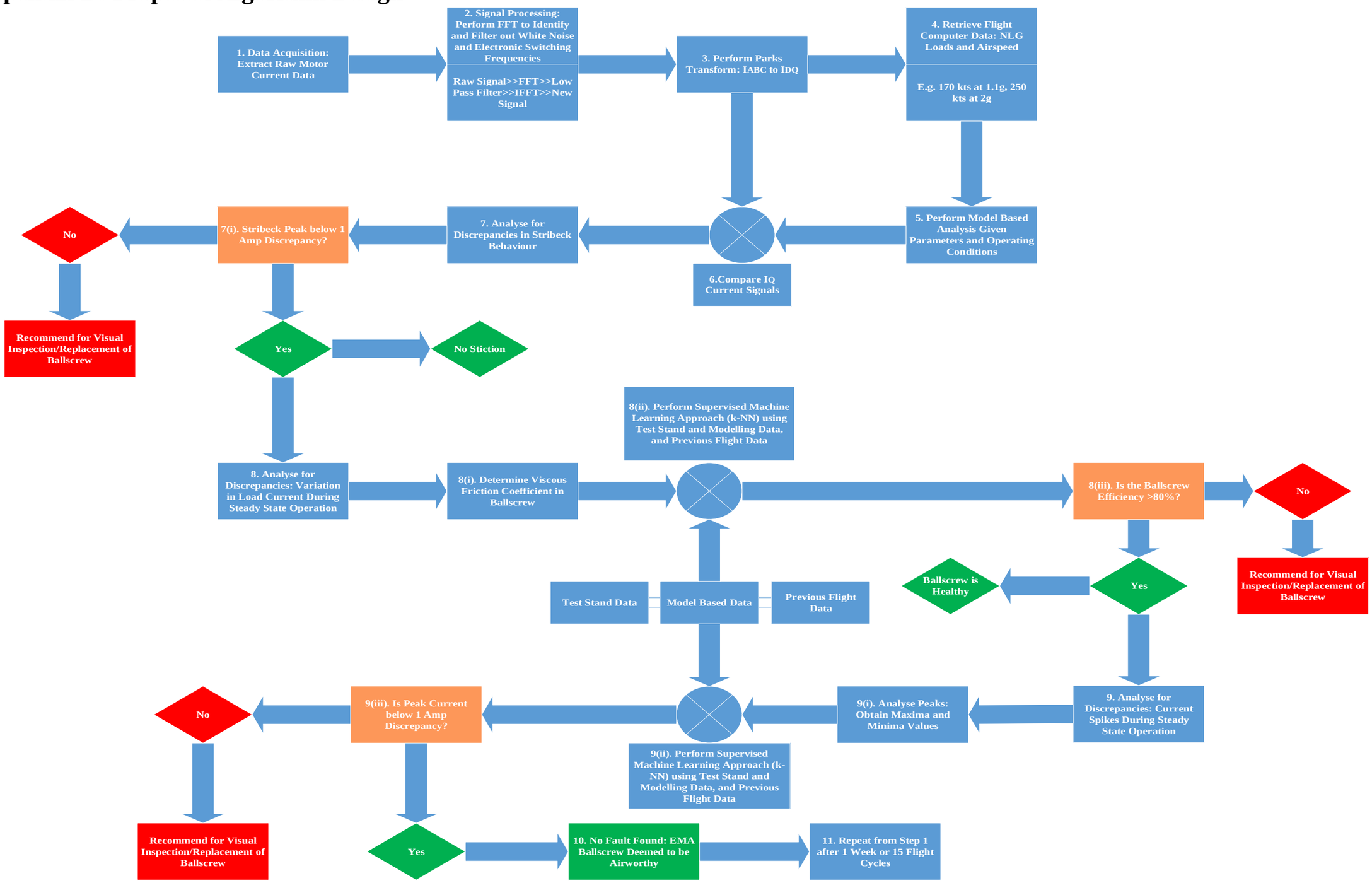

Figure 57. Proposed Algorithm Design.